Characterization of CFTR chloride channel

Yang, Jie

2009

Yang, J. (2009). Characterization of CFTR chloride channel. Doctoral thesis, Nanyang Technological University, Singapore.

https://hdl.handle.net/10356/19294

https://doi.org/10.32657/10356/19294

NANYANG TECHNOLOGICAL UNIVERSITY

CHARACTERIZATION OF CFTR CHLORIDE CHANNEL

YANG JIE

SCHOOL OF BIOLOGICAL SCIENCES

2009

CHARACTERIZATION OF CFTR CHLORIDE CHANNEL

YANG JIE

School of Biological Sciences

A thesis submitted to the Nanyang Technological University
in partial fulfillment of the requirement for the
degree of Doctor of Philosophy

2009

Acknowledgement

I express my special and deepest gratitude to my supervisors Dr. Alex Gong, Dr. Valerie Lin and Prof. Alex Law for their kindly guidance and encouragement during the process of the whole study. I am also thankful for the financial support of the doctoral scholarship from Nanyang Technology University during my PhD study.

I sincerely thank Dr. Alex Gong for his patient instruction in doing my project. His forthrightness and serious attitude about science gave me deep impression and had a huge effect on me. Thanks also go to Ms. Ge Ning, Mr. Qian Feng and Mr. Xue Jiugang for their help and friendship.

I thank Ms. Xing Chang and Ms. Ng Lifang for helping me in doing site-directed mutagenesis and preparing the necessaries.

Thanks to Ms. Sun Yang, Ms. Hua Hua and all the labmates working in Dr. Lin's group for their help and kind share of the utilities.

Finally, I give special thanks to all of my friends in School of Biological Sciences and my parents for their supports in these years.

Contents

Summary

Cystic fibrosis (CF) is an inherited disease caused by mutations in a single gene which encodes the cystic fibrosis transmembrane conductance regulator (CFTR), a member of ATP-binding cassette (ABC) proteins superfamily. Since the genetic basis of CF was resolved in 1989 when the CFTR gene was cloned and disease-associated mutations were identified, remarkable progress have been made in understanding CF and CFTR. However, there is no cure for CF or effective control of the destruction of the lungs and pancreas of CF patients. What's more, despite the progress in elucidating domains involved in CFTR channels function, the structure basis for chloride conductance through CFTR remains incompletely understood. For example, the possible interactions among the CFTR proteins have not been demonstrated at the cell membranes if they can form a dimer or an oligomer. Therefore, we tested whether CFTR is monomeric or oligomeric by analyzing the population of channel conductance from cells co-expressing two mutants with different single channel properties. And our results suggest that CFTR channel pore is made up from a monomer. However, our findings also provide direct functional evidence supporting the notion that CFTR can exist as dimer or even multimer in the cell membranes.

Meanwhile, we also investigated structure fluctuations in CFTR, as an anion channel, which is activated by phosphorylation of the R domain via cAMP-activated protein kinase A (PKA) and ATP binding and hydrolysis at the two NBDs. We tested the interdomain interaction between R domain and MSD/NBD domains, and the interaction

between MSD domains and NBD domains. Our results suggest that R domain which is predominantly unstructured would allow multiple different phosphoserines to stimulate CFTR chloride channel. The unstructured R domain has such a large flexibility to interact with NBDs and MSDs that it can not only regulate the gating of CFTR channel pore but also affect the channel properties. Our results also suggest that interdomain interaction between NBD and MSD domains can change the CFTR channel pore conformation thereby to affect the channel pore properties.

Finally, we focused our work on CF gene therapy. There is tremendous interest in gene therapy treatments for CF after the identification of the CFTR gene. Gene therapy offers the potential of correcting the underlying cause, overwhelming traditional treatments which fall far short of a cure and are aimed primarily at improving the quality of patients. Give the assumption that CFTR gene can be genetically modified to maximize its lost function; we constructed some CFTR genes to achieve CFTR gain of function mutants which can compensate the losses of CFTR Cl^- channel function and hence be potentially useful to the gene therapy. We identified some crucial sites which are potential residues for gene therapy, such as R334, F337, T338, T339 and S341. We do believe that by continuing to identify the potential CFTR mutants and by maintaining a strong focus on improving CFTR gene function, gene therapy will surely improve the outcome of CF therapy.

List of Figures

List of Tables

List of Abbreviations

3T3	3-day transfer, inoculum 3 x 10^5 cells
ABC	ATP-binding cassette
ADP	adenosine diphosphate
AMP	adenosine monophosphate
AMP-PNP	adenylyl imidodiphosphate
ATP	adenosine-5'-triphosphate
BHK	baby hamster kidney
CAL	CFTR-associated ligand
Calu-3	Caucasian lung adenocarcinoma cancer cell
cAMP	cyclic adenosine monophosphate
CAP	CFTR-associated protein
CF	cystic fibrosis
CFTR	cystic fibrosis transmembrane conductance regulator
CHO	chinese hamster ovary
CsA	cyclosporine A
DM	deltamethrin
DMEM	dulbecco's modified eagle's medium
DPC	diphenylamine-2-carboxylic acid
DTRL	carboxy-terminal amino acids of CFTR
E_{Rev}	reversal potential
E3KARP	NHE3 kinase A regulatory protein

E. coli	Escherichia coli
ENaC	epithelial sodium channel
EBP50	ERM-binding phosphoprotcin-50
GSH	γ-glutamyl-cysteinyl-glycine
Hsc	heat shock protein cognate
Hsp	heat shock protein
HT-29/B6	human caucasian colon adenocarcinoma grade II
I/I_0	control current remains
K_d	dissociation constant
LB	Luria-Bertani
MEM	minimum essential medium
MSD	membrane-spanning domain
NBD	nucleotide binding domain
NHERF	Na^+/H^+ exchanger regulating factor
NPPB	natriuretic peptide precursor B
P_o	open probability
PDZ	post synaptic density protein 95
PIP(2)	phosphatidylinositol 4,5-bisphosphate
PKA	protein kinase A
PKC	protein kinase C
PP1	protein phosphatase 1
PP2A	protein phosphatase 2A
PP2B	protein phosphatase 2B

PPi	pyrophosphate
RD	regulatory domain
Shank	SH3 and multiple ankyrin repeat domains 2
SLC26	solute-linked carrier 26
SLC26T	solute-linked carrier 26 transporters
SLC26T DRA	solute-linked carrier 26 transporters down-regulated in adenoma
STAS	sulphate transporter and antisigma factor antagonist
TM	transmembrane segment
ClC-0 channel	voltage-gated chloride channel
WT	wild type

1 Introduction

1.1 Cystic Fibrosis (CF) and Cystic Fibrosis Transmembrane Conductance Regulator (CFTR)

Cystic fibrosis (CF) is the most common inherited disease in Caucasian population, affecting about 1 in every 2,500 children born. It is much rarer in people of Africans or Asians. In CF patients, the body produces abnormally thick, sticky mucus. It clogs the lungs and leads to the dysfunction of normal constant flow of mucus which can remove debris and bacteria over the surfaces of the air passages. In fact, due to the thick mucus, which provides an ideal environment for bacterial growth and gives rise to the bacterial chest infections, CF patients have to spend their lifetime in struggling with persistent coughing, wheezing, and shortness of breath with ordinary activities. Moreover, the mucus obstructs the pancreas, preventing digestive enzymes from reaching the intestines to help break down and absorb food (Pilewski and Frizzell, 1999). Cystic fibrosis is also a cause of infertility. The majority of adult males with CF (99%) are characterized by congenital bilateral absence of vas deferens (CBAVD). CBAVD is encountered in 1-2% of infertile males without CF. Men with CBAVD but without CF gene mutations have a high incidence of urinary tract malformations (Dork et al., 1997). Females with CF are found to be less fertile than normal healthy women. In females with CF, delayed puberty and amenorrhoea are common due to malnutrition. CFTR mutations are also associated with congenital absence of the uterus and vagina (CAUV). In CF females delayed puberty and amenorrhoea are common due to malnutrition as the main cause (Stead et al.,

1987). Due to the progressive lung destruction, pancreatic disease and other symptoms, the life expectancy of CF patients is very short, normally under 30 years old.

During the past two decades, concern of CF has grown vigorously in science, medicine, and society. It has advanced from innumerable speculations about its cause to a precise definition of causative mutations. However, despite the remarkable progress made in understanding CF, currently, there is no cure for this disease or effective control of the destruction of the lungs and pancreas (Quinton, 1999).

The genetic basis of CF was resolved in 1989 when the cystic fibrosis transmembrane conductance regulator (CFTR) gene was cloned and disease-associated mutations were identified (Riordan et al., 1989). The CFTR protein is a multi-functional protein (Barinaga, 1992; Hasegawa et al., 1992; Schwiebert et al., 1999), its most important role is as a nucleotide-dependent, phosphorylation-regulated Cl^- channel in apical membranes of epithelial cell (Anderson et al., 1991; Cheng et al., 1991; Schultz et al., 1999). The loss of CFTR chloride channel function is the primary cause of cystic fibrosis (McIntosh and Cutting, 1992). CFTR is expressed in many different epithelial tissues, and as a result, CF is associated with lung, pancreatic, gastrointestinal, and reproductive disease (Pilewski and Frizzell, 1999).

CFTR mutations can be categorized into five major classes: the total absence of CFTR; defects in CFTR folding and trafficking leading to reduced amounts of mature CFTR; abnormal regulation of Cl^- conduction in an otherwise mature CFTR; decreased Cl^-

conduction in a fully processed CFTR; and decreased CFTR synthesis (Pilewski and Frizzell, 1999). An additional class of CFTR mutations has been recently been proposed by Haardt et al. (Haardt et al., 1999) and discussed by Zielenski as Class VI (Zielenski, 2000), which cause accelerated turnover of protein from the cell surface, resulting in decreased CFTR activity. From a physiological perspective, the loss of CFTR Cl^- channel function is the primary mechanism for all six classes of CFTR mutations.

At present, more than 1000 allele mutants have been identified to date (Bobadilla et al., 2002). Among the 1000 mutants, ΔF508 is present in approximately 70% of CF patients (Macek et al., 1990). It corresponds to a specific deletion of three base pairs, which result in the loss of a phenylalanine residue at amino acid position 508 of the putative product of the CF gene. Most other mutations have not yet been defined. Although most of the reported mutations in CFTR are rare and unclassified, it may be possible to use genotype-phenotype correlation to determine the best approach for new pharmacological treatments. Therefore, an understanding of the function of the protein product and its defective function in CF should yield important new insights into the pathogenesis and potential therapy of this disease.

1.2 Structure of CFTR

CFTR is a member of the large ATP-binding cassette (ABC) family of membrane proteins, most members of which act as ATP-dependent transmembrane pumps of a wide range of substances. The CFTR protein is made up of two homologous repeats, each containing six transmembrane (TM) regions followed by a cytoplasmic nucleotide

binding domain (NBD). These two halves are joined by a cytoplasmic regulatory (R) domain, a structure that is unique to CFTR in the ABC family, which contains multiple consensus sequence sites for phosphorylation by protein kinase A (PKA). The originally suggested roles of the NBDs and the R domain, in channel regulation by ATP binding and hydrolysis and activation by PKA-dependent phosphorylation, have subsequently been borne out experimentally (Gadsby and Nairn, 1999; Sheppard and Welsh, 1999). Two highly conserved motifs which are contained in both NBDs of the ABC proteins: Walker A (GXXGXGKS/T) which is involved in coordinating the β- and γ-phosphates of ATP and Walker B (ϕϕϕϕD, where ϕ is a hydrophobic residue) are located in NBDs of CFTR. In contrast, the primary structure of CFTR give little clue as to the location of the channel pore region through which Cl^- ions cross the membrane, and as a result, the structure of this region is still relatively poorly defined. To date, most studies have concentrated on TM6, which clearly contributes to the pore and plays an apparently dominant role in determining its permeation properties (Gong and Linsdell, 2003a, b, c). Although other TMs are generally presumed to contribute to the pore (Dawson et al., 1999), strong evidence supporting such a role is lacking. Establishing the roles of different TMs is of obvious importance in determining the overall architecture of the pore. Furthermore, specific amino acid residues within the TMs that line the pore undoubtedly form the binding sites for the most CFTR channel inhibitors (Gong et al., 2002a; Gong et al., 2002b).

Despite the progress in elucidating domains involved in CFTR channels function, the structural basis for chloride conductance through CFTR remains incompletely understood.

Fundamental questions remain as to how many CFTR polypeptides constitute the channel, although there are controversial reports concerning whether CFTR channel is a monomer (Chen et al., 2002; Marshall et al., 1994) or a dimer (Eskandari et al., 1998; Ramjeesingh et al., 2003; Ramjeesingh et al., 2001; Schillers et al., 2004; Zerhusen et al., 1999). Furthermore, the possible interactions among the CFTR proteins have not been demonstrated in the cell membranes if they can form a dimer or an oligomer. Quaternary structure of CFTR at the cell membranes is fundamental important to understand the molecular basis for cystic fibrosis pathogenesis. Since nearly all known ion channels are homo- or hetero-oligomers (Hille, 2001), the possibility that CFTR may posses a quaternary structure also has to be considered.

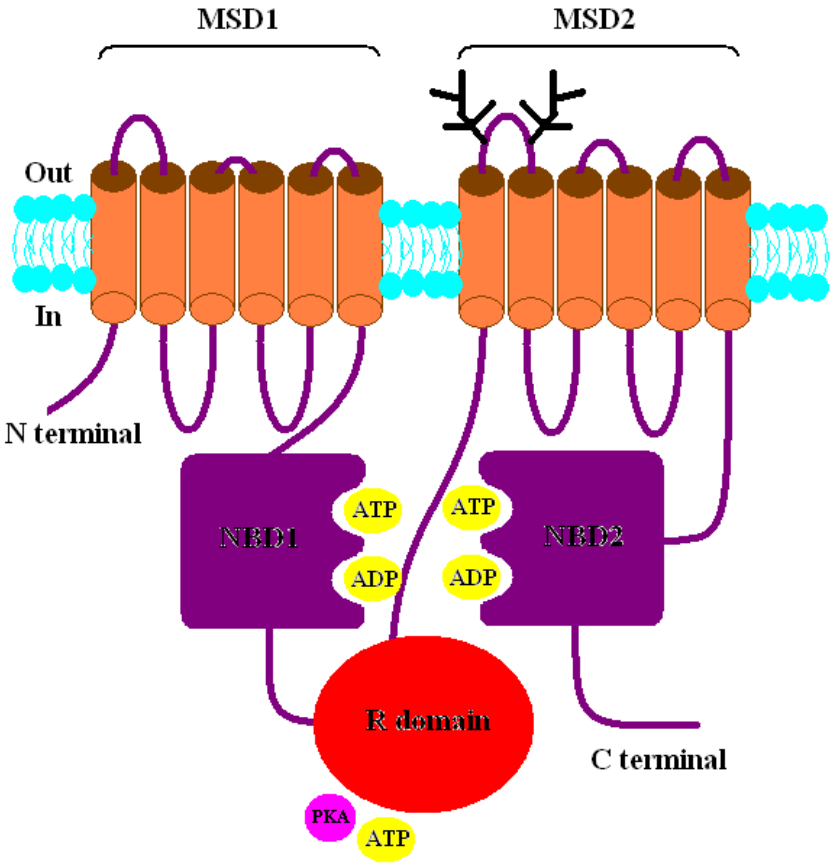

Fig. 1.1 The proposed domain structure of CFTR

CFTR Channel gating is modulated by R domain phosphorylation and the ATP hydrolysis at NBDs. MSD, membrane-spanning domain; NBD, nucleotide binding domain; R domain, regulatory domain.

1.3 Function of CFTR

1.3.1 Primary Function as Anion Channel

CFTR is functionally distinct in performing as an ion channel although its architectural similarity to ABC transporter family members. CFTR was first stated either be the chloride channel or a regulator of a separate channel protein (Riordan et al., 1989). Later, strong evidence indicates that CFTR polypeptide itself mediates a characteristic epithelial anion conductance despite the vast reports of influences of the CFTR on other channels and transporters (Kunzelmann, 2001; Lee et al., 1999). Now the chloride-selective permeation path though CFTR has been studied extensively in electrophysiological fields, as with all Cl^- channels, CFTR is much less selective than most cation channels (K^+, Na^+, Ca^{2+}), allowing most small anions to permeate to some extent (Gong and Linsdell, 2003a). The anion permeability sequence is similar to the classical Hofmeister or lyotropic sequence (SCN^-> I^-> NO_3^-> Br^-> Cl^-> F^-) with anions which are more easily dehydrated (lyotropic) having a higher permeability than anions which retain their waters of hydration more strongly (kosmotropes)(Gong and Linsdell, 2003a).

While cystic fibrosis transmembrane conductance regulator is well known to function as a Cl^- channel, CFTR is also involved in the transport of other physiologically important anions such as HCO_3^- (implicated in pH regulation of pancreatic ducts) (Gray et al., 2001), glutathione (implicated in the regulation of oxidative stressing airways) (Linsdell and Hanrahan, 1998b) and larger organic anions (some native antibiotics) (Linsdell and Hanrahan, 1998a). In fact, permeation of anions other than Cl^- such as HCO_3^- through CFTR may be physiologically relevant (Poulsen et al., 1994). This has been observed in

the airways including submucosal glands; the gastro-intestinal tract; the liver and gallbladder and the pancreas (Gray et al., 2001). Under physiological conditions, the secreted HCO_3^- rich fluid and electrolytes serve to flush the digestive enzymes from the acini and ducts of the pancreas. Thus, the impaired HCO_3^- secretion results in poor clearance of the digestive enzymes, and their premature activation eventually causes the destruction of pancreas in CF. Defective HCO_3^- and fluid secretion are hallmarks of the pathophysiology of the pancreas of cystic fibrosis patients. It has been shown that a similar defect in HCO_3^- secretion can also be found in the airway mucosa (Smith et al., 1994). Several studies have addressed the question of whether CFTR per se conducts HCO_3^- and suggested that CFTR does have a finite permeability for HCO_3^- ions (Wine, 2003), but this permeability is at best 26% of that for Cl^- ions. At this point, it seems justified to question whether this seemingly low permeability might in fact be sufficient to permit HCO_3^- through CFTR. The results with primary cultures of human bronchial epithelial cells and Calu-3 cells suggest HCO_3^- secretion in the airway may be more important than has previously been appreciated. Despite the crucial role of HCO_3^- in buffering pH, little is known about the relationship between cause of CF pathology and the molecular defects arising from specific mutations. Mutations in CFTR that impair the conductance of the channel for HCO_3^- are expected to increase the severity of the disease in those epithelia where HCO_3^- secretion is essential for the normal physiology of the organ. Impaired HCO_3^- secretion in the pancreas and small intestine in CF patients has been known for many years. Some mutations in the CFTR channel protein causing cystic fibrosis disrupt the vital physiological function of HCO_3^- transport.

It is also reported that the Cl^- and HCO_3^- conducting functions of CFTR can be regulated differentially by intracellular glutamate and ATP (Reddy and Quinton, 2003). Furthermore, due to their distinct regulatory properties, disease-causing mutations may exert distinguishable effects on HCO_3^- and Cl^- flux. For example, the CF mutation CFTR R117H retains near-normal HCO_3^- conductance, despite a substantive reduction of Cl^- conductance.

Similarly, conductance of another physiologically important anion, glutathione, is regulated differently from Cl^- (Linsdell and Hanrahan, 1998b). Glutathione conductance exhibited a distinctive dependence on nucleotide interaction. The structure of the conductance pore through CFTR may be malleable and dependent on the nucleotide occupancy of the cytosolic domains (nucleotide-binding domains). Like HCO_3^- flux, glutathione flux is an important consideration in understanding normal tissue physiology. Glutathione is a major extracellular and intracellular antioxidant. Lack of an efflux path in the apical membrane of respiratory epithelia may be expected to alter the concentration of glutathione in the airway surface fluid and impact negatively on the antioxidant load in this tissue.

Studies have shown that expression of CFTR is associated with enhanced glutathione (GSH) efflux from airway epithelial cells, implicating a role for CFTR in the control of oxidative stress in the airways. To define the mechanism underlying CFTR-associated GSH flux, wild type and mutant CFTR proteins expressed in Sf9 membranes were studied, as well as purified and reconstituted CFTR. CFTR-expressing membrane

vesicles mediate nucleotide-activated GSH flux, which is disrupted in the R347D pore mutant, and in the Walker A K464A and K1250A mutants. Further, purified CFTR protein alone directly mediates nucleotide-dependent GSH flux. Interestingly, although ATP supports GSH flux through CFTR, this activity is enhanced in the presence of the non-hydrolyzable ATP analog AMP-PNP. These findings corroborate previous suggestions that CFTR pore properties can vary with the nature of the nucleotide interaction. In conclusion, GSH flux is an intrinsic function of CFTR and prompt future examination of the role of this function in airway biology in health and disease (Kogan et al., 2003).

Many scientists reported ATP release also associated with CFTR expression in human airway epithelial cells (Cantiello, 2001; Schwiebert, 1999; Schwiebert et al., 1995), C127 cells (Prat et al., 1996; Rotoli et al., 1996), red blood cells from normal and CF patients upon mechanical stress (Sprague et al., 1998), cardiac myocytes (Lader et al., 2000a; Lader et al., 2000b) and retinal pigment epithelium cells (Reigada and Mitchell, 2005). ATP serves not only as an energy source for all cell types but as an extracellular messenger for autocrine and paracrine signalling. It is released from the cell via several different purinergic signal efflux pathways. ATP and its Mg^{2+} and/or H^{+} salts exist in anionic forms at physiological pH and may exit cells via some anion channel if the pore physically permits this. If anionic forms of ATP are released via the CFTR channel, then actual ATP-mediated conductance should be measurable in CFTR-expressing cells under certain experimental conditions. Reisin et al. (Reisin et al., 1994) were the first to detect such a conductance in C127/CFTR cells. When both pipette and bath contained ATP

solutions, a 4.8 pS channel could be observed with a reversal potential of around 0 mV which was independent of employed cations (Na^+, Mg^{2+} or $Tris^+$), suggesting that the current was anionic. The channels were activated by PKA and inhibited by diphenylamine-2-carboxylate (DPC), indicating that the currents were related to or mediated by CFTR. Schwiebert et al. (Schwiebert et al., 1995) also demonstrated the presence of a glibenclamide-sensitive 6 pS channel in human airway epithelial cells bearing either normal or mutant CFTR, using symmetrical ATP solutions (140 mM TrisATP). The reversal potential shifted by -22 mV when 140 mM TrisCl was present on one side, indicating that the channel was permeable to chloride ions as well. Cantiello and coworkers repeatedly observed PKA-stimulated whole-cell and single-channel ATP-mediated currents from shark rectal gland cells (Cantiello et al., 1997) as well as from rat (Lader et al., 2000b) and mouse (Lader et al., 2000a) cardiac myocytes in primary culture. However, it must be pointed out that one cannot completely rule out a possible contamination of Cl^- currents in the currents measured during these patch-clamp experiments, because the shank of the patch pipette was back-filled with Cl^- containing solution which may have been pushed down into a Cl^- free, ATP-containing tip region by hydrostatic pressure.

1.4 Mechanism of Anion Permeation

1.4.1 Functional Probes of CFTR Pore

Small permeant anions, $Au(CN)_2^-$ and $Pt(NO_2)_4^{2-}$, as functional probes of the CFTR pore region were used to identify amino acid residues in the key TM6 region that contribute to

the processes of anion binding and selectivity and provide clues concerning the mechanism of Cl^- permeation through the pore (Gong et al., 2002a; Gong and Linsdell, 2003a; Linsdell and Gong, 2002). Lyotropic anions, as well as showing a high permeability in CFTR, bind relatively tightly within the CFTR pore. Experimentally, this is manifested in two ways. First, lyotropic anions with high permeability often show low conductance, suggesting a longer retention time within the pore than less permeant anions (Gong and Linsdell, 2003b). Secondly, lyotropic anions are effective open channel blockers of Cl^- permeation (Gong and Linsdell, 2003b, 2004), suggesting that they bind tightly enough within the pore to slow the overall rate of flux. Although both anion permeability and anion binding in CFTR show a similar lyotropic sequence, recent evidence suggests that these two facets of the permeation mechanism are only weakly interdependent (Smith et al., 2001). This suggests that distinct structural loci are primarily responsible for determining CFTR anion selectivity and intrapore anion binding.

1.4.2 Crucial Role of TM6 in Formation of the CFTR Channel Pore

Despite extensive investigations in the intervening dozen years, neither the exact segments of the polypeptide which form the pore nor the number of CFTR molecules per pore have been determined with certainty. Most obvious is the need for a high-resolution three dimensional structure that would clearly define the pore. The influence of charged residues within membrane-spanning segments on anion selectivity supported the reasonable assumption that these putative transmembrane helices contribute to the pore. Site mutations in TM6 have been used to identify the structural determinants of CFTR pore function and to provide clues concerning the mechanism of Cl^- permeation through

the pore. As the helix that includes a greater number of charged amino acids than any other, TM6 has functional important residues: K335 and R347 influence anion selectivity and Cl^- conductance (Tabcharani et al., 1997); R347 confers anomalous molefraction effects and protocol-dependent block by I^- (Tabcharani et al., 1997); T338 and T339 together control the permeability of the channel to polyatomic anions due to the control of a narrow region (Linsdell et al., 1997a); R334W and R347P, disease-associated mutations, alter the kinetics and conductance of single channel (Sheppard et al., 1993) and T351, R352 and Q353 form the anion/cation selectivity filter (Cheung and Akabas, 1997; Guinamard and Akabas, 1999).

Most recently, the interaction between different anions bound within the CFTR pore has been investigated. Multiple anions bind simultaneously within the pore, and bound anions experience mutual repulsion (probably of an electrostatic nature) that speeds their exit from the pore (Gong et al., 2002a; Gong and Linsdell, 2003a, c). We believe that this repulsion may be crucial part of the normal rapid throughput of Cl^- ions in CFTR, and possibly all anion-selective channels. A key anion binding site (R334) near the external end of TM6 plays a crucial role in coordinating the concurrent binding of multiple anions (Gong and Linsdell, 2003b, 2004). These results suggested that R334 makes a strong contribution to anion binding in the CFTR pore. Previous experiments also revealed other properties of R334 mutants. All mutations at this position induced inward rectification of the I-V relationship (Gong and Linsdell, 2003b, 2004).

1.4.3 Multiple Transmembrane Domains are involved in Formation of the CFTR Channel Pore

Previous investigations of CFTR pore structure have stressed the importance of TM6, and at the same time failed to find strong evidences for the involvement of other TMs (Dawson et al., 1999; Gong and Linsdell, 2003b; McCarty, 2000). A major role of TM6 has been confirmed in extensive studies employing mutagenesis and chemical modification at several positions (Gong et al., 2002a; Gong and Linsdell, 2003b). These modifications strongly impacted fundamental properties of the channel, including conductance, anion selectivity and occupancy, and inhibition by blockers. Nevertheless, it is widely presumed that other TMs must play some roles in forming the pore and determining its functional properties (McCarty, 2000). Previous work showed that TM5, which is adjacent to TM6 and separated from it by only a very short extracellular loop, plays a much less important role than in TM6 in forming the pore (Ge et al., 2004). G314 and V317 in TM5 were suggested to contribute to the pore on the basis of the finding that these mutations alter conduction properties (Mastrocola et al., 1998). TM11 and TM12 also were reported to contribute to the pore from selectivity studies and an analysis of the effects of mutations in these domains on interactions with channel blockers (McDonough et al., 1994; Zhang et al., 2000a; Zhang et al., 2000b). Mutations S1118 in TM11 and T1134 in TM12 altered the affinity and voltage-dependence of blockage by DPC or NPPB (Zhang et al., 2000b). Based on these studies a hypothesis suggested that CFTR channel pore consists of surfaces provided by transmembrane helices 5, 6, 11 and 12 and the pore of CFTR is asymmetric (McCarty, 2000).

1.4.4 CFTR Channel Pore is structurally Asymmetrical in terms of "Sidedness" (Intracellular vs Extracellular)

The CFTR channel shows linear current-voltage relationship when symmetrical Cl^- concentrations present in both sides of membrane. However, all of the CFTR channel blockers described above act either preferentially or exclusively from the cytoplasmic side of the membrane. This suggests that drug binding sites within the pore are more easily accessible from their cytoplasmic end. This functional asymmetry has led to the suggestion that the CFTR pore is structurally asymmetric, with a wide inner vestibule containing binding sites with which large channel blockers may interact (Gong et al., 2002b; Gong et al., 2002c; Gong and Wong, 2000; Gong et al., 2000). The pore is presumed to narrow towards its extracellular end, forming a restricted region where discrimination between different permeant anions takes place (Gong et al., 2002b; Gong et al., 2002c; Gong and Wong, 2000; Gong et al., 2000). Previous research on TM6 has identified binding sites in the CFTR pore for permeant anions and for the large organic molecule lonidamine (Gong et al., 2002a; Gong et al., 2002b; Gong and Linsdell, 2003b). However, the overall molecular pharmacology of the pore is not well understood, more comprehensive studies are required to establish and refine a useful structural model of pore-inhibitor interactions.

1.4.5 Multiple Anion Binding Sites Exist Throughout the CFTR Channel Pore

As we mentioned previously that multiple anions bind simultaneously within the pore, and that bound anions experience mutual repulsion (probably of an electrostatic nature) that speeds up their exit from the pore (Gong et al., 2002a; Gong and Linsdell, 2003a, c).

We believe that this repulsion may be crucial part of the normal rapid throughput of Cl^- ions in CFTR, and possibly all anion-selective channels. A key anion binding site (R334) near the external end of TM6 plays a crucial role in coordinating the concurrent binding of multiple anions (Gong and Linsdell, 2003b, 2004). Previous results showed that multiple amino acid residues in the CFTR pore region contribute to anion binding sites in TM6 (Gong and Linsdell, 2003a, b, c, 2004), and we hypothesize that other similar amino acid residues are also involved in the anion binding in other pore forming TMs. For example, Mutations S1118 in TM11 and T1134 in TM12 altered the affinity and voltage-dependence of blockage by DPC or NPPB (Zhang et al., 2000b). To find these residues, further work need to be carried out.

1.4.6 Interaction between anions simultaneously bound to these sites is a crucial aspect of the normal permeation mechanism

The existence of multiple anion binding sites is also consistent with the functional evidence that the CFTR pore can accommodate more than one anion at the same time (Gong and Linsdell, 2003a, b, c, 2004). Such multi-ion pore behavior results from electrostatic interactions between ions bound simultaneously within the confines of channel pores. Such electrostatic interactions have been shown to be crucially important in the permeation and selectivity processes of other channel types. We assume that the best probes of multi-ion pore behavior are permeant ions that bind within the pore with high affinity (Gong and Linsdell, 2003a, b, c, 2004). The potential interactions between Cl^- and high-affinity permeant ions such as $Au(CN)_2^-$, SCN^- and ClO_4^- within the pore coupling with the identification of the molecular basis of permeant ion binding, is used to

identify interacting binding sites within the pore. And several different types of interactions between permeant and blocking anions are possible within channel pores. Most simply, if both permeant and blocking anions bind to a common site, competition between the two will reduce the apparent affinity of the blocker. Some interesting evidence showed that the direction in which $Au(CN)_2^-$ exit the pore can be modulated by interactions with other anions and by mutations within the pore. Identification of the location of the "barrier" to divalent anion permeation is important structurally since these pseudohalides block Cl^- permeation in CFTR, potentially making them useful as probes of intrapore anion binding sites. If we are able to determine at the molecular level a point in the channel beyond which these anions cannot permeate, then their blocking effects must occur between the sides of the membrane at which they are applied at this point. This kind of approach has the potential to characterize distinct anion binding sites on either side of a well-defined intrapore permeation barrier. Such information would be highly useful in investigating the proposed structural asymmetry in the pore.

1.5 Regulation of CFTR Channel Activity

1.5.1 Phosphorylation of the R domain regulates CFTR channel gating

The presence of the unique R-domain, rich in consensus sites for phosphorylation by PKA and PKC, suggests that some control by phosphorylation is likely. Under normal circumstances, phosphorylation by PKA (and PKC) is obligatory for activation of gating by ATP binding. Conformational changes at the level of the R-domain and the whole protein have been observed on PKA phosphorylation (Grimard et al., 2004). However, the R-domain itself is not highly structured when either phosphorylated or

dephosphorylated (Ostedgaard et al., 2000). Phosphorylation of the R domain stimulates CFTR channel activity and may also influence its interactions with other proteins. Regulation by PKA and PKC are well established although other serine-threonine and tyrosine kinases may also have a role. Sites that become conspicuously phosphorylated under in vivo conditions are $RRNS_{660}I$, $KRKNS_{700}I$, $RKVS_{795}L$ and $RRLS_{813}$ Q. Phosphorylation of other sites (i.e., $RKFS_{712}I$, $RIS_{753}V$ and $RRQS_{768}V$) has been detected in vitro, presumably because kinase activity is higher (or phosphatase activity lower) in vitro than in intact cells. The role of consensus sequences that are not detectably phosphorylated in vivo are rather mysterious probably have important roles since they can support ~ 50% channel activity and are highly conserved between species despite sequence divergence within the R domain. Some PKA sites (S737, S768) down-regulate channel activity when phosphorylated (Csanady et al., 2005; Vais et al., 2004).

Protein kinase C (PKC) is much less effective in activating CFTR channels compared to PKA (<10%) but does enhance CFTR responsiveness to PKA by increasing the rate and magnitude of PKA activation and helping to maintain CFTR in a PKA-responsive state. Several PKC consensus sequences are essential for CFTR to be competent for gating, and at least one of these is actually phosphorylated by PKC. There is also evidence for inhibitory PKC sites on the R domain (Chappe et al., 2004).

Interestingly, Himmel and Nagel reported that phosphatidylinositol 4,5-bisphosphate (PIP(2)) activates human CFTR, resulting from ATP responsiveness of PIP(2)-treated CFTR. PIP(2) alone is not sufficient to open CFTR, but ATP opens nonphosphorylated

CFTR after application of PIP(2) (Himmel and Nagel, 2004). They suggested that regulation of CFTR by PIP(2) is a previously unrecognized, alternative mechanism to control chloride conductance.

1.5.2 Nucleotides are required for CFTR gating

CFTR channel activity is also regulated by nucleotide binding and ATP hydrolysis. The relationship between ATPase activity at the NBDs of CFTR and channel gating has been interpreted in different ways. ATP hydrolysis is generally believed to be energetically coupled to the transport of solutes by other transport ATPase, but ion permeation through channels is driven only by the electrochemical gradients of the ions. Nucleotides bind to both NBDs, but NBD1 is the site of stable ATP binding and NBD2 is the primary site for ATP hydrolysis (Aleksandrov et al., 2001). Therefore, the effects of mutations in the two NBDs are non-equivalent. For example, the ATPase activity exhibited by CFTR K464A in NBD1 was decreased by 70-80%, whereas the ATPase activity of CFTR K1250A in NBD2 was approximately 1% of wild-type activity. Hence, there may be one primary catalytic site formed by the NBDs of CFTR (involving the Walk A lysine in NBD2 K1250) and one modulatory site (involving the Walker lysine in NBD1 K464) (Basso et al., 2003). While this property is consistent with its membership in the ABC superfamily, intrinsic ATP hydrolysis has not been linked to the gating mechanism for any other channel to date. Therefore, investigations of the structure-function relationships of CFTR are exciting because they lead researchers into uncharted areas. ATP is required for CFTR channel gating, but CFTR activity has been recorded in nominally Mg-free solutions that should prevent hydrolysis. Moreover, the temperature dependence of CFTR

gating in planar bilayers suggests that the open and closed states of CFTR have similar free energies and therefore ATP hydrolysis energy is not required for closing the channel and it has been proposed that the energy comes instead from the interaction of MgATP with CFTR. Different functions have been ascribed to NBD1 and NBD2 based on electrophysiological studies of mutant channels. Photoaffinity labelling studies with 8-azido-alpha -32P-ATP indicate that nucleotides bind stably at NBD1 whereas rapid ATP turnover occurs at NBD2.

CFTR is an anion channel in the ATP binding cassette (ABC) transporter family. Like other ABC transporters, it can hydrolyze ATP. Yet while ATP hydrolysis influences channel gating, it has long seemed puzzling that CFTR would require this reaction because anions flow passively through CFTR. Moreover, no other ion channel is known to require the large energy of ATP hydrolysis to gate. It was found that CFTR also has adenylate kinase activity (ATP + AMP <=> ADP + ADP) that regulates gating. When functioning as an adenylate kinase, CFTR showed positive cooperativity for ATP suggesting its two nucleotide binding domains may dimerize. Thus, channel activity could be regulated by two different enzymatic reactions, ATPase and adenylate kinase, that share a common ATP binding site in the second nucleotide binding domain. At physiologic nucleotide concentrations, adenylate kinase activity, rather than ATPase activity may control gating, and therefore involve little energy consumption (Randak and Welsh, 2003).

1.5.3 CFTR is down-regulated by a membrane-associated protein phosphatase

CFTR channels run down soon after membrane patches are excised from cAMP-stimulated cells. This spontaneous decline in open probability (Po) has been attributed to phosphatase activity in the excised patch because channels could be reactivated by exposure to MgATP + PKA. Rundown is not inhibited significantly by high concentrations of okadaic acid, and does not require Ca or calmodulin, indicating that it is not mediated by PP1, PP2A or PP2B. However, rundown is sensitive to the alkaline phosphatase inhibitors levamisole and bromotetramisole at high concentrations (> 200 μM) that inhibit all four types of serine/threonine phosphatases in biochemical studies. Reducing Mg^{2+} concentration slows rundown of CFTR channel activity in excised patches, consistent with the dependence of PP2C phosphatase activity on millimolar concentrations of Mg^{2+}. In patches from T84 cell monolayers, deactivation of cAMP-stimulated currents was also insensitive to okadaic acid and calyculin A, suggesting most CFTR deactivation in epithelia is also mediated by PP2C. PP2C is the main phosphatase physically associated with CFTR but it is not yet known if this interaction is direct or mediated by other proteins.

The activity of the CFTR Cl^- channel is dependent on its phosphorylation status set by kinases and phosphatases. Protein phosphatase 2B (PP2B) and protein kinase C (PKC) are potential regulators of CFTR. Treating CFTR-expressing 3T3 cells with either of the two specific PP2B blockers cyclosporin A (CsA, 1 microM) or deltamethrin (DM, 30 nM) caused rapid activation of CFTR in cell-attached patches. As determined by noise analysis of multi channel patches, DM- or CsA-activated CFTR displayed gating kinetics

comparable to those of forskolin-activated CFTR. After activation of CFTR by blocking PP2B, CFTR still inactivated. CFTR-mediated currents were, on average, 6.1 times larger when cells were stimulated by forskolin during PP2B block compared to stimulation by forskolin alone. This suggests that, in CFTR-expressing 3T3 cells, a phosphorylation site of CFTR is regulated by cellular PKA, PP2B and another phosphatase. However, in the epithelial cell lines Calu-3 and HT-29/B6, CsA and DM had no effect on CFTR activity in both cell-attached patch-clamp and transepithelial experiments. In contrast, when exogenous PP2B was added to patches excised from 3T3 or Calu-3 cells, PKA-activated CFTR currents were quickly inactivated. This indicates that free exogenous PP2B can inactivate CFTR in patches from both cell types. We propose that in order to regulate CFTR in an intact cell, PP2B may require a selective subcellular localization to become active. When excised patches were PKC-phosphorylated, the gating kinetics of CFTR was significantly different from those of PKA-phosphorylated CFTR. Addition of PP2B also inactivates PKC-activated CFTR, showing the indiscriminate dephosphorylation of different phosphorylation sites by PP2B (Fischer et al., 1998).

1.5.4 CFTR Interacts Physically and Functionally Up-Regulates Other Proteins

Intermolecular interactions of mature CFTR have been detected primarily with the N- and C-terminal tails, and these interactions have some impact not only on channel functions but also on localizations and processing within the cell. The C terminus of CFTR has a consensus sequence recognized by PDZ domains, and several PDZ-domain binding proteins have been shown to bind to it (Raghuram et al., 2001; Wang et al., 2000). These interactions may serve several functions, including enhancement of CFTR channel gating

through dimerization on dinging bivalent PDZ domain proteins (Raghuram et al., 2001; Wang et al., 2000). CFTR may be associated in a regulatory complex with other proteins at the plasma membrane where it has been reported to affect other transport proteins such as the epithelial sodium channel (ENaC). The best characterized interaction is that involving the amino terminal tail (N-tail) of CFTR and syntaxin 1A (Bilan et al., 2004). Syntaxin 1A is part of the vesicle fusion apparatus at neuronal synapses and is also expressed in airway epithelium. It binds to the N-tail of CFTR and inhibits its channel activity, apparently by disrupting interaction of the N-tail with the R domain of CFTR. The carboxy-terminal amino acids of CFTR (DTRL) form a motif that binds PDZ (Post synaptic density 95, Discs large, ZO-1) domains in scaffolding/adaptor proteins such as EBP50 (also called NHERF for sodium hydrogen exchange regulatory factor). Other PDZ proteins such as E3KARP, CAL (CFTR associated ligand), CAP70, and Shank2 has also been proposed to bind to the C terminus of CFTR and regulate its maturation, oligomeric state, channel gating, or phosphorylation (Cheng et al., 2004; Kim et al., 2004). Shank2, one of these scaffolding proteins, showed a strong interaction with CFTR by yeast two-hybrid assays. Shank2-CFTR interaction was verified by co-immunoprecipitation experiments in mammalian cells. Notably, this interaction was abolished by mutations in the PDZ domain of Shank2. Protein phosphorylation, HCO_3^- transport and Cl^- current by CFTR were measured in NIH 3T3 cells with heterologous expression of Shank2. Of interest, expression of Shank2 suppressed cAMP-induced phosphorylation and activation of CFTR. Importantly, loss of Shank2 by stable transfection of antisense-hShank2 plasmid strongly increased CFTR currents in colonic T84 cells, in which CFTR and Shank2 were natively expressed. Results indicate that

Shank2 negatively regulates CFTR and that this may play a significant role in maintaining epithelial homeostasis under normal and diseased conditions such as those presented by secretory diarrhea (Kim et al., 2004). The carboxy terminal truncation mutants of CFTR result in the decreased cell surface stability of the CFTR protein. Therefore, future studies may be directed toward determining whether the decreased cell expression of C terminus mutants can be corrected by pharmacological agents that enhace their phosphorylation status, i.e., phosphatase inhibitors. Whether protein-protein interactions mediate CFTR's effects on other transporters such as the epithelial sodium channel ENaC remains to be established.

The Na^+-H^+ exchanger regulatory factor (NHE-RF) is a cytoplasmic phosphoprotein that was first found to be involved in protein kinase A-mediated regulation of ion transport. NHE-RF contains two distinct protein interaction PDZ domains: NHE-RF-PDZ1 and NHE-RF-PDZ2. However, their binding partners are currently unknown. Because PDZ domains usually bind to specific short linear C-terminal sequences, affinity selection of random peptides for specific sequences that interact with the NHE-RF PDZ domains has been carried out and NHE-RF-PDZ1 is found to be capable of binding to the CFTR C-terminus. The specific and tight association suggests a potential regulatory role of NHE-RF in CFTR function (Wang et al., 1998).

CFTR gene encodes a chloride channel protein that belongs to the superfamily of ATP binding cassette (ABC) transporters. Phosphorylation by protein kinase A in the presence of ATP activates the CFTR-mediated chloride conductance of the apical membranes. A

novel hydrophilic CFTR binding protein, CAP70, has been identified, which is also concentrated on the apical surfaces. CAP70 consists of four PDZ domains, three of which are capable of binding to the CFTR C terminus. Linking at least two CFTR molecules via cytoplasmic C-terminal binding by either multivalent CAP70 or a bivalent monoclonal antibody potentates the CFTR chloride channel activity. Thus, the CFTR channel can be switched to a more active conducting state via a modification of intermolecular CFTR-CFTR contact that is enhanced by an accessory protein (Wang et al., 2000).

Chloride and bicarbonate secretion are vital functions of epithelia, as highlighted by cystic fibrosis and diseases associated with mutations in members of the SLC26 chloride-bicarbonate exchangers. Many SLC26 transporters (SLC26T) are expressed in the luminal membrane together with CFTR, which activates electrogenic chloride-bicarbonate exchange by SLC26T. However, the ability of SLC26T to regulate CFTR and the molecular mechanism of their interaction are not known. It is reported a reciprocal regulatory interaction between the SLC26T DRA, SLC26A6 and CFTR. DRA markedly activates CFTR by increasing its overall open probability sixfold. Activation of CFTR by DRA was facilitated by their PDZ ligands and binding of the SLC26T STAS domain to the CFTR R domain. Binding of the STAS and R domains is regulated by PKA-mediated phosphorylation of the R domain. Notably, CFTR and SLC26T co-localize in the luminal membrane and recombinant STAS domain activates CFTR in native duct cells. These findings provide a new understanding of epithelial chloride and bicarbonate transport and may have important implications for both cystic fibrosis and diseases associated with SLC26T (Ko et al., 2004).

The CHIP ubiquitin ligase turns molecular chaperones into protein degradation factors. CHIP associates with the chaperones Hsc70 and Hsp90 during the regulation of signaling pathways and during protein quality control, and directs chaperone-bound clients to the proteasome for degradation. Obviously, this destructive activity should be carefully controlled. The cochaperone HspBP1 was identified as an inhibitor of CHIP. HspBP1 attenuates the ubiquitin ligase activity of CHIP when complexed with Hsc70. As a consequence, HspBP1 interferes with the CHIP-induced degradation of immature forms of CFTR and stimulates CFTR maturation. These data reveal a novel regulatory mechanism that determines folding and degradation activities of molecular chaperones (Alberti et al., 2004).

Aquaporins (AQPs) can provide the molecular routes for transport of water through many epithelial thissues. In ocular epithelia, fluid transport generally involves secondary active chloride transport, which creates the osmotic gradient to drive transepithelial water transport (Schreiber et al., 2000). Several previous papers also mentioned that CFTR can interact with aquaporins and enhance osmotic water permeability when activated by cAMP (Kunzelmann, 1999; Schwiebert et al., 1999). The enhanced water permeability can be detected both in *Xenopus* oocytes and human airway epithelial cells. However the mechanisms are still not clear. Rainer Schreiber et al. reported that AQP 3 cloned from *Xenopus laevis* was regulated by CFTR (Schreiber et al., 2000). The interaction required stimulation of wild type CFTR by cAMP and an intact first nucleotide binding domain as demonstrated for other CFTR-protein interactions. Christine Pietrement et al. (Pietrement

et al., 2008) proposed that CFTR is an important regulator of AQP9 and that the interaction between AQP9, NHERF1 and CFTR may facilitate the activation of AQP9 by cAMP.

1.6 CF Therapy

More recent developments in CF therapy have concentrated on increasing supportive care include, enhanced nutritional support in the form of supplements. Recombinant enzymatic proteins given via enzyme replacement therapy are currently in Phase III development and can now be used to treat the nutrient malabsorption. Although more than 80 clinical trials are currently ongoing for CF worldwide, the majority of these trials again target either the symptomatic features of the disease rather than the disease itself. Over the years, various attempts to treat CF were met with varying degrees of success. Some newer novel attempts to treat CF include small molecules, many of which are now in development. PTC Therapeutics (with PTC 124) and Vertex Pharmaceuticals (with VX770), respectively, are two companies developing therapeutics that attempting to rescue CFTR function. PTC 124 achieves this by preventing read-through abnormal truncation of the protein. Other companies are attempting to restore ion channel balance at the cell surface. Inspire Pharmaceuticals are developing Denufosol (INS 3721, these proceedings) and is currently in Phase III while Parion Sciences have Parion 552-02 in Phase II. A role for mucolytics to thin the mucus still exists and remains an interesting and viable target being pursued (e.g. Lo-Mucin and N-acetylcysteine). Finally, development of supportive care medicines including anti-infectives and antibiotics are also being actively developed to treat the secondary complications, chronic exacerbations

in the hope that these medicines will increase the quality of life of sufferers with few hospitalizations.(Alexis et al., 2006; Brown, 2008; Dalemans et al., 1991; Meyer et al., 2000; Saeed et al., 2007; Strausbaugh and Davis, 2007)

1.6.1 Genetics Approaches to CF diagnosis

CF has been considered a candidate for gene therapy since the discovery of the CFTR gene in 1989. As an autosomal recessive disorder that primarily affects the epithelial cells in the intestine, respiratory system, pancreas, gall bladder and sweat glands (Rowntree and Harris, 2003), CF has many reasons to be chosen for gene therapy. Firstly, it is a monogenic autosomal recessive disease; secondly, small amounts of functional CFTR protein are sufficient to restore chloride transport; finally, the lung is the main affected organ and can be reached by nebulized gene therapy (Proesmans et al., 2008). As with other genetic diseases, gene therapy as a treatment modality for cystic fibrosis has attracted significant interest since the discovery of the CFTR gene.

Early studies suggested and showed that by providing a normal copy of the CFTR cDNA sequence to damaged cells they could fix the genetic defect and the correction of as few as 6-10% of epithelia might be therapeutic (Johnson et al., 1992). The fundamental principle of gene therapy for cystic fibrosis is to deliver a normal copy of the CFTR DNA to airway epithelia using a delivery vehicle (vector) by instillation or as an aerosol (Rosenfeld et al., 1992). Whatever the mechanism used, scientists recognize the respiratory epithelium as one of the most challenging targets for the practical applicant of gene therapy. Difficulties include delivery of the vector to the cell, lack of persistent gene

expression, immune responses to viral gene products, and directing viral vectors towards on the apical surface of the epithelial cells. In spite of many basic and applied experiments were completed, the goal of attaining clinically relevant and persistent correction of the cystic fibrosis defect in humans has not been achieved. There have been major obstacles which have limited the efficiency of gene transfer, gene expression and gene persistence (Grubb et al., 1994). When higher doses of viral vector were instilled to overcome this problem, there were host complications of inflammation and immune reactions. Restoration of CFTR function will be the primary consideration for curing the disease. The gain of function mutants of CFTR can compensate the loss of its function.

1.6.2 CFTR gain of function

CF-causing mutations are either severe and result in complete loss of Cl^- channel function through different molecular mechanisms, or mildly alter conductance properties of normal CFTR. So, can an effective gene therapy treatment be achieved through the CFTR gene gain of function mutants? Can the engineered CFTR gene forms with artificially increased conductance, higher open probability or favoring the physiological important anion permeation, such as HCO_3^-, be used to maximize the efficacy of CF gene therapy and eventually give us the opportunity to cure the CF disease that work in a patient- or mutant-specific manner?

We do not know the exact mechanism of CFTR mutation and the number and type of CFTR gain of function mutants in nature. However we believe that we can genetically modify the CFTR gene to get a better one. It is the so called wild type CFTR gene today

it may be not the wild type anymore tomorrow, as the evolution is never ever stopping. Despite stunning advances in genomic technologies and drug discovery, drug therapy often improves CF disease symptoms but does not cure the disease (Super, 2000). The main causes of this failure in CF cure may attributable to genetic variability, to the scarce knowledge of CF biochemistry, and to poor understanding of the mechanism of anion permeation in CFTR. Although proof-of-principle for gene transfer to CF patients has been established, efficiency is generally very low by using wild type CFTR gene (Super, 2000). Successful gene therapy and drug therapy should, hypothetically, converge at a common end point, that is to restore the normal functions of CFTR protein. Thus, we hypothesize that CFTR gene can be genetically modified to maximize its lost function. These specific new gene forms, because of their maximized functions, can efficiently compensate the functional losses in various CF patients even at under lower efficiency of gene transfer, the most common problem in all gene therapy.

Table 1.1 Classes of CFTR gain of Function

Class	Mechanism
Type I	augmenting the amplitude of channel conductance
Type II	diverting the direction of anion movement through open CFTR channel (rectification)
Type III	favouring physiological important ion permeation (channel selectivity)
Type IV	enhancing channel open probability
Type V	enhancing gating
Type VI	interacting physically and functionally up-regulating other proteins

1.7 Objectives

Despite its fundamental importance as well as relevance to the molecular mechanism underlying the disease of CF, the structural basis for CFTR is as yet unknown, and the

possible interactions among the CFTR proteins have not been demonstrated. Just as we mentioned previously, fundamental questions remain as to how many CFTR polypeptides constitute the channel, although there are controversial reports concerning whether CFTR channel is a monomer (Chen et al., 2002; Marshall et al., 1994) or a dimmer (Eskandari et al., 1998; Ramjeesingh et al., 2003; Ramjeesingh et al., 2001; Schillers et al., 2004; Zerhusen et al., 1999). Furthermore, the possible interactions among the CFTR proteins have not been demonstrated at the cell membranes if they can form a dimer or an oligomer. Here, based on single channel conductance, we tested whether CFTR is monomeric or oligomeric by analyzing the population of channel conductance from cells co-expressing two mutants with different single channel properties. We hope our findings on the CFTR monomer channel pore with dependent-gating and (or) coupled-gating in the CFTR oligomer can solve many contradictions regarding whether CFTR is a monomer or a dimer among previous reports.

Proteins have a flexible structure, and their atoms exhibit considerable fluctuations under normal operating conditions. However, apart from some enzyme reactions involving ligand binding, our understanding of the role of flexibility in ion channels remains mostly incomplete. Here we also investigated this question in CFTR, as an anion channel, which is activated by phosphorylation of the R domain via cAMP-activated protein kinase A (PKA) and ATP binding and hydrolysis at the two NBDs (Baukrowitz et al., 1994; Gadsby et al., 1998; Quinton and Reddy, 1992). We tested the interdomain interaction between R domain and MSD/NBD domains, and the interaction between MSD domains and NBD domains. We hope the interdomain cooperation between R domain and

MSD/NBD domains or the interaction between MSD domains and NBD domains can provide more information for the flexibility of CFTR which was supposed to be important in channel gating mechanism (Vergani et al., 2005b).

There is tremendous interest in gene therapy for CF after the identification of the CFTR gene. Gene therapy offers the potential of correcting the underlying cause, overwhelming traditional treatments which fall far short of a cure and are aimed primarily at improving the quality of patients. Nowadays, despite of a variety of epithelial tissues of organs affected by CF, most gene therapy studies target the airway epithelium since CF lung disease is the major cause of morbidity and mortality. The fundamental principle of these gene therapies is to deliver a normal copy of the CFTR DNA to airway epithelia using a delivery vehicle by instillation or as an aerosol. Give the assumption that CFTR gene can be genetically modified to maximize its lost function; we constructed some CFTR genes to achieve CFTR gain of function mutants which can compensate the losses of CFTR Cl^- channel function and hence be potentially useful to the gene therapy.

Previous work showed that some CFTR mutations can be used to maximize the efficacy of CF gene therapy by increasing single channel conductance (T338A), raising open probability (K1250A), rectifying Cl^- currents (S341A, R334 mutants), or favoring physiological important anion permeation, such as HCO_3^- . Based on these gains, we constructed some CFTR gene forms. We hope these artificial CFTR gene forms will solve the problem of efficacy in gene therapy and may eventually give us the opportunity to cure the CF disease that work in a patient- or mutant-specific manner. This is a

potential new line of treatment that offers renewed hope to cystic fibrosis patients suffer throughout the world.

2 Materials and Methods

2.1 Site-Directed Mutagenesis

2.1.1 Bacterial Strain and Culture Media

Escherichia coli DH5α was purchased from Invitrogen (Carlsbad, CA, USA). Kanamycin sulphate was purchased from US Biological (MA, USA). 100 mg of kanamycin in 10 ml of Milli-Q water was dissolved, filter-sterilized and stored at -20 ℃. 3 ml per 1 L medium was added. Luria-Bertani (LB) medium was prepared by dissolving 10 g bacto-tryptone, 5 g bacto-yeast extract and 5 g NaCl in 1000 ml ddH_2O. The medium was adjusted to pH 7.0 with 1N NaOH and autoclave at 121 ℃ for 20 mins. For preparing LB agar plates, 2% agar was added in the LB medium and autoclaved. Plates were poured after the LB agar cooled to about 50-60 ℃. After sterilization, antibiotics can be added aseptically to the medium if necessary. SOC medium was prepared by dissolving 20 g bacto-tryptone, 5 g bacto-yeast extract, 0.584 g NaCl, 0.186 g KCl, 2.033g $MgCl_2$, 2.468 g $MgSO_4$ and 3.604 g glucose in 1000 ml ddH_2O. 10% glycerol was prepared by dissolving 100 ml of glycerol in 1000 ml ddH_2O. All the media and solutions should be sterilized by autoclave at 121 ℃ for 20 mins.

2.1.2 Plasmids and Subcloning

CFTR in the pNUT vector was kindly provided by Dr Lee Chee Tsui, Hospital for Sick Children, Toronto, Canada. To visualize cells transiently transfected with CFTR, the CFTR cDNA was subcloned from the pNUT vector into the bicistronic pIRES2-EGFP

vector (Figure 2.1, Clontech, USA). pIRES2-EGFP was first digested with *Eco*R I and *Bam*H I at 37 ^{o}C for 2 hrs. The 5300 bp fragment was purified through gel extraction and used as backbone. The targeting CFTR cDNA fragment (4700 bp) from pNUT-CFTR was also digested with *Eco*R I and *Bam*H I. The stoichiometry of targeting fragment to backbone was 3:1 in 20 μl ligation reactions with 1 μl T_4 DNA ligase (Roche). The reactions were kept at 16 ^{o}C overnight and then mixed with 100 μl DH5α competent cells. The mixture was kept at 0 ^{o}C for 30 min, followed by heat shock at 42 ^{o}C for 2 min, then incubated at 0 ^{o}C for 5 min; cells were recovered by adding 880 μl LB media and shaking at 37 ^{o}C, 230 rpm for 40 min. After incubation, bacteria cells were centrifugated at 2000xg for 10 min. Supernatant was discarded and cell pellet was resuspended with 100 μl fresh LB media and plated onto LB agar plates with 30 μg/ml kanamycin. LB agar plate was incubated at 37 ^{o}C overnight. Isolated colonies were inoculated into LB media with 30 μg/ml kanamycin. Cultures were incubated at 37 ^{o}C, shaking 250-300 rpm overnight. The plasmid was purified by mini-prep kit (Qiagen) and analyzed by digestion and sequencing. The product plasmid was named as pIRES2-EGFP-wt-CFTR.

2.1.3 Site-Directed Mutagenesis

To construct different site-specific CFTR mutants, we designed the mutagenesis primers based on the transcription codes of amino acids. Site-directed Mutagenesis of CFTR was then carried out within the pIRES2-EGFP vector using the QuickChange XL Site-Directed Mutagenesis Kit (Stratagene, USA) as previously described (Gong and Linsdell, 2003a, b, c, 2004; Linsdell and Gong, 2002). Briefly, the thermal cycling mixture contained a final concentration of 100-200 ng pIRES2-EGFP-CFTR plasmid DNA, 1.5 x

Pfu reaction buffer, 250 ng of each of two synthesized complementary oligonucleotide primers which contain the designed mutation, 500 μM each of dNTPs and 5 U *Pfu* Turbo DNA polymerase. Temperature cycling was performed using an Eppendorf Master Cycler (Eppendorf, Singapore), with a short (30 s) denaturing step at 95 ℃ followed by 20 cycles of denaturation (95 ℃ for 30 s), annealing (55 -60 ℃ for 60 s) and extension (68 ℃ for 20 min). Following cycling, DNA was treated with *Dpn*I for 2 h at 37 ℃ to digest template DNA, transformed into competent *Escherichia coli* DH5α cells and grown overnight on LB agar plates containing 30 μg ml^{-1} kanamycin. Five to ten separate colonies were selected and expanded, and plasmid DNA was isolated for confirmation of the desired mutation by DNA sequencing (Research Biolab Pte. Ltd, Singapore).

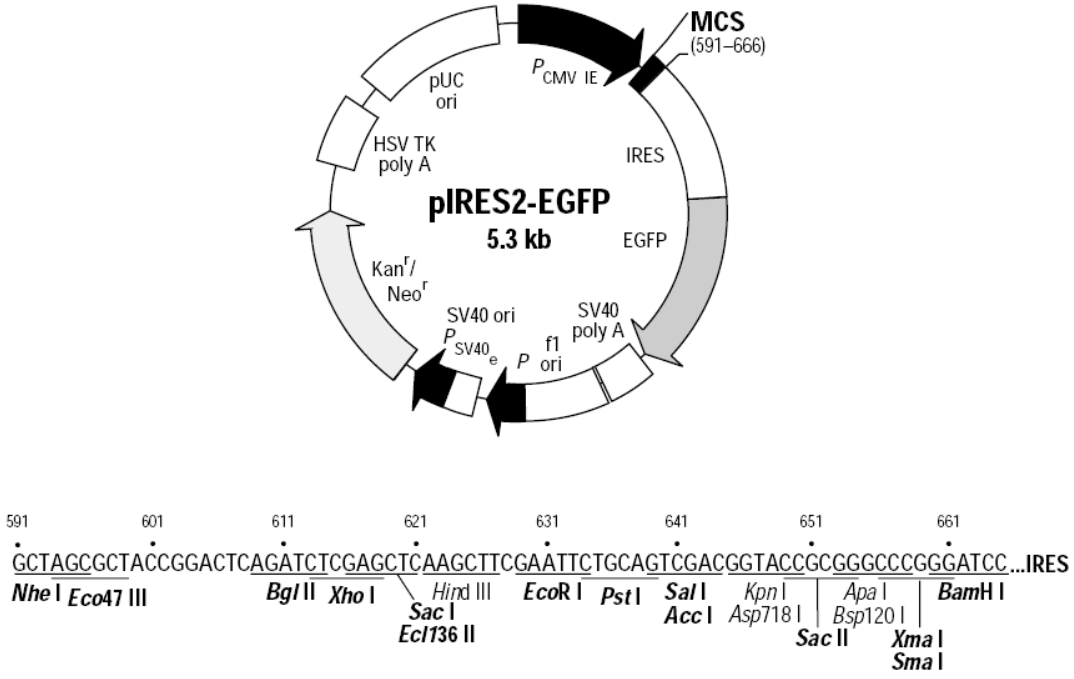

Fig. 2.1 Restriction Map and Multiple Cloning Site (MCS) of pIRES2-EGFP Vector

Unique restriction sites are in bold.

2.1.4 Preparation of DH5α Competent Cells

1 µl or 10 µl loop was used; a little of the bacteria stock stored at -80 ℃ was picked up and inoculated 5ml LB (no antibiotics). The bacteria were incubated at 37 ℃ with shaking, overnight. Then 5ml overnight culture was transferred into 200 ml LB (no antibiotics) in a 500 ml flask. The flash was incubate at 37 ℃, 250 rpm, for approximately 2.5 hrs until OD_{600} = 0.5 (±0.05). The culture was spined at 6000 rpm, at 4 ℃, for 10 min. Cells were resuspended in 100 ml of 0.1 M $MgCl_2$, and then were vortexed to resuspend on ice for 5 min. Then the culture was spined at 6000 rpm, 4 ℃, for 10 min. Cells were resuspended in 20 ml of 0.1 M $CaCl_2$, the medium were pipette up and down to resuspend. The culture was incubated at 4 ℃ overnight. After this step, cells are fragile, be gentle during further handling. The culture was spined at 4000rpm at 4 ℃ for 10 min. Cells were resuspended in 10ml of 86% $CaCl_2$ (w/v, 0.1 M), 14% glycerol (w/v). This step should be very gentle. A serological pipette should be carefully used to gently pipette up and down until the pellet is completely homogenized. This resuspension should be done on ice as much as possible. The cells were aliquoted into 0.6 ml eppendorf tubes, 100 µl per tube. Store at -80 ℃.

2.1.5 Transformation by Electroporation

Tthe electroporation apparatus was set to 2500 V. 20 µl of fresh or thawed untransformed competent *E. coli* cells were saved as control. 1 ml of SOC medium was added in 15 ml centrifuge tube and incubated at 37 ℃ for 1hour with shaking at 250 rpm. 1 µl of plasmid DNA (about 5 pg to 0.5 µg) was added into the microcentrifuge tube containing fresh or

thawed competent cells (on ice). Mixed well. The mixture was transferred into an electroporation cuvette that has been chilled for 5 min on ice. The cuvette was shaked gently to settle the cells to the bottom and the ice was wiped from the cuvette with Kimwipe tissue. The cuvette was placed into the sample chamber immediately then closed the chamber. The "Pulse" key was pressed twice. After the beep signal, the cuvette was removed. Immediately 1 ml of SOC medium was added for cell recovery. The misture was mixed well and transferred to a 15 ml centrifuge tube. 100 µl original was spread in 30×, 900× and 2700× diluted cultures onto labelled LB plates containing 30 µg ml^{-1} kanamycin. Incubated overnight at 37 ℃. 3 single colonies of *E. coli* cells were selected and each one of them was aseptically inoculated into 5 ml of LB medium containing kanamycin in 50 ml centrifuge tubes. Incubated at 37℃ with shaking at 250 rpm for 18 to 24 hrs until the cell density reaches an OD_{600} of 2 to 3. Two 100 µl aliquots of transformed culture were aseptically transfered in microcentrifuge tubes. 100 µl of 100% glycerol was added into each tube and mixed well. The transformed cells can be kept at -80 ℃ for future use. The rest of the culture can be used for DNA extraction by Mini-prep (Invitrogen) or Maxi-prep kits (Qiagen). The concentration of extracted DNA was determined by spectrophotometer.

2.2 Cell Culture and Transfection

Experiments were carried out on Chinese hamster ovary (CHO) and baby hamster kidney (BHK) cells from American Tissue Culture Collection (ATCC), transiently transfected with wild type or mutated human CFTR, prepared as described previously (Gong et al., 2002a; Gong et al., 2002b; Gong and Linsdell, 2003a, b, c, 2004; Gong et al., 2002c).

BHK cells were grown at 37℃ in 5% CO_2 in phenol red Dulbecco's Modified Eagle Medium supplemented with 5% fetal bovine serum, 100 Uml^{-1} penicillin-streptomycin, and 0.25 μg ml^{-1} fungizone (all from Life Technologies, USA). CHO cells were routinely maintained in phenol red Minimum Essential Medium Alpha Modification (Life Technologies) supplemented with 8% FCS, 100 Uml^{-1} penicillin-streptomycin and 0.25 μg ml^{-1} fungizone. For patch clamp recording, cells were seeded onto 22 mm glass coverslips and transfected with the pIRES2-EGFP vector containing wild type or mutated CFTR cDNA. Briefly, plasmid DNA was pre-incubated with Lipofectamine 2000 reagent (Invitrogen) or Superfect reagents (Qiagen) for 15 min. Complexed DNA was then diluted in supplement-free medium to a final concentration of 0.5 μg ml^{-1} and added to the cell culture dishes. After 3-6 hours at 37 ℃ and 5% CO_2, the medium was completely replaced with growth medium. Transiently transfected CHO or BHK cells could be identified by fluorescence microscopy within 24 hours and used for patch clamp recording 1 to 3 days after transfection.

2.3 Patch Clamp Recording

Electrophysiological data were recorded from excised, inside-out patches of membrane from the transfected CHO or BHK cells using the patch clamp technique (Gong et al., 2002a; Gong et al., 2002b; Gong and Linsdell, 2003a, b, c, 2004; Gong et al., 2002c). Briefly, CFTR channels were activated after patch excision by exposure to 50 nM protein kinase A catalytic subunit (PKA) plus 1 mM MgATP. For single channel recording, the extracellular (pipette) solution contained: 150 mM Na gluconate, 10 mM N-tris[hydroxymethyl] methyl-2-aminoethanesulfonate (TES), 2 mM $MgCl_2$. Intracellular

solution contained: 150 mM NaCl, 10 mM N-tris[hydroxymethyl] methyl-2-aminoethanesulfonate (TES), 2 mM $MgCl_2$. For macroscopic current-voltage relationship recording, symmetric concentration of chloride was added at both sides of the excised cell membrane. To estimate anion permeability, NaCl in the extracellular solution (pipette) was replaced by 150 mM NaX, where X^- represents one of the monovalent anions we used other than Cl^- such as 150 mM NaBr or 150 mM NaSCN. For the iodide permeability experiment, the intracellular (bath) solution containing 150 mM NaCl was replaced by 150 mM NaI to avoid electrode oxidation in pipette. Dicyanoaurate (Stock solution = 200 mM, used final concentrations were indicated in the results) was used as probe to characterize the physical properties of the CFTR channel pore (Linsdell and Gong, 2002). All of the solutions were adjusted to pH 7.4 with NaOH or HCl and filtered with 0.22 um syringe filter (Life Technologies).

Given voltages were corrected for liquid junction potentials calculated using Clampex 9.2 software (Axon Instruments, USA). Pipette resistances were 6-10 MΩ for single channel recordings and around 2 MΩ for macroscopic excised patches. Currents were filtered at 50 Hz for single channel recording or 1 kHz for the macroscopic inside-out recording using an 8-pole Bessel filter (Frequency Devices, USA), amplified using an Axopatch 200B amplifier (Axon Instruments), digitized at 250 Hz for single channel recording or 5 kHz for the macroscopic inside-out recording using a DigiData 1322A interface and analyzed using Clampfit 9.2 (Axon Instruments). Macroscopic current-voltage (*I-V*) relationships were constructed using depolarizing voltage ramp protocols as described previously (Gong et al., 2002a; Gong and Linsdell, 2003a; Gong et al., 2002c).

Macroscopic current were elicited with voltage ramp protocol from -100 mV to 60 mV within 500 ms. Current amplitude was at the beginning (20 ms) and end (480 ms). The 20 ms-time point was selected to ensure that the cell membrane capacitive current did not contribute to the current measured and was used for calculating the inhibition ratio of $Au(CN)_2^-$ blockade and the rectification ratio. Currents in the absence of PKA has been subtracted so that the data shown are only of currents through PKA-activated CFTR channels.

2.4 Data Analysis

Rectification of the I-V relationship was quantified as the rectification ratio, the slope conductance at -50 mV as a fraction of that at +50 mV. The macroscopic current reversal potential (E_{Rev}) was estimated by reading the zero current potential of the leak-subtracted I-V relationship. Under strictly biionic conditions and assuming zero cation permeability, with monovalent anions A in the intracellular solution and B in the extracellular solution, the relative permeability of these two anions was given by Goldman-Hodgkin-Katz voltage equation as described in literature review:

$$P_A/P_B = \exp (E_{Rev} F/RT) \quad (1)$$

Where E_{Rev} is the estimated current reversal potential, F is the Faraday constant ($9.648*10^4$ C/mol), R is the Gas constant (8.314 J/K·mol), and T is the absolute temperature in Kelvin (Sheppard et al., 2004).

The dissociation constant of the blocker (K_d) was calculated by the Woodhull model of voltage-dependent block (Gong et al., 2002b) using SigmaPlot 9.0:

$$I/I_0 = K_d(V) / \{Kd(V) + [B]\} \quad (2)$$

$$K_d(V) = K_d(0) \exp(-z \delta VF/RT) \quad (3)$$

Where I/I_0 is the fractional of the control current remaining following addition of blocker, [B] is the blocker concentration (um), $K_d(V)$ is the voltage dependent dissociation constant, $K_d(0)$ is the dissociation constant of the blocker at zero membrane potential, z is the valence of the blocker (a value of -1 is assumed for dicyanoaurate), V is the membrane potential, δ is the fraction of the transmembrane electric field transversed by blockers in reaching their binding site within the pore from the intracellular solution, and F, R and T have their normal thermodynamic meanings (Zhou et al., 2002).

Dwell time is the period during which a dynamic process remains halted in order that another process may occur. Here we analyzed histograms of closed times to estimate the open and close state of wild type CFTR and different CFTR mutants. Dwell time distributions were fit by a single exponential curve:

$$F(t) = \sum_{i=1}^{n} A_i e^{-t/\tau i} + C \quad (4)$$

All the experiments were performed at room temperature, 20-25 ˚C. Mean values were given as mean ± S.E. Statistical comparisons between mutants were carried out using Student's two-tailed *t*-test, with $P < 0.05$ being considered statistically significant. Unless stated otherwise, all chemicals were from Sigma-Aldrich, USA.

3 Stoichiometry and Novel Gating Mechanisms within the CFTR Channel Complexes

3.1 Introduction

Our approach to study CFTR stoichiometry is based on single channel conductance. Because most oligomeric pore-forming proteins organize their subunits around the pore (Liu et al., 1996), an oligomeric channel comprised of different subunits each with a different channel conductance should usually exhibit a hybrid conductance that is intermediate to those of the two constituents. In contrast, two co-existing monomers should simply reveal two discrete conductance populations. Thus, we tested whether CFTR is monomeric or oligomeric by analyzing the population of channel conductance from cells co-expressing two mutants with different single channel properties. We have previously shown that the sixth transmembrane helix of CFTR has a profound influence on chloride conductance (Gong and Linsdell, 2003a; Linsdell, 2005b, 2006; Linsdell et al., 2000; Linsdell and Gong, 2002). For example, mutant R334K dramatically decreases chloride conductance while the mutation of T338A enhances chloride conduction (Gong and Linsdell, 2004; Linsdell, 2006). Here, we created five mutations (two single mutations-R334K, T338A; three double mutations-R334K/T338A, T338A/T339A, T338A/S341A) within the proposed channel pore as they significantly affect the CFTR channel conductance and one mutation in NBD domain which affect the channel gating (K1250A). One complication in using single channel conductance to characterize the stoichiometry of CFTR is that wild type CFTR itself has a very small conductance at

about 6-8 pS. To facilitate detection of the possible hybridizing channels, we paired mutants that exhibit distinct channel conductances and used a chloride concentration gradient. To maximize channel kinetics, all recordings were made in presence of 2 mM MgATP and 50 nM PKA.

3.2 Single Channel Conductance of Wild Type CFTR and Mutants

Before co-expressing wild type CFTR and mutants for single channel analysis to assess CFTR stoichiometry, we used single-channel recordings in excised inside-out patches to detect the single channel conductance of wild type CFTR and mutants. Single-channel current amplitudes at -50 mV are 0.61, 0.32, 0.78, 0.60, 0.42, 1.16 and 0.4 pA for wild type CFTR, R334K, T338A, K1250A, R334K/T338A, T338A/T339A, and T338A/S341A, respectively (Fig. 3.1 and Fig. 3.2).

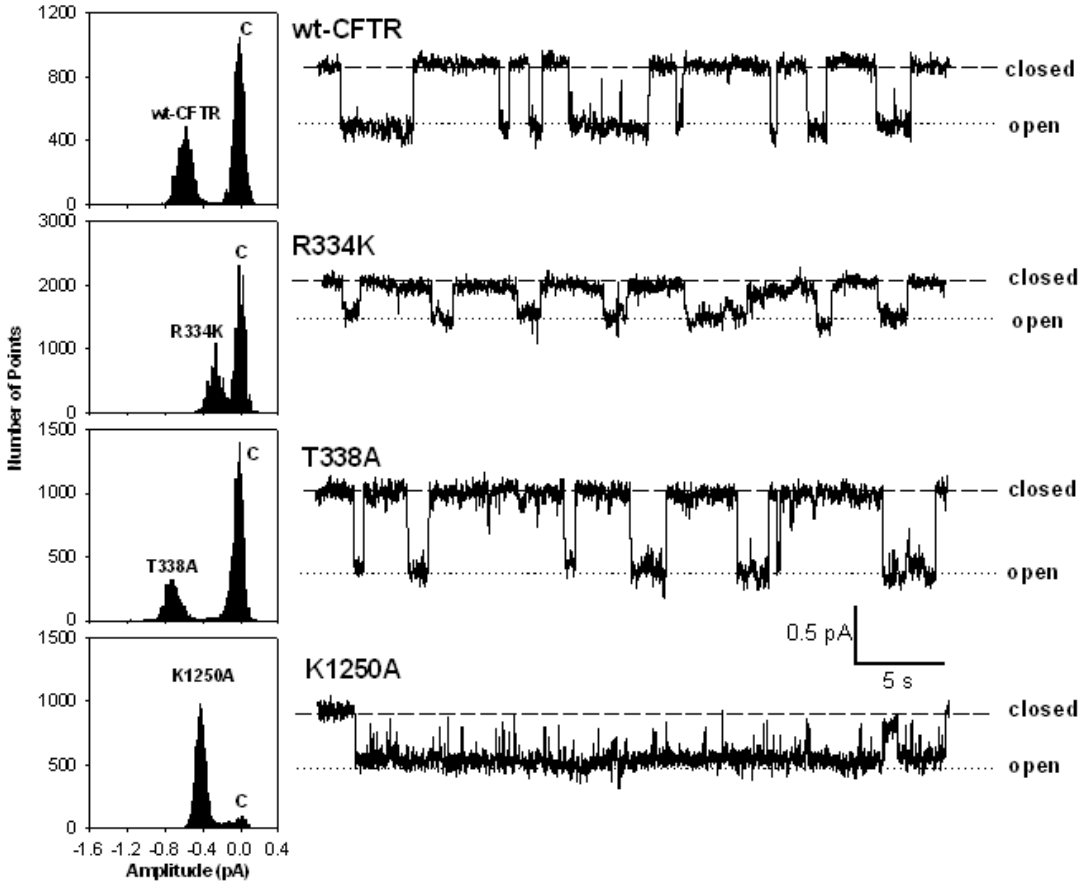

Fig. 3.1 Examples of single channel currents of wt-CFTR, single mutants R334K, T338A, K1250A

Examples of single channel currents of wt-CFTR, single mutants R334K, T338A and K1250A recorded from inside-out patches at membrane potentials of -50 mV. In each case, the open and closed states of the channel are indicated by the short dashed lines and dotted lines, respectively. The unitary current amplitudes are demonstrated from all point histograms prepared from these current traces, and as indicated. Single-channel current amplitudes at -50 mV are 0.61, 0.32, 0.78 and 0.60 pA for wt-CFTR, R334K, T338A, and K1250A, respectively.

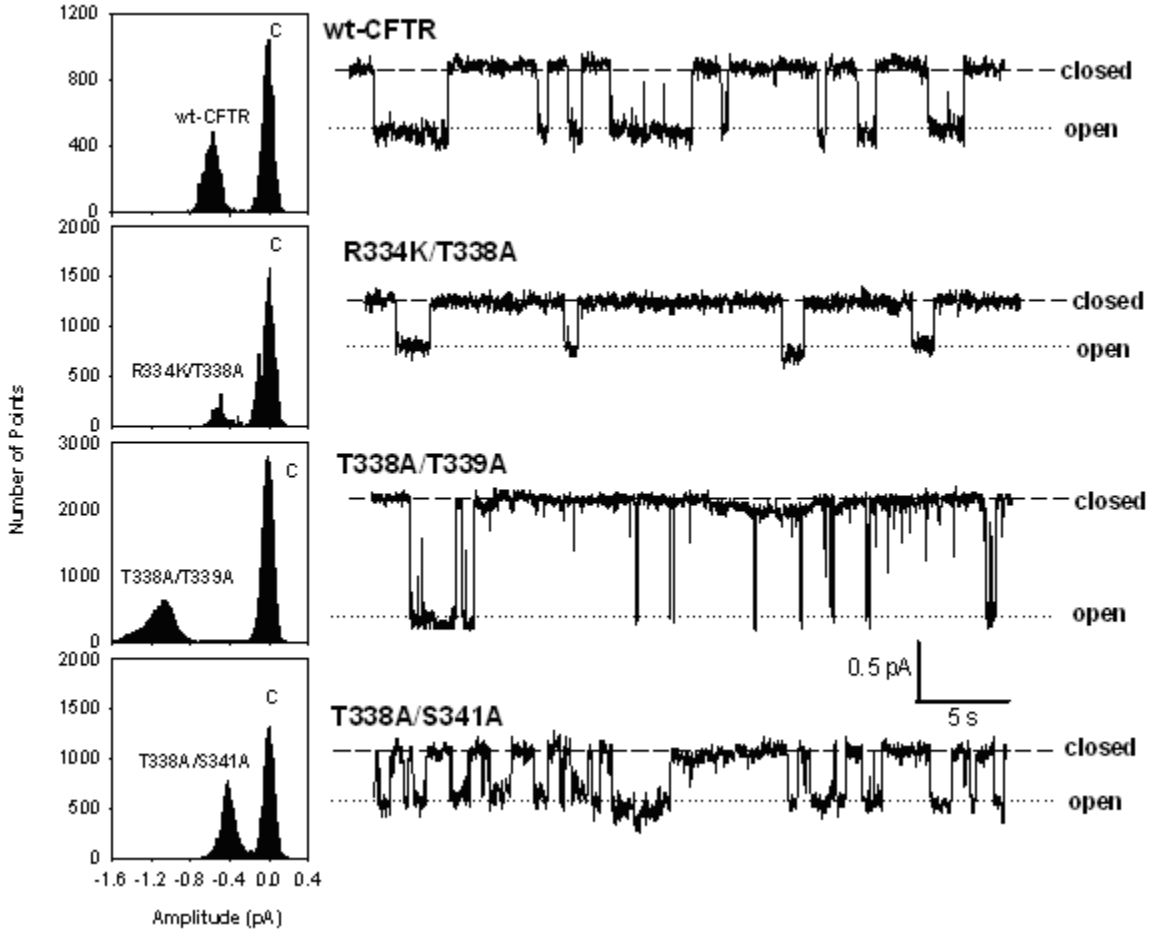

Fig. 3.2 Examples of single channel currents of wt-CFTR, double mutants R334K/T338A, T338A/T339A and T338A/S341A

Examples of single channel currents of wt-CFTR, double mutants R334K/T338A, T338A/T339A and T338A/S341A recorded from inside-out patches at membrane potentials of -50 mV. In each case, the open and closed states of the channel are indicated by the short dashed lines and dotted lines, respectively. The unitary current amplitudes are demonstrated from all point histograms prepared from these current traces, and as indicated. Single-channel current amplitudes at -50 mV are 0.61, 0.42, 1.16 and 0.4 pA for wt-CFTR R334K/T338A, T338A/T339A and T338A/S341A, respectively.

3.3 Co-expression of Low Conduction Mutants with Normal Conduction High Conduction Mutants

To assess CFTR stoichiometry, we co-expressed approximately equal amount of a low conduction mutant (R334K) with a normal conduction species (wild type CFTR), or a low conduction mutant (R334K) with a high conduction mutant (T338A) for single channel analysis. As shown in Fig. 3.3, co-transfections of R334K and wild type CFTR (or T338A) in CHO cells lead to the expressions of channels with two distinct conductances. In both pairs of combinations (R334K and wild type CFTR; R334K and T338A), the observed single channel conductances were comprised of each co-expressed conduction mutants. No hybrid channel (intermediate or any other than expected single channel conductances of the transfected mutants) was detected from the at least 10 patches which contained two channels for each co-transfection experiments.

The data from our studies of pore-forming mutants show that no hybrid channel could be detected in about more than 20 patches. However, another possibility is that CFTR proteins form a dimer by other domains such as nucleotide binding domains instead of the common configuration of pore-forming domains (equivalent to subunits of other ion channels).

Earlier work showed that two highly conserved nucleotide-binding domains (NBDs) that control channel gating through their interactions with ATP (Anderson et al., 1991). Structural studies have suggested that the two NBDs form a dimer clamping two nucletotides at the NBD:NBD interface (Hanrahan and Wioland, 2004). Mutation of

conserved Walker A motif lysine residues (K464 in NBD1 or K1250 in NBD2) inhibited ATP hydrolysis. For instance, K1250A mutation alters channel function, reducing the open probability (P_0) by slowing the opening rate while prolonging the burst duration (see supplement figure). Taking the similar assumption as the channel pore-forming mutants as above, we co-expressed a pore-forming mutant T338A (or R334K) and a mutant K1250A which affects CFTR gating into CHO cells to investigate the stoichiometry of CFTR proteins. As clearly shown in Fig. 3.3, the observed channel populations were comprised of either K1250A or T338A, no channel with a hybrid single channel property was detected from the 10 patches for the co-transfection experiments of K1250A and T338A (or R334K with K1250A).

3.4 Co-expression of Single Mutants with Double Mutants

We also created three double mutants (R334K/T338A, T338A/T339A and T338A/S341A). The single channel conductances of these three double mutants exhibited either an intermediate conductance for R334K/T338A double mutant or the synergy conductances for T338A/T339A double mutant (larger than the current amplitudes of their individual mutants) and T338A/S341A (smaller than the current amplitudes of their individual mutants). The results of double mutant experiments imply that mutations at two different sites of CFTR channel pore region will affect their single channel property. We next co-expressed a double mutant R334K/T338A (or T338A/S341A) and a single mutant R334K (or T338A) which is mutated at the corresponded site of one of the double mutation into CHO cells or co-expressed a double mutant T338A/T339A and a single

mutant at different site (R334K). Not to our surprise, Fig. 3.4 shows only the individual mutant's single channel properties, no detectable mixed channels were observed.

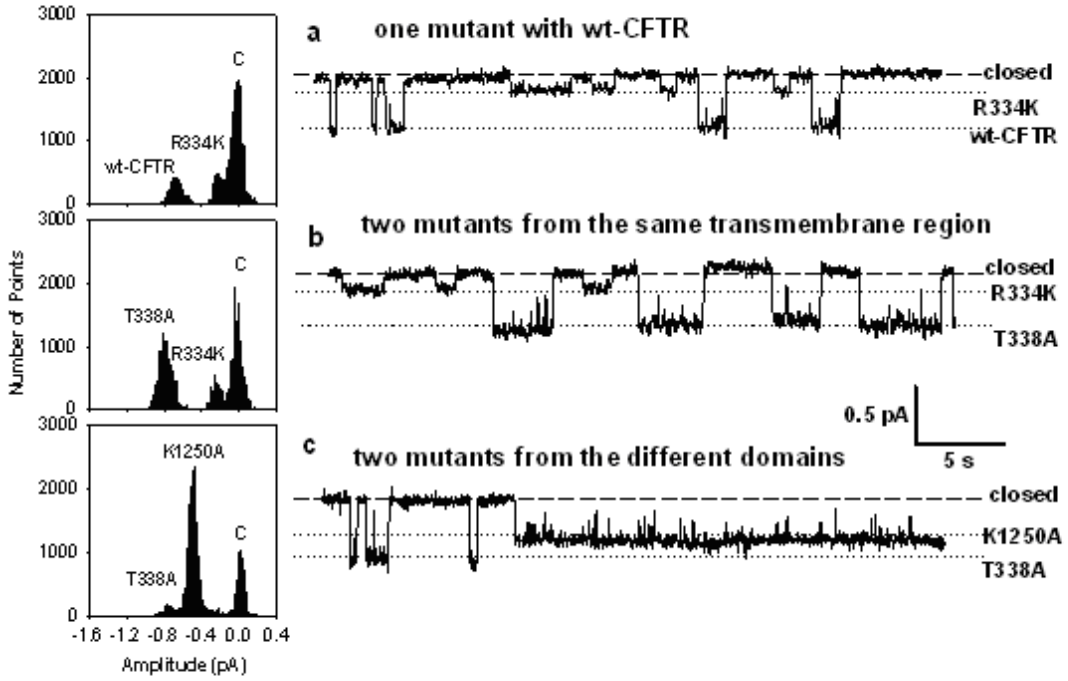

Fig. 3.3 Co-expression of wt-CFTR and single mutants

No detectable hybrid conducting channels from CHO cell membranes co-transfected with approximately equal amounts of wt-CFTR and R334K (**a**), or two distinct conduction CFTR mutants (R334K and T338A) (**b**), or one gating CFTR variant (K1250A) plus one conduction variant (T338A) (**c**). Single channel current amplitudes for all of the mutants are matched with those as shown in the figure 3.1 recorded at same conditions. In each case, the open and closed states of the channel are indicated by the short dashed lines and the dotted lines, respectively. The unitary current amplitudes are demonstrated from all point histograms (left panel) prepared from these current traces, and as indicated. The membrane potential was held at -50 mV.

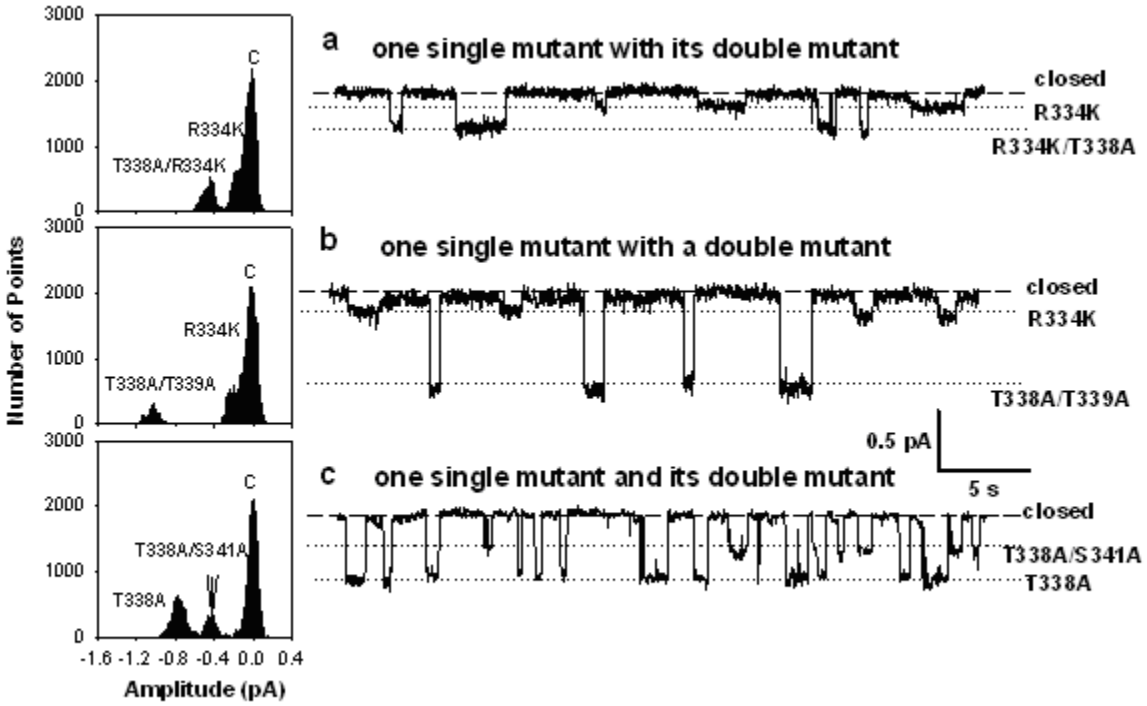

Fig. 3.4 Co-expression of single mutants and double mutants

No detectable hybrid conducting channels from CHO cell membranes co-transfected with approximately equal amounts of a single mutant (R334K) with a complementary double mutant (R334K/T338A) (**a**), or a single mutant (R334K) with a very high-conduction double mutant (T338A/T339A) (**b**), or with a double mutant (T338A/S341A) and a single mutant (T338A) (**c**). Single channel current amplitudes for all of the mutants are matched with those as shown in the figure 3.2 recorded at same conditions. In each case, the open and closed states of the channel are indicated by the short dashed lines and the dotted lines, respectively. The unitary current amplitudes are demonstrated from all point histograms (left panel) prepared from these current traces, and as indicated. The membrane potential was held at -50 mV.

3.5 Inhibitory Effects of $Au(CN)_2^-$ On Co-expressing Wild Type CFTR and T338A-CFTR mutant

Although an oligomeric channel comprised of different subunits with different channel conductance should exhibit a hybrid conductance, the conductance sometimes may not be distinguishable enough, especially when its conductance is very small, such as the CFTR chloride channels. To further confirm these mutated individual CFTR channels, our experiments were extended by testing the sensitivity of the channels to $Au(CN)_2^-$. Highly lyotropic anions (i.e. those with low free energies of hydration), such as the pseudohalide $Au(CN)_2^-$, hold great potentials as functional and structural probes of Cl^- channel pores. Our previous results show that the effects of intracellular $Au(CN)_2^-$ on wild type CFTR and T338A-CFTR macroscopic currents were very different; i.e. very strong inhibition for wild type CFTR and very weak inhibition for T338A at the negative membrane potentials (Gong et al., 2002a). Here we used the molecular probe ($Au(CN)_2^-$) of CFTR channel pore and the distinct blocking properties of wild type CFTR and T338A to detect any hybrid CFTR channels coexpressed wild type CFTR and T338A. Fig. 3.5 shows the similarity to our previous results of macroscopic patch experiments (Gong et al., 2002a), the inhibitory effects of 100 μM $Au(CN)_2^-$ were very weakened in T338A (Fig. 3.5b and 3.5d), especially at very negative membrane voltage potential (Fig. 3.5e), while the inhibitory effects of 100 μM $Au(CN)_2^-$ were very strong in wild type CFTR with less voltage dependent block (Fig. 3.5b, 3.5c and 3.5e). The blocking experiment of 100 μM $Au(CN)_2^-$ in co-expressing wild type CFTR and T338A-CFTR mutant indicates that the observed single channel populations were indeed comprised of either wild type CFTR or T338A, no hybrid channel population was observed in our 7-12 patches.

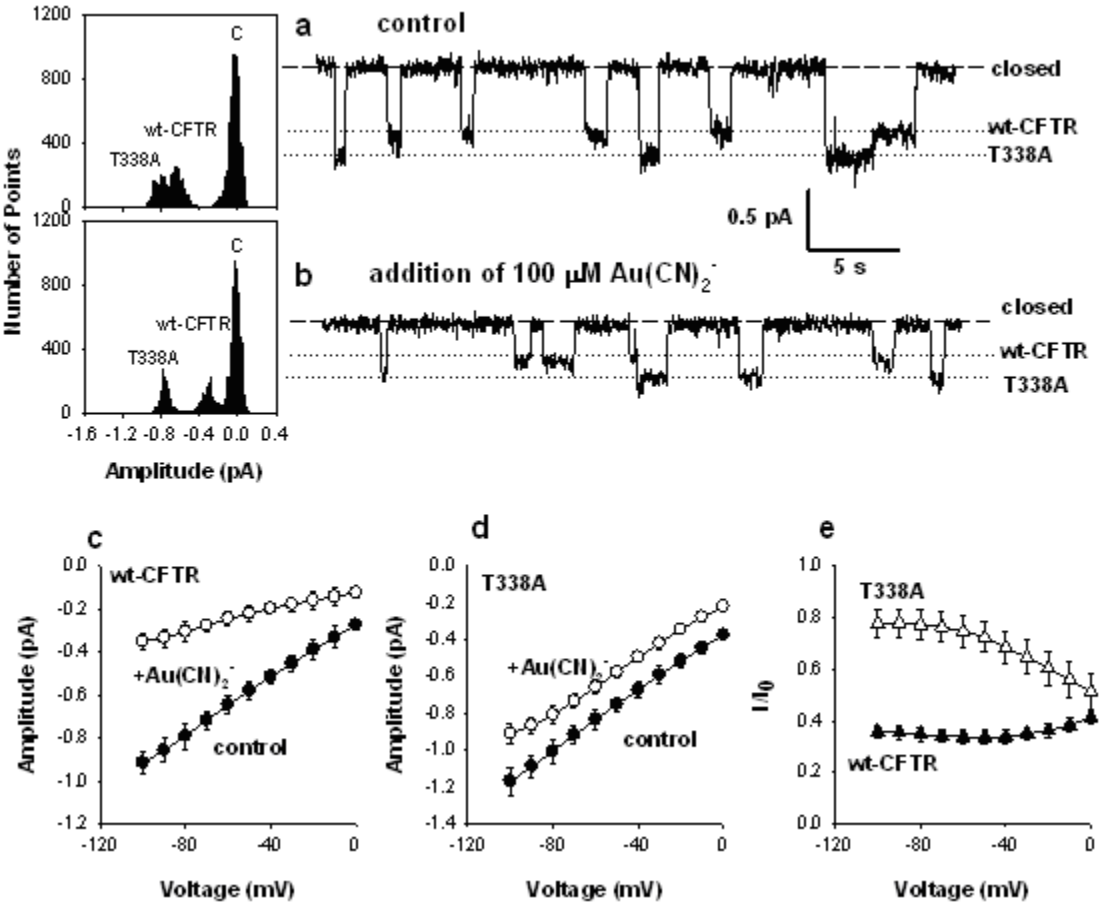

Fig. 3.5 Inhibitory Effects of $Au(CN)_2^-$ in co-expressing wt-CFTR and T338A-CFTR mutant

The CFTR channel pore sensitive probe $Au(CN)_2^-$ ions were used to confirm the single channel populations in the CHO cells cotransfected with wt-CFTR and T338A single mutant. No hybrid channel was detected by a CFTR channel pore sensitive probe $Au(CN)_2^-$ ion. Currents were recorded in the absence of $Au(CN)_2^-$ (**a**) or with $Au(CN)_2^-$ (100 μM) (**b**) present in the intracellular solution. The membrane potential was held at -50 mV. In both wt-CFTR and T338A, $Au(CN)_2^-$ causes a reduction in unitary current amplitude (**c** and **d**). However, $Au(CN)_2^-$ blocked wt-CFTR currents more severely than in the T338A mutant, as shown in panel **e**. Fractional unitary currents remaining (I/I_0) following addition of 100 μM $Au(CN)_2^-$ to the intracellular solution at -50 mV have no significances for both wt-CFTR and T338A in the co-expressed and single (either wt-CFTR or T338A) expressed CHO cells .

3.6 Single Channel of Wild Type CFTR Recorded in BHK Cells

The data from all of our single channel recordings obtained from CHO cells provides evidence that strongly suggests that CFTR monomer forms a single CFTR channel pore. Why are there several reports which indicated that CFTR could form a dimer (Eskandari et al., 1998; Marshall et al., 1994; Ramjeesingh et al., 2003; Ramjeesingh et al., 2001; Schillers et al., 2004) and what are the possible implications or interactions between CFTR dimer proteins? To answer these questions, we switched our experimental cell lines from the Chinese hamster ovary (CHO) cells to the baby hamster kidney (BHK) cells. BHK cells which expressed high level CFTR proteins are used for macroscopic current recording, while CHO cells are used for single channel recording as CFTR protein expression level is low (Gong et al., 2002a; Gong and Linsdell, 2003a, c, 2004). To facilitate CFTR protein dimerization or oligomerization and test whether wild type CFTR proteins form a dimer or a multimer, we patched the BHK cells stable transfected wild type CFTR. Single channel recordings with less than two CFTR channels were indeed not very easy to be recorded frequently. In most cases there were several channels shown in the recordings which render these single channels difficult to be analyzed. Nevertheless, we recorded more than ten patches in which only two CFTR single channels were shown in the recordings. Among these patches, based on the gating kinetics of these recordings with two CFTR channels, we can categorize three different types of single channel kinetics with two wild type CFTR channels (Fig. 3.6): 1) those in which two CFTR channels opened independently (Fig. 3.6a); 2) those with two CFTR channels opened (Fig. 3.6b) as the gating behaviour very similar to that of the two barrel pores of a ClC channel (Dutzler, 2004; Dutzler et al., 2003; Pusch, 2004); and 3) those

that one of the CFTR channel was locked in open state for several minutes (Fig. 3.6c). In ~50% patches, two channels opening and closing (gating) independently in the inside-out patch configuration were observed (Fig. 3.6a). In these experiments, one channel opened to the 0.45 pA level and a second channel was clearly apparent, opening independently of the first. A current amplitude histogram (Fig. 3.6d) revealed three discrete peaks corresponding to closed channels (0 pA) and openings to the full amplitude for one channel (0.45 pA) or for two channels (0.9 pA). We have observed that the maximal open probability (P_o) rarely exceeded 0.5 in excised inside-out patches of both CHO and BHK cells in numerous studies if two CFTR channels opened independently. However, approximately 30% patches with two CFTR channels show a pattern as Fig. 3.6b with high P_o. The mean open probability exceeded 0.5 as shown in Fig. 3.6g. We have also observed in less than 10% of our recordings shows one of the CFTR channel were locked in open state for several minutes (Fig. 3.6c) under the exactly same concentrations of MgATP, PKA and other recording conditions. However, the P_o of each individual channel was different from that of the other recordings. For example, the probabilities of the three current levels showed a multinomial distribution. These results together indicate that the two CFTR channels have equal conductance and different P_o (Fig. 3.6c) and challenge the principle of independent gating of CFTR channels.

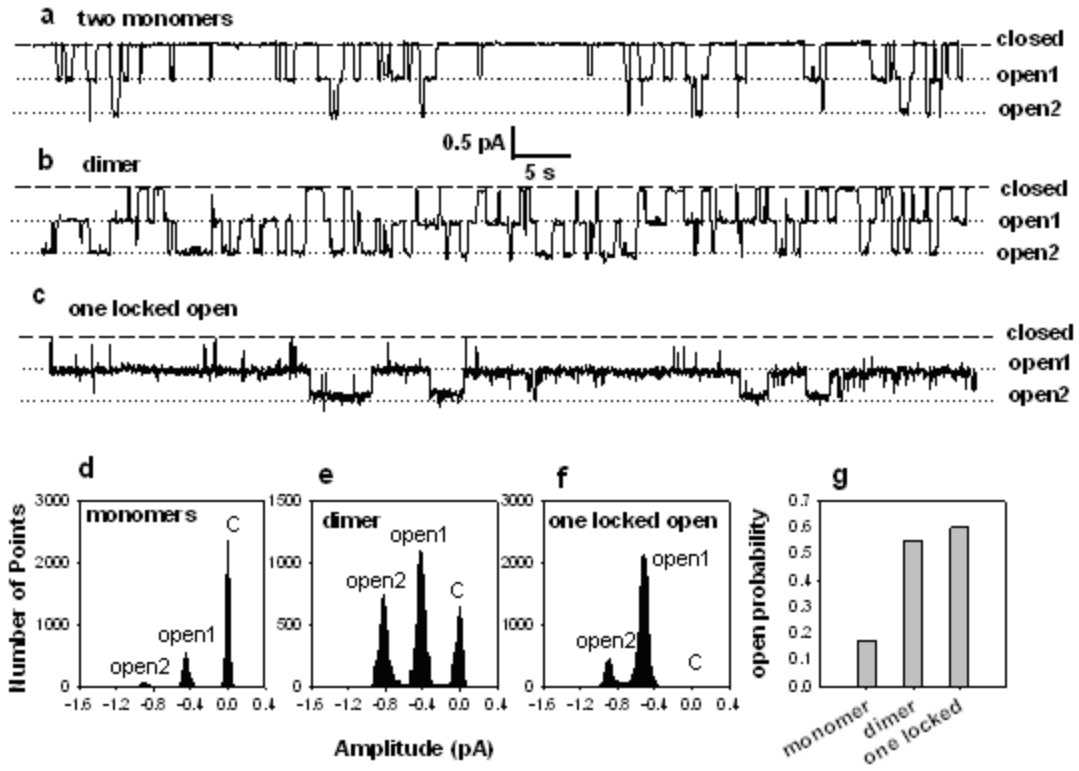

Fig. 3.6 Three different types of single channel kinetics of two CFTR channels in BHK cells

Three different types of single channel kinetics of two CFTR channels in BHK cells stable transfected with wt-CFTR, recorded from inside-out patches at membrane potentials of -50 mV under symmetrical chloride concentration (154 mM) (**a** to **c**). The open and closed states of the channel are indicated by the short dashed lines and the dotted lines, respectively. The unitary current amplitudes and abundance of events for closed and openings of the two CFTR channels are demonstrated from all point histograms prepared from these current traces, and as indicated (**d** to **f**). Based on the gating kinetics of these three recordings, we propose that the first recording was from CFTR monomers (**a** and **d**), the second one was from CFTR dimer (**b** and **e**), and the third one from CFTR trimer (**c** and **f**) in the stable transfected BHK cells. Note that a low mean open probability (P_o<0.5) of the CFTR individual channels in monomer and high mean open probability(P_o>0.5) of CFTR channels in multimer (**g**).

3.7 Gating Behaviour of Co-expressed T338A/T339A with R334K

To study the underlying molecular mechanism of the novel gating behaviour and possible CFTR interprotein interactions and maximize possibility of CFTR oligomer formation, we co-transfected BHK cells with two very distinct CFTR mutants- a double mutant (T338A/T339A) with very large single channel conductance and a single mutant (R334K) with a small conductance but still observable into BHK cells. In one of patches as shown in Fig. 3.7, we recorded a single channel trace that is very interesting to us. The histogram and single trace clearly displayed three distinct clusters of points corresponding to the double mutant T338A/T339A with the current amplitude of 1.2 pA and two new single channels with current amplitudes of 1.4 and 1.6 pA, labelled as R334K1 and R334K2, respectively. This pattern is very different from the monomer expression studies, where we observed two channels with expected channel conductance. However, closer inspection of the single channel trace as expanded in Fig. (3.7a)B to (3.7a)E and the all-point histograms reveals that these two new channels were very much likely to reflect the contributions of R334K and T338A/T339A channels open simultaneously. The 1.4 pA channel current amplitude was an addition of a single channel current of the double mutant T338A/T339A (1.2 pA) and current of the mutant R334K (0.2 pA). The 1.6 pA channel current was an addition of one T338A/T339A channel current and currents of two R334K channels.

Significantly, in certain period of recording as shown in Fig. (3.7a)B and (3.7a)C, two R334K channels were observed in the recording; channel opening to the 1.4-pA level (one R334K) and a second channel opening to 1.6 pA (two R334K channels). A current

amplitude histogram (Fig. (3.7a)B) revealed three discrete peaks corresponding to 1.2 pA (opening of only CFTR T338A/T339A mutant) and openings to 1.4 (simultaneously openings of one R334K channel and one T338A/T339A channel) and 1.6 (simultaneously openings of two R334K channels and one T338A/T339A channel). In about 20% of recording period (shown as Fig. 3.7c), channels were observed that only opened to 1.2 pA and 1.6 pA, without the openings of 1.4 pA. Current amplitude histogram (Fig. 3.7c) revealed two discrete peaks corresponding to the opened channel of T338A/T339A (1.2 pA) and openings to 1.6 pA (twice the normal current amplitude of single R334K mutant plus the current amplitude of the double mutant T338A/T339A).

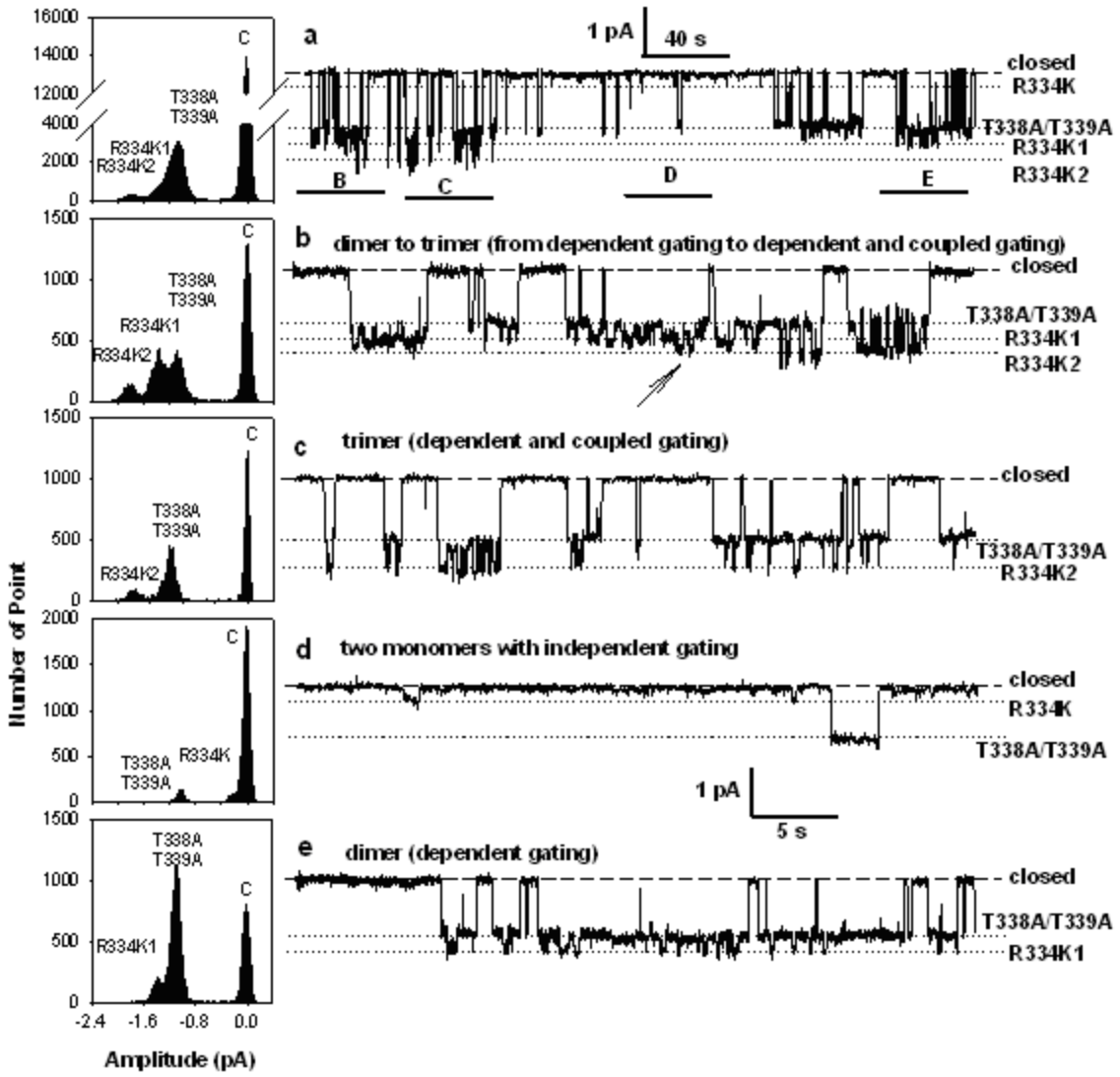

Fig. 3.7 Dynamic CFTR monomer, dimer and tritimer formation

Dynamic CFTR monomer, dimer and tritimer formation in a BHK cell cotransfected with a double mutant (T338A/T339A) and a single mutant R334K. Example trace of single channel currents of the BHK cell recorded from cell free inside-out patch at membrane potentials of -50 mV (**a**). As shown in more detail expanded sections (Panels **b**-**e**) at higher time base, individual T338A/T339A and R334K single channel currents are rarely seen from this recording (**d**), instead, R334K channels were opened when the T338A/T339A channels were activated as shown in Panel b, Panel c and Panel d. A third channel of 0.4 pA was seen in part of Panel b and Panel c, which has a double size of current amplitude of R334K single channel (coupled gating – two R334K channels gating are coupled).

4 Flexibility of the CFTR Chloride Channel Pore – CFTR Interdomain Interactions beyond the Channel Gating

4.1 Introduction

Proteins have a flexible structure, and their atoms exhibit considerable fluctuations under normal operating conditions. However, apart from some enzyme reactions involving ligand binding, our understanding of the role of flexibility in ion channels remains mostly incomplete. Here we investigate this question in CFTR that forms an anion channel. CFTR, as a chloride channel, is activated by phosphorylation of the R domain via cAMP-activated PKA and ATP binding and hydrolysis at the two NBD domains (Baukrowitz et al., 1994; Gadsby et al., 1998; Quinton and Reddy, 1992). This large and irregularly formed R domain may need a complicated intermolecular cooperation to conduct its function in delicate regulation of channel gating because of the scattered distributed phosphorylation sites in R domain which has nine dibasic (e.g., R,R/K,X,S/T) consensus sequences, five monobasic (e.g., R/K,X,S/T) sites, and numerous potential low-affinity sites for phosphorylation by PKA (Chang et al., 1993; Chappe et al., 2004; Dahan et al., 2001). Such an intermolecular cooperation can also provide more chances for NBDs dimerization which was supposed to be important in channel gating (Vergani et al., 2005b). And among these important phosphorylation sites in R domain for CFTR regulation by PKA, most are stimulatory (S660, S700, S795, S813 et al.), while S737 and S768 are inhibitory due to the possibility that individual phosphoserines have differential sensitivity to PKA (Wilkinson et al., 1997). Some R domain missense mutations that had been identified in CF patients were also functionally characterized. Interestingly, two

mutations, H620Q and A800G were reported to increase intrinsic chloride transport activities. Therefore, we created five mutants (four single mutants-H620Q, A800G, S737A, S768A; one double mutant-S737A/S768A) to gain a better insight into the structure and function of the R domain.

Opening and closing of CFTR channel pore have been linked to ATP binding and hydrolysis at two NBDs of CFTR (Carson et al., 1995; Gunderson and Kopito, 1995). Lots of evidences have demonstrated that NBDs can dimerize upon binding ATP (Hopfner et al., 2000; Smith et al., 2002) and this ATP-driven dimerization of NBDs was supposed to be involved in CFTR channel opening (Lewis et al., 2004; Vergani et al., 2005b). The region around F508 is suggested to be involved in coupling the NBD engine to conformational changes of the MSDs that open and close the CFTR channel (Dalemans et al., 1991). Vergani and his colleague demonstrated that R555 (NBD1) and T1246 (NBD2) are energetically coupled in open, channel therefore suggested that NBDs undergo dynamic reorganization during channel gating (Vergani et al., 2005b). Here we also created three mutants (one double mutant-T338A/T339A; two triple mutants-T338A/T339A/R555K, T338A/T339A/K1250A) to detect the interaction between NBDs and MSDs.

4.2 Single Channel Activity of CFTR Mutants

Single channel conductance, the flow rate of ions, is the most economical description of the behaviour of an ion channel. The Cl^- currents in the cells of the CFTR mutants in CF patients are completely lost or partially decreased. So sustaining CFTR channel

conductance is very crucial for maintaining normal airway surface liquid volume. To obtain a brief knowing about the flexibility of the CFTR chloride channel pore, that is, to see how the CFTR interdomain interactions affect the single channel conductance, here we investigated the single channel activity of these CFTR mutants. To compare these single channel conductances, a low extracellular Cl^- concentration was applied so that only inward currents due to Cl^- efflux were recorded. Expression of these mutants in Chinese hamster ovary (CHO) cells led to the appearance of PKA- and ATP-dependent Cl^- channel currents in excised membrane patches. Representative recordings of single channel currents are recorded at 0 mV and -50 mV membrane potential.

H620Q and A800G are two missense mutants that had been recognized in CF patients and these two mutants are reported to result in increased intrinsic chloride transport activities (Vankeerberghen et al., 1998). Here we measured the single channel conductance of H620Q and A800G at 0 mV and -50 mV membrane potential, respectively. Fig. 4.1 and Fig. 4.2 show the examples of single channel conductance of wild type CFTR, H620Q and A800G. As we can see from Fig. 4.1, wild type CFTR carried a conductance of 3.5 pS at 0 mV while H620Q and A800G carried 3.3 pS and 2.9 pS respectively. At -50 mV, wild type CFTR carried a conductance of 6.1 pS; for H620Q and A800G, the single channel conductance is 6.1 pS and 4.5 pS respectively. (Fig. 4.2) Single channel current amplitude histograms of wild type CFTR, H620Q and A800G at membrane potential of 0 mV and -50 mV are also shown in Fig. 4.1 and Fig. 4.2. Consistent with the results of single channel conductance recording, the histograms show that H620Q carried a normal single channel conductance almost the same as wild type CFTR while A800G drastically decreased the single channel conductance.

As for the other mutants in R domain (S737A, S768A and S737A/S768A), we also measured their single channel conductance at 0 mV and -50 mV membrane potential. (Fig. 4.3 and Fig. 4.4) Interestingly, S737A and S768A showed a normal single channel conductance almost the same as wild type CFTR at 0 mV and -50 mV. (at 0 mV, 3.5 pS for wild type CFTR and 3.8 pS, 3.7 pS for S737A and S768A respectively; at -50 mV, 6.1 pS for wild type CFTR, 6.8 pS, 6.4 pS for S737A and S768A respectively) While, S737A/S768A `showed a drastic decrease in the single channel conductance: at 0 mV 2.6 pS and at -50 mV 4.9 pS. The single channel current amplitude histograms also showed the same results. (Fig. 4.3 and Fig. 4.4)

Compared with the single channel recordings of the other three mutants T338A/T339A, T338A/T339A/R555K and T338A/T339A/K1250A (Fig. 4.5 and Fig. 4.6) suggests that T338/T339A carried a significant increased single channel conductance. This result also confirms the previous result from other researchers (Ge et al., 2004). But both the triple mutants T338A/T339A/R555K and T338A/T339A/K1250A showed a normal single channel conductance as wild type CFTR.

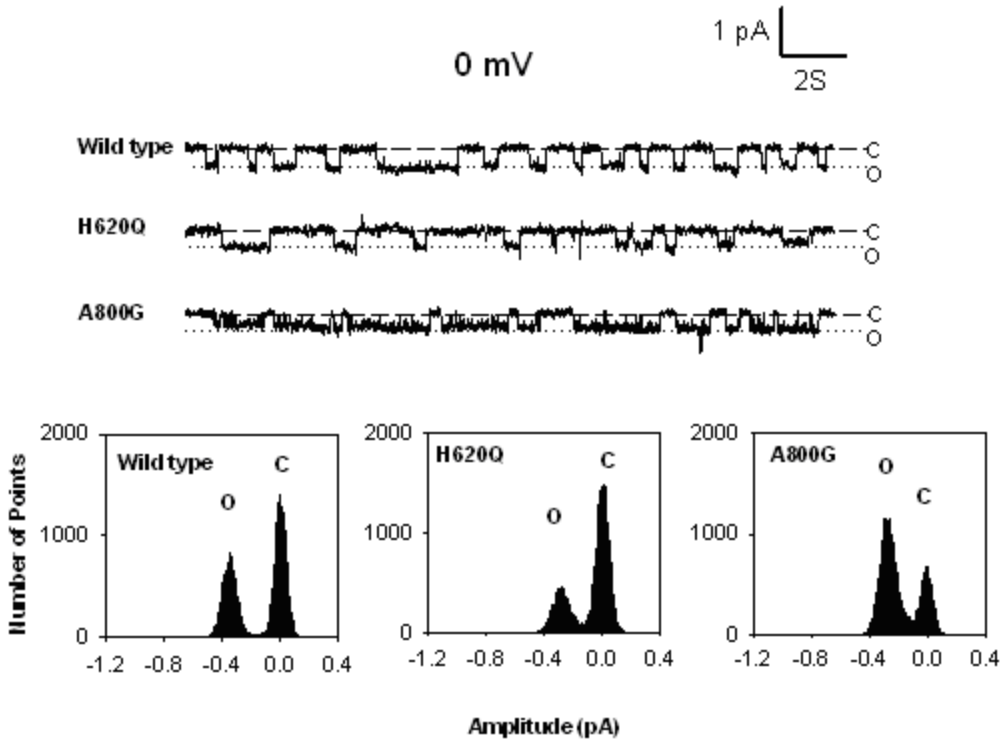

Fig. 4.1 Examples of single channel currents of wt-CFTR, single mutants H620Q, A800G

Examples of single channel currents of wt-CFTR, single mutants H620Q and A800G recorded from inside-out patches at membrane potentials of 0 mV. In each case, the open and closed states of the channel are indicated by the short dashed lines and dotted lines, respectively. The unitary current amplitudes are demonstrated from all point histograms prepared from these current traces, and as indicated. Single-channel current amplitudes at 0 mV are 0.35, 0.33 and 0.29 pA for wt-CFTR, H620Q and A800G, respectively.

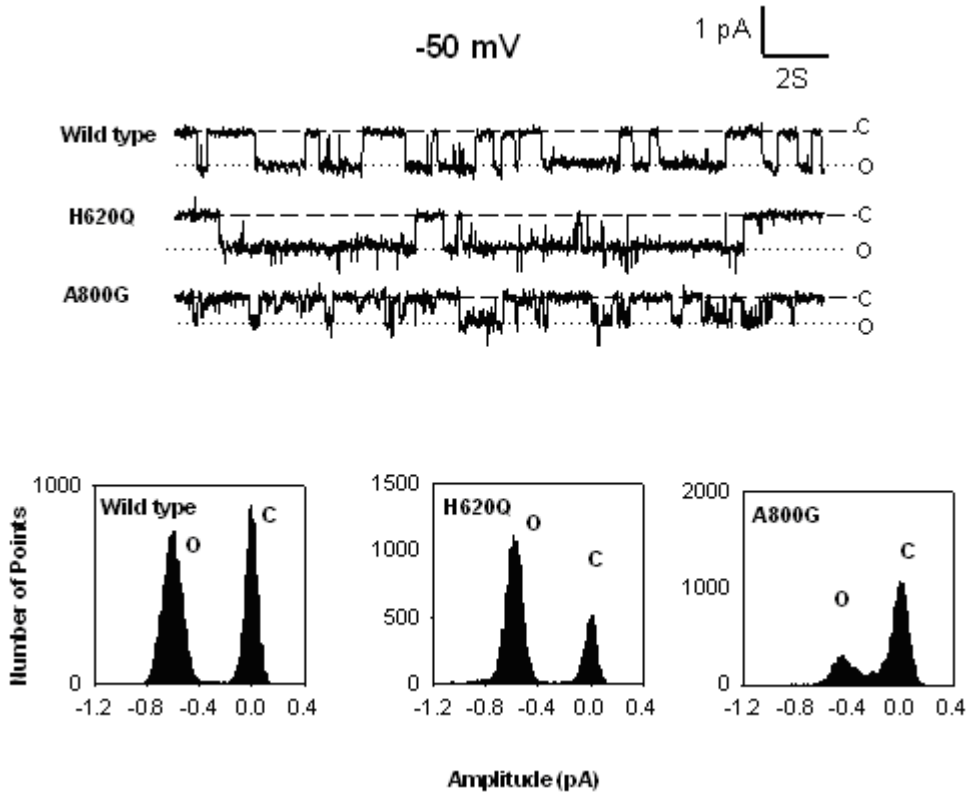

Fig. 4.2 Examples of single channel currents of wt-CFTR, single mutants H620Q, A800G

Examples of single channel currents of wt-CFTR, single mutants H620Q and A800G recorded from inside-out patches at membrane potentials of -50 mV. In each case, the open and closed states of the channel are indicated by the short dashed lines and dotted lines, respectively. The unitary current amplitudes are demonstrated from all point histograms prepared from these current traces, and as indicated. Single-channel current amplitudes at -50 mV are 0.61, 0.61 and 0.45 pA for wt-CFTR, H620Q and A800G, respectively.

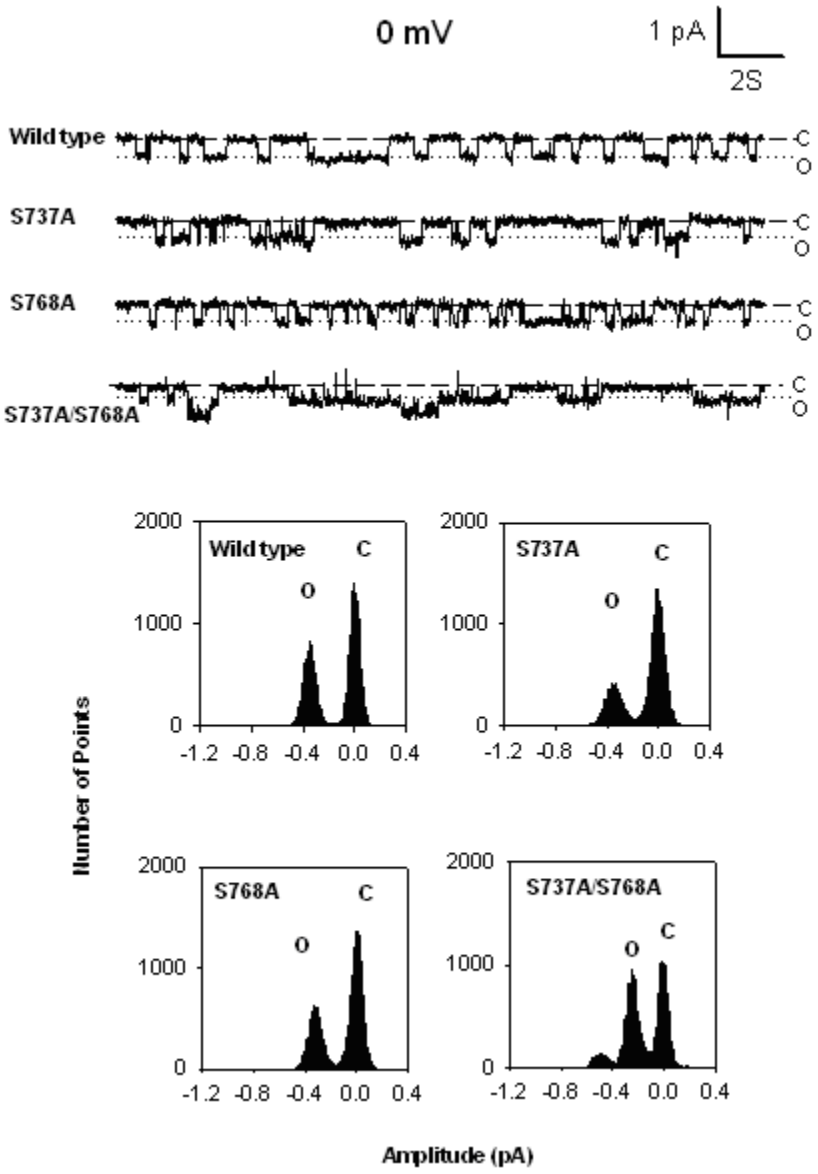

Fig. 4.3 Examples of single channel currents of wt-CFTR, mutants S737A, S768A and S737A/S768A

Examples of single channel currents of wt-CFTR, single mutants S737A and S768A, double mutant S737A/S768A recorded from inside-out patches at membrane potentials of 0 mV. In each case, the open and closed states of the channel are indicated by the short dashed lines and dotted lines, respectively. The unitary current amplitudes are demonstrated from all point histograms prepared from these current traces, and as indicated. Single-channel current amplitudes at 0 mV are 0.35, 0.38, 0.37 and 0.26 pA for wt-CFTR, S737A, S768A and S737A/S768A, respectively.

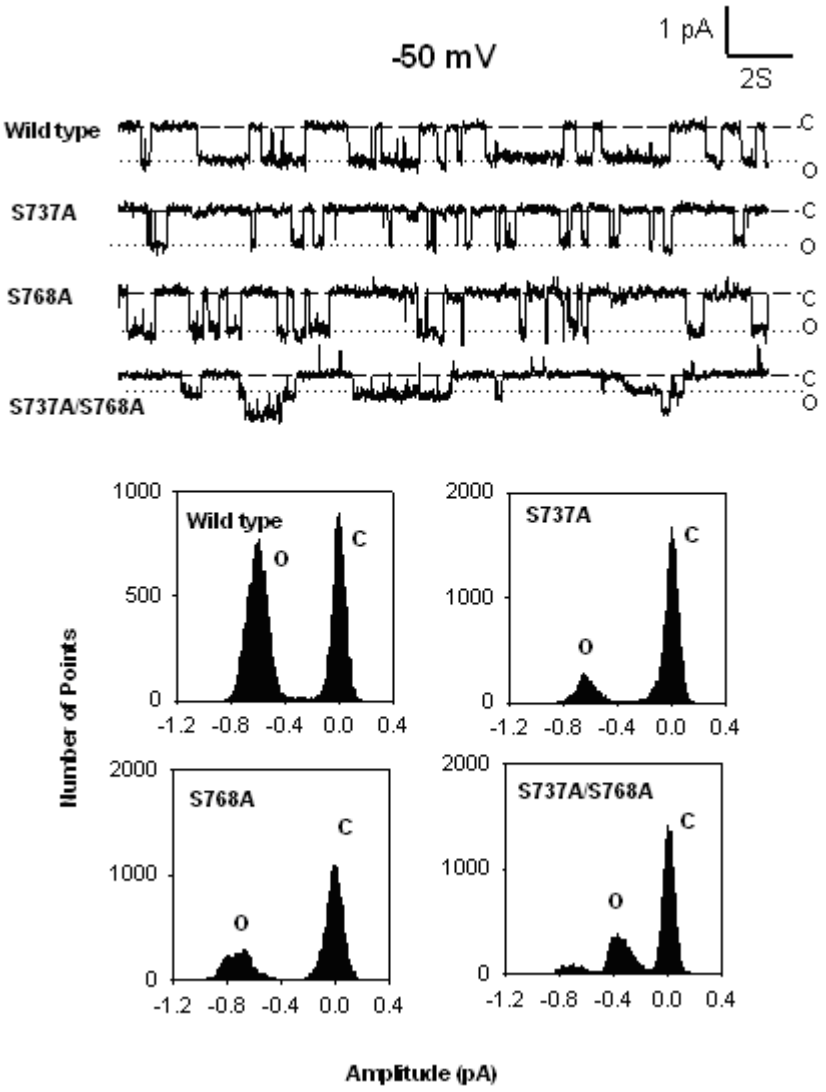

Fig. 4.4 Examples of single channel currents of wt-CFTR, mutants S737A, S768A and S737A/S768A

Examples of single channel currents of wt-CFTR, single mutants S737A and S768A, double mutant S737A/S768A recorded from inside-out patches at membrane potentials of -50 mV. In each case, the open and closed states of the channel are indicated by the short dashed lines and dotted lines, respectively. The unitary current amplitudes are demonstrated from all point histograms prepared from these current traces, and as indicated. Single-channel current amplitudes at -50 mV are 0.61, 0.68, 0.64 and 0.39 pA for wt-CFTR, S737A, S768A and S737A/S768A, respectively.

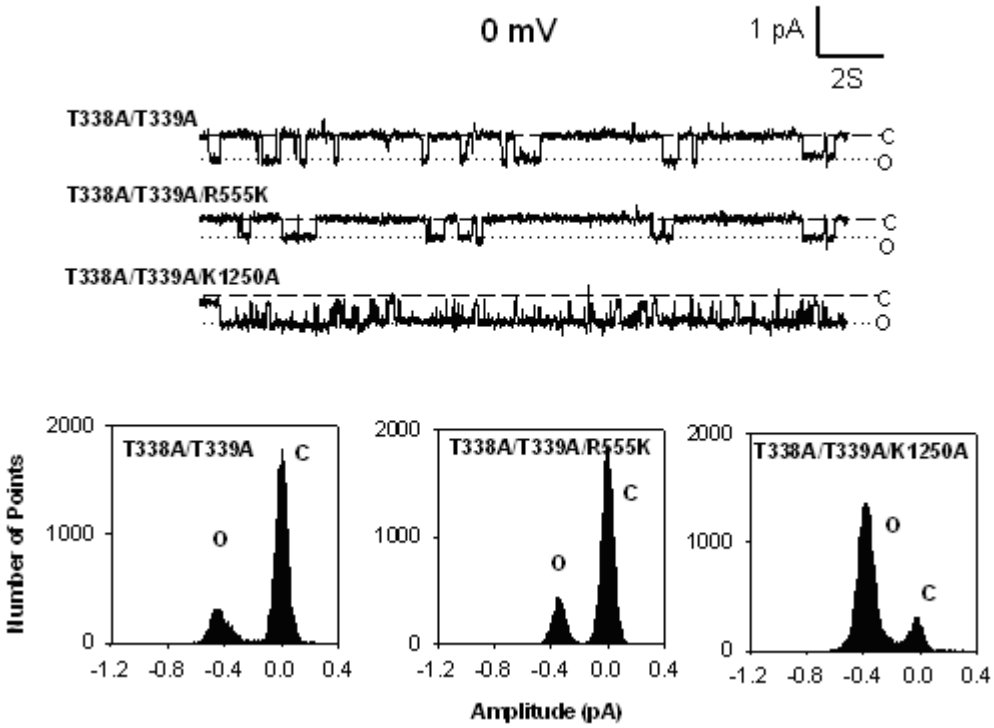

Fig. 4.5 Examples of single channel currents of double mutant T338A/T339A, triple mutants T338A/T339A/R555K, T338A/T339A/K1250A

Examples of single channel currents of double mutant T338A/T339A, triple mutants T338A/T339A/R555K, T338A/T339A/K1250A recorded from inside-out patches at membrane potentials of 0 mV. In each case, the open and closed states of the channel are indicated by the short dashed lines and dotted lines, respectively. The unitary current amplitudes are demonstrated from all point histograms prepared from these current traces, and as indicated. Single-channel current amplitudes at 0 mV are 0.49, 0.32 and 0.37 pA for T338A/T339A, T338A/T339A/R555K and T338A/T339A/K1250A, respectively.

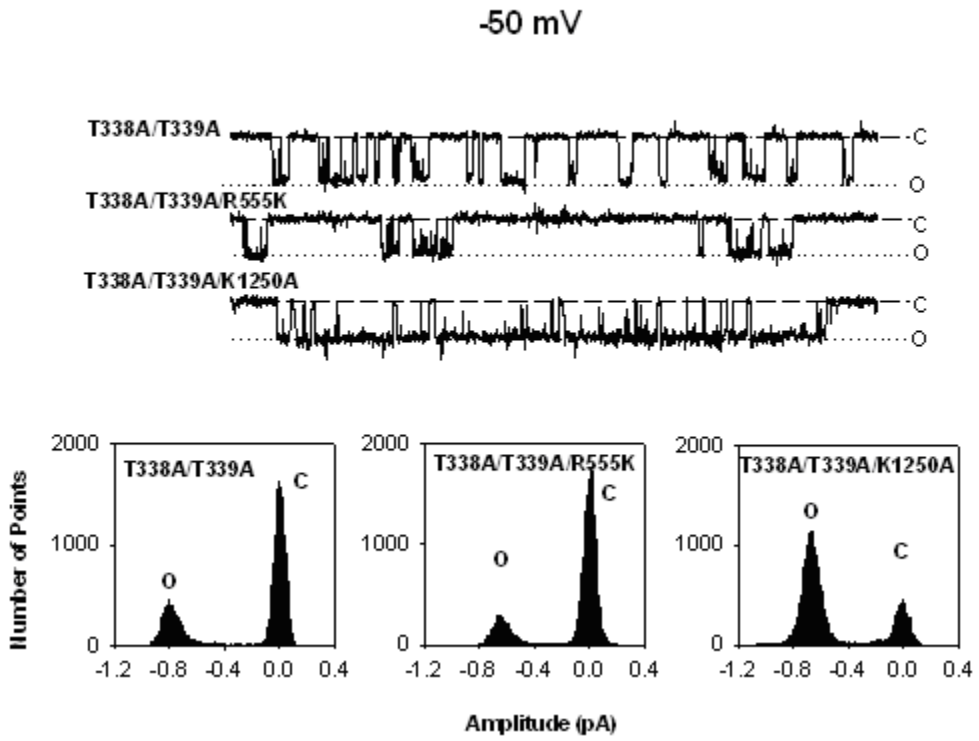

Fig. 4.6 Examples of single channel currents of double mutant T338A/T339A, triple mutants T338A/T339A/R555K, T338A/T339A/K1250A

Examples of single channel currents of double mutant T338A/T339A, triple mutants T338A/T339A/R555K, T338A/T339A/K1250A recorded from inside-out patches at membrane potentials of -50 mV. In each case, the open and closed states of the channel are indicated by the short dashed lines and dotted lines, respectively. The unitary current amplitudes are demonstrated from all point histograms prepared from these current traces, and as indicated. Single-channel current amplitudes at -50 mV are 0.89, 0.65 and 0.66 pA for T338A/T339A, T338A/T339A/R555K and T338A/T339A/K1250A, respectively.

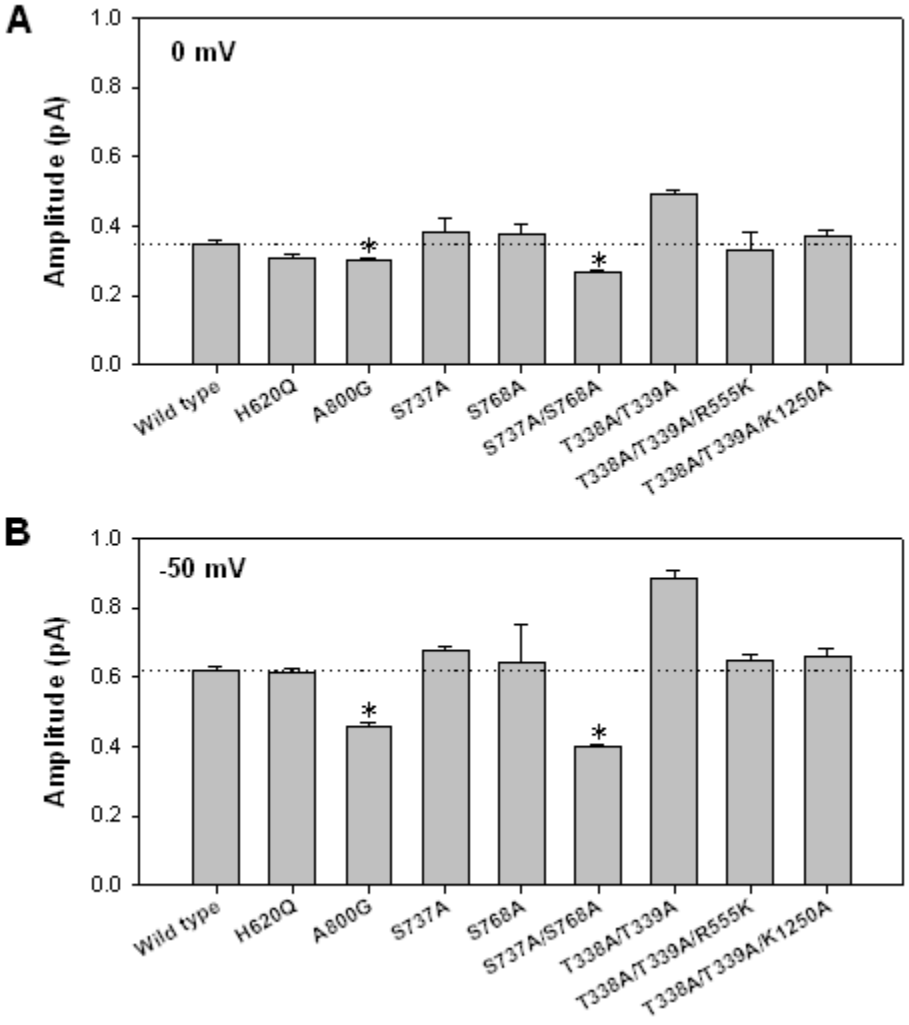

Fig. 4.7 Single channel current amplitudes of wt-CFTR and different CFTR channel variants

Single channel current amplitudes from individual patches of wt-CFTR and different CFTR channel mutants at 0 mV (A) and -50 mV (B) membrane potential were calculated and compared. *Asterisks* indicate a significant difference from wild type CFTR. Mean of data from three to ten patches.

4.3 Single Channel Kinetics of CFTR Mutants

4.3.1 Closed Dwell Time

Fig. 4.8 shows the closed time histograms of wild type CFTR, H620Q and A800G at 0 mV. The mean closed time constant τ_c of wild type CFTR, H620Q and A800G was 474.6 ms, 382.2 ms and 69.7 ms, respectively. The open states of mutant H620Q and A800G were longer than that of wild type CFTR. The same results were obtained in mutants S737A, S768A and S737A/S768A, as shown in Fig. 4.9, the mean closed time constants τ_c of S737A, S768A and S737A/S768A are 123.0 ms, 151.1 ms and 103.5 ms, respectively. And from Fig. 4.10 we can see that the double mutant T338A/T339A showed a shorter τ_c than wild type CFTR: 110.7 ms. Similar to the result of T338A/T339A, triple mutants T338A/T339A/R555K and T338A/T339A/K1250A also showed shorter τ_c than wild type CFTR. The τ_c of tripe mutants T338A/T339A/R555K and T338A/T339A/K1250A were 132.4 ms and 114.6 ms, respectively.

Fig 4.11A compared the τ_c of wild type CFTR and all the above mutants. As we can see from Fig. 4.11A, all the mutants (H620Q, A800G, S737A, S768A, S737A/S768, T338A/T339A, T338A/ T339A/R555K, T338A/T339A/K1250A) showed a shorter mean closed time than wild type CFTR. (Mean of data from 5 minute intervals and 5~10 patches.)

4.3.2 Interevent Interval

We also compared the interevent intervals of wild type CFTR and these mutants. As shown in Fig. 4.11B, the interevent interval for wild type CFTR was 1346.6 ± 397.9 ms, while the interevent interval for those other mutants were all smaller than that of wild type CFTR. Table. 4.1 shows the interevent intervals of mutants.

Table. 4.1 Interevent Intervals (ms)

	Interevent Interval (ms)
Wild type	1346.6 ± 397.9
H620Q	431.1 ± 66.1
A800G	137.4 ± 8.2
S737A	306.2 ±70.0
S768A	350.0 ±40.6
S737A/S768A	390.7 ±116.4
T338A/T339A	604.6 ±219.7
T338A/T339A/R555K	331.3 ±38.2
T.338A/T339A/K1250A	344.2 ±111.7

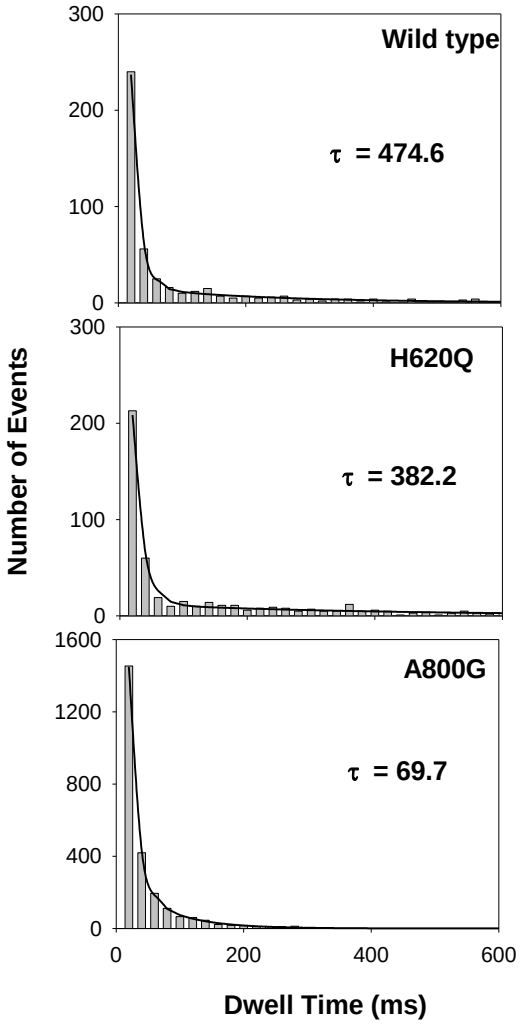

Fig. 4.8 Examples of closed time histograms obtained from single channel recordings of wt-CFTR, H620Q and A800G

Examples of closed time histograms obtained from single channel recordings of wt-CFTR, H620Q and A800G. Tracings were obtained at 0 mV membrane potential. Data are closed dwell time analysis of 1 channel. The continuous line is the fit of a one-component exponential function and the time constants (τ) are shown for each distribution.

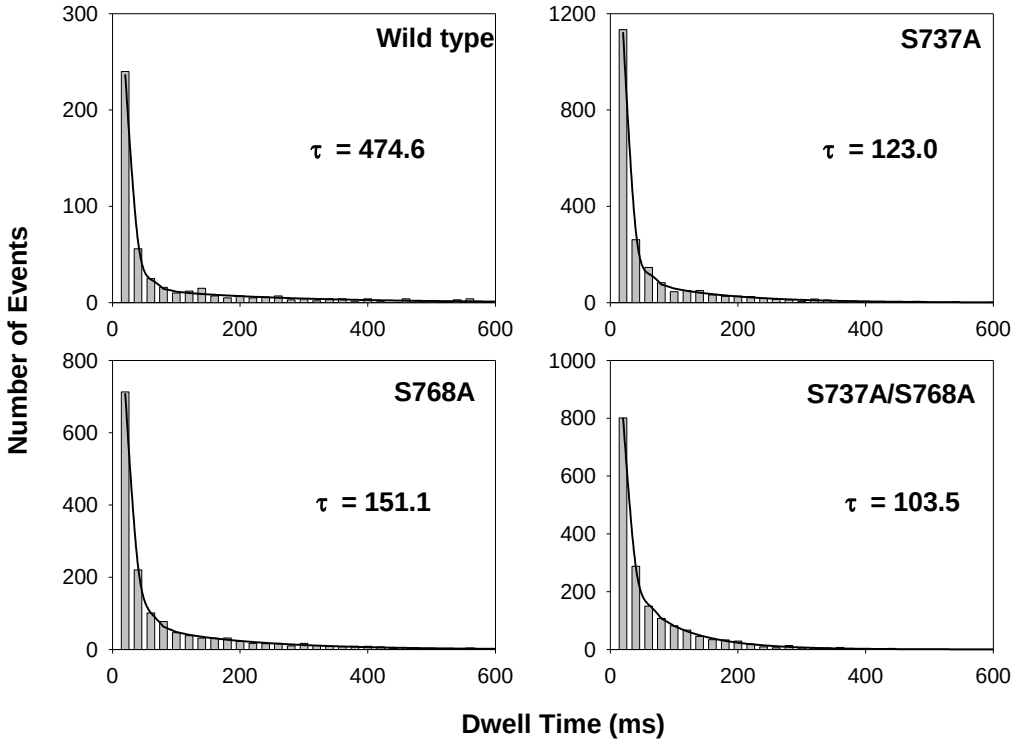

Fig. 4.9 Examples of closed time histograms obtained from single channel recordings of wt-CFTR, S737A, S768A and S737A/S768A

Examples of closed time histograms obtained from single channel recordings of wt-CFTR, S737A, S768A and S737A/S768A. Tracings were obtained at 0 mV membrane potential. Data are closed dwell time analysis of 1 channel. The continuous line is the fit of a one-component exponential function and the time constants (τ) are shown for each distribution.

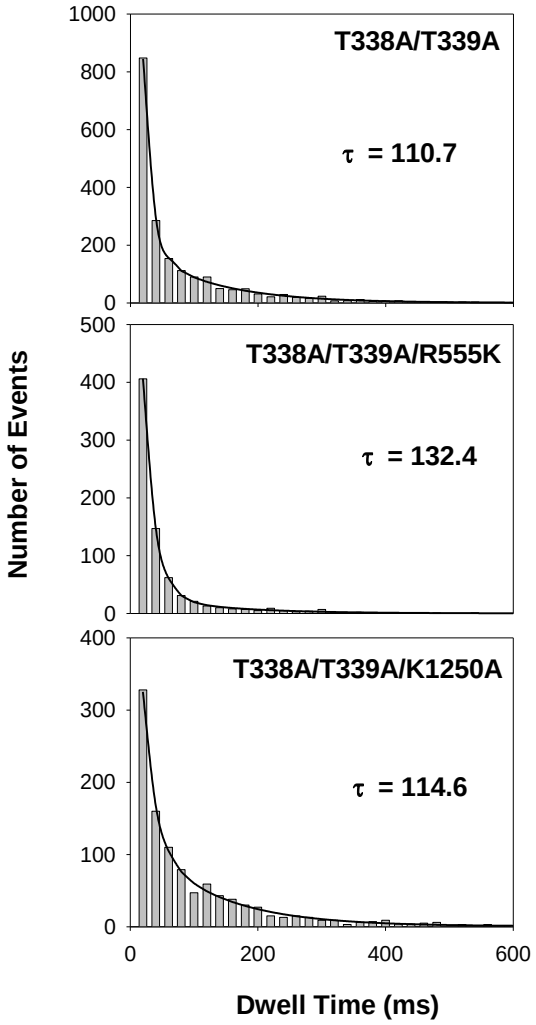

Fig. 4.10 Examples of closed time histograms obtained from single channel recordings of T338A/T339A, T338A/T339A/R555K and T338A/T339A/K1250A

Examples of closed time histograms obtained from single channel recordings of T338A/T339A, T338A/T339A/R555K and T338A/T339A/K1250A. Tracings were obtained at 0 mV membrane potential. Data are closed dwell time analysis of 1 channel. The continuous line is the fit of a one-component exponential function and the time constants (τ) are shown for each distribution.

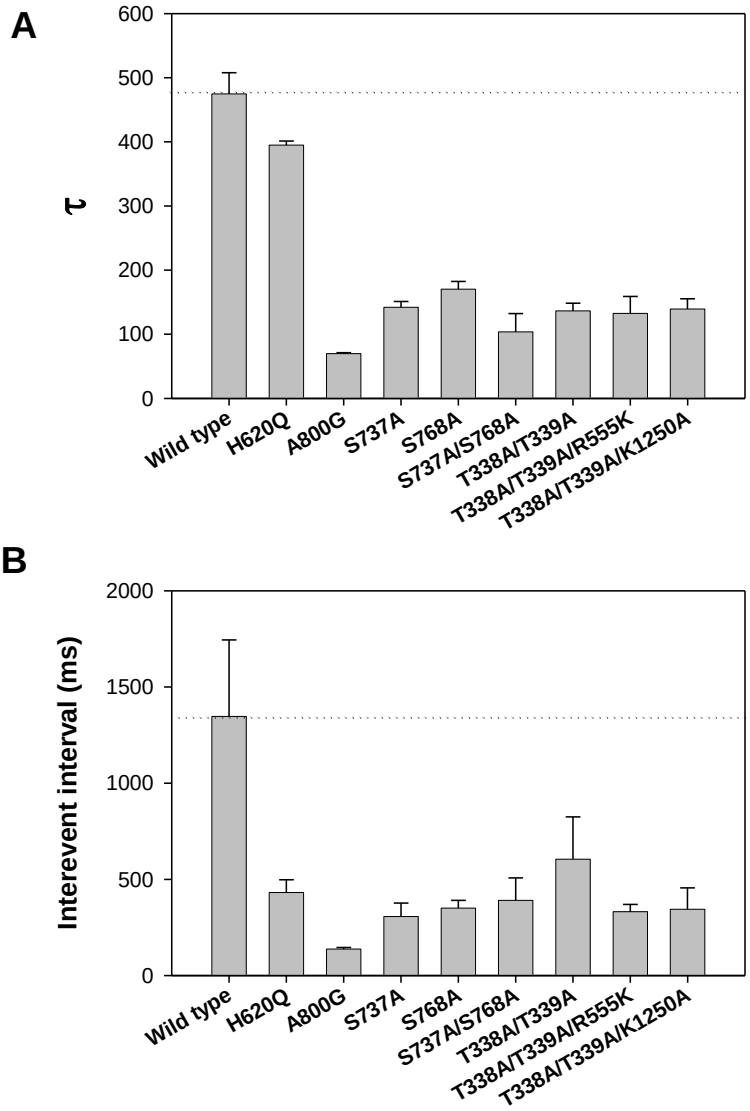

Fig. 4.11 Mean closed time constant τ (ms) and interevent interval (ms) of wt-CFTR and mutants

Panel A shows the mean closed time constant τ of wt-CFTR and other 8 mutants. Each data were from 5 minutes intervals and 5~10 patches. Panel B shows the interevent intervals of wt-CFTR and mutants. Each data also were from 5 minutes intervals and 5~10 patches.

4.3.3 Open Probability

To determine how these mutations altered CFTR Cl^- channel gating, we also analyzed single channel open state probability (P_o). Fig. 4.12 shows that in the presence of ATP and PKA, all of the variants had a similar P_o compared with wild type CFTR (0.25±0.09, n=5) except T338A/T339A/K1250A which had a P_o of 0.73±0.03 (n=5). Previous work shows that mutant K1250A can slow the rate of ATP hydrolysis thereby decrease the P_o (Carson et al., 1995). However, it is not conflicted with our result because mutant T338A/T339A/K1250A was very difficult to activate, but once it was activated, the channel opening would last a long time. Our recordings were calculated from the time near activation.

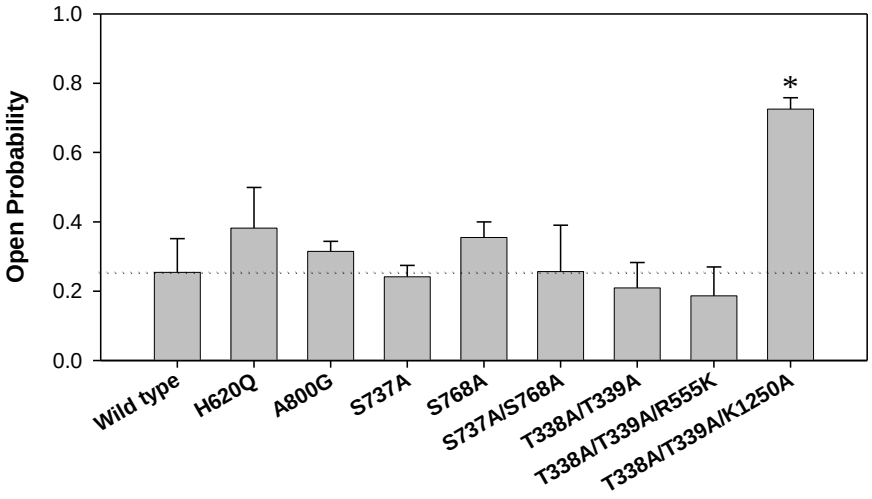

Fig. 4.12 Po for wt-CFTR and other 9 mutants.

All measurements were made in the presence of ATP and PKA with membrane potential clamped at -50 mV. *Asterisks* indicate statistical significance ($p<0.001$) relative to wild type CFTR. Mean of data of 5~10 patches.

4.4 Inhibitory Effects Of $Au(CN)_2^-$ In Wild Type CFTR And Mutants

To explore the interdomain interaction of CFTR, besides the single channel properties, we also studied the sensitivity of the channels to $Au(CN)_2^-$. As we mentioned previously, highly lyotropic anions (i.e. those with low free energies of hydration), such as the pseudohalide $Au(CN)_2^-$, hold great potentials as functional and structural probes of Cl^- channel pores. Our previous results also show that the effects of intracellular $Au(CN)_2^-$ on wild type CFTR and T338A-CFTR macroscopic currents are very different; i.e. very strong inhibition for wild type CFTR and very weak inhibition for T338A at the negative membrane potentials (Gong et al., 2002a). Here we used the molecular probe ($Au(CN)_2^-$) of CFTR channel pore and the distinct blocking properties of wild type CFTR and T338A to detect the inhibitory effects of the probe in A800G, S737A/S768A, T338A/T339A/R555K and T338/T339A/K1250A which showed a lower single channel conductance than wild type CFTR and T338A/T339A.

Fig. 4.13 shows the inhibitory effects of $Au(CN)_2^-$ in wild type CFTR , A800G and S737A/S768A. The inhibitory effects of 100 μM $Au(CN)_2^-$ were stronger in A800G and S737A/S768A than in wild type CFTR, especially at very negative potential. The inhibitory effects of 1 M $Au(CN)_2^-$ were also stronger in A800G and S737A/S768A than in wild type CFTR, but not so obvious as 100 μM $Au(CN)_2^-$.

Our results also confirmed that the effects of intracellular $Au(CN)_2^-$ on wild type CFTR and T338A/T339A macroscopic currents were very different; i.e. very strong inhibition

for wild type CFTR and very weak inhibition for T338A/T339A at the negative membrane potentials. And the other two triple mutants T338A/T339A/R555K and T338A/T339A/K1250A showed similar inhibitory effects as T338A/T339A as can see from Fig. 4.14.

Based on the macroscopic current-voltage (*I-V*) relationships of wild type CFTR and mutations (Fig. 4.13A, Fig. 4.14A), we quantified the rectification of the *I-V* relationship as the "rectification ratio", the slope conductance at -50 mV as a fraction of that at +50 mV (Gong and Linsdell, 2003b). Fig. 4.15 shows the rectification ratio of wild type CFTR and the mutations. We can see that A800G, S737A/S768A, T338A/T339A had no significant difference from wild type CFTR, while T338A/T339A/R555K and T338A/T339A/K1250A both showed significant difference from wild type CFTR.

Fig. 4.16 shows the $K_d(0)$ and δ of the blocking effects of 100 μM intracellular $Au(CN)_2^-$. $K_d(0)$ of all mutations was similar as that of wild type CFTR (Fig. 4.16A); while the δ value of T338A/T339A, T338A/T339A/R555K and T338A/T339A/K1250A showed significant difference from δ of wild type CFTR. Mutant A800G and S737A/S768A showed similar δ value as wild type CFTR.

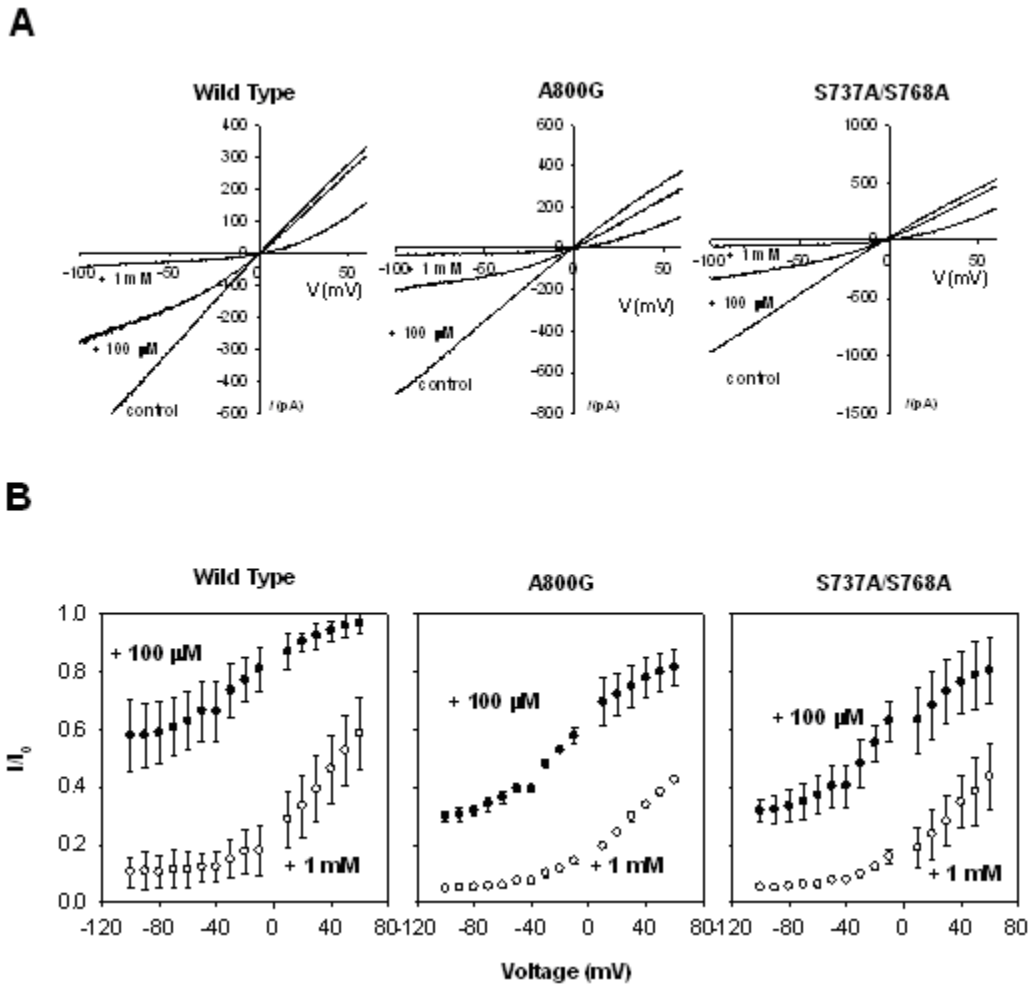

Fig. 4.13 Inhibitory Effects of $Au(CN)_2^-$ in wt-CFTR , A800G and S737A/S768A

Panel A shows examples of leak-subtracted macroscopic currents recorded in inside-out membrane patches following maximal activation with 50 nM PKA, 1 mM MgATP under symmetrical 154 mM Cl^- concentrations. In each case, currents were recorded before (*Control*) and after additions of 100 µM and 1 mM $Au(CN)_2^-$ to the intracellular solution. Panel B shows the mean fractions of control current remaining (I/I_0) following additions of 100 µM and 1 mM $Au(CN)_2^-$ to the intracellular solution as a function of membrane potential. Mean of data from five to seven patches.

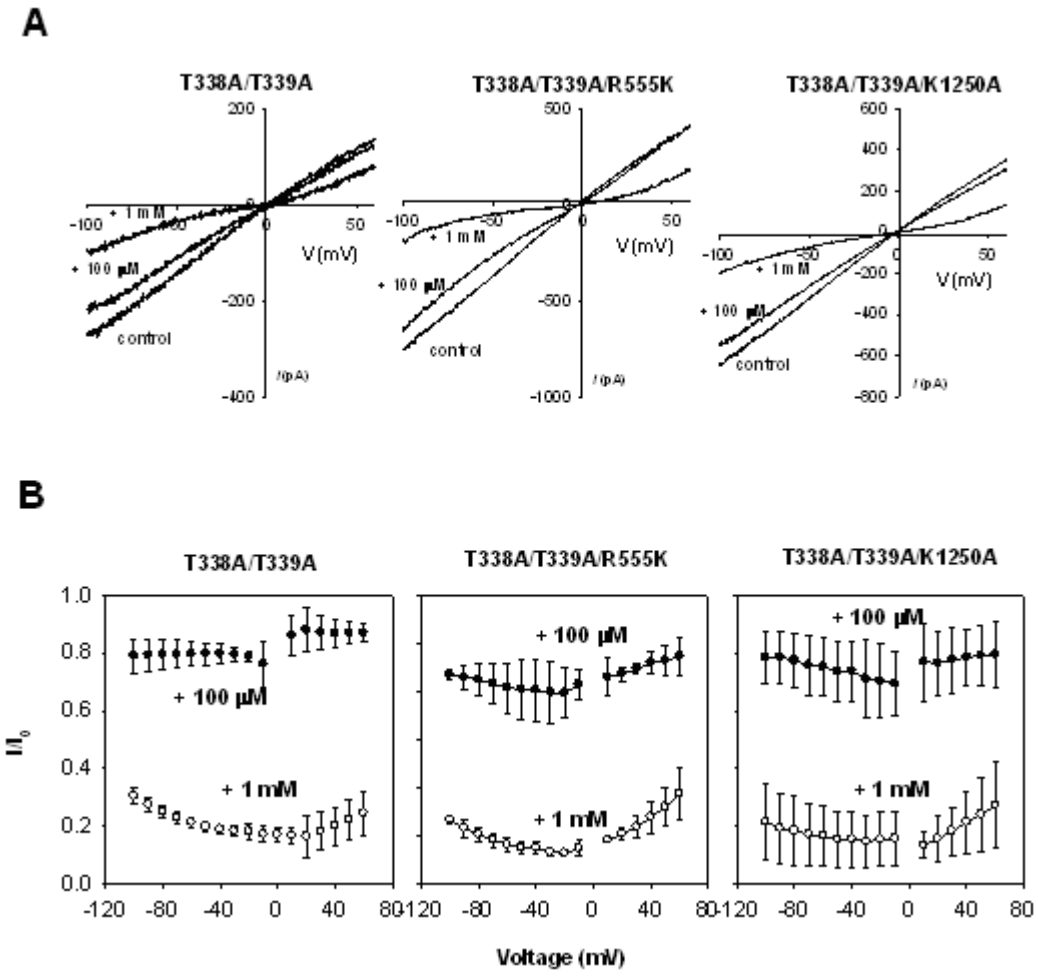

Fig. 4.14 Inhibitory Effects of $Au(CN)_2^-$ in T338A/T339A, T338A/T339A/R555K and T338A/T339A/K1250A

Panel A shows examples of leak-subtracted macroscopic currents recorded in inside-out membrane patches following maximal activation with 50 nM PKA, 1 mM MgATP under symmetrical 154 mM Cl^- concentrations. In each case, currents were recorded before (*Control*) and after additions of 100 µM and 1 mM $Au(CN)_2^-$ to the intracellular solution. Panel B shows the mean fractions of control current remaining (I/I_0) following additions of 100 µM and 1 mM $Au(CN)_2^-$ to the intracellular solution as a function of membrane potential. Mean of data from five to seven patches.

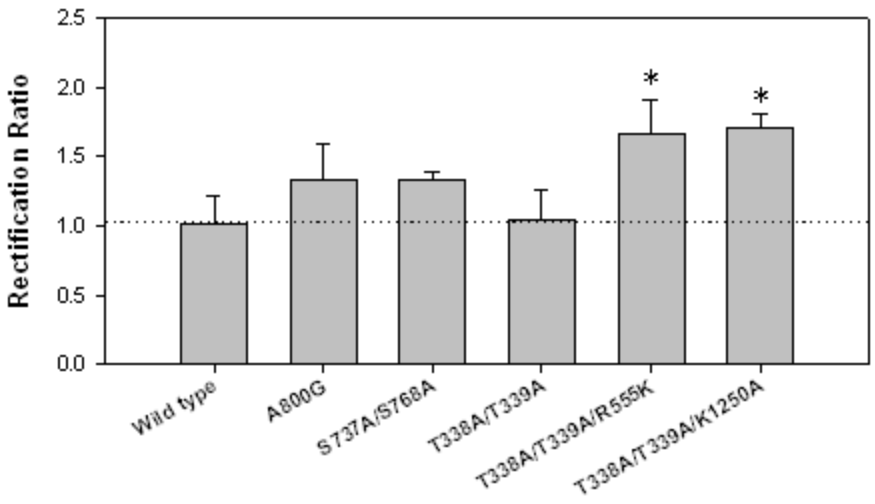

Fig. 4.15 Effect of mutations on rectification of the macroscopic I-V relationship

Rectification was quantified as the rectification ratio as described above, such that a ratio greater than one reflects inward rectification and a ratio less than one outward rectification of the *I-V* curve. *Asterisks* indicate significantly different from wild type CFTR. Mean of data from three to six patches.

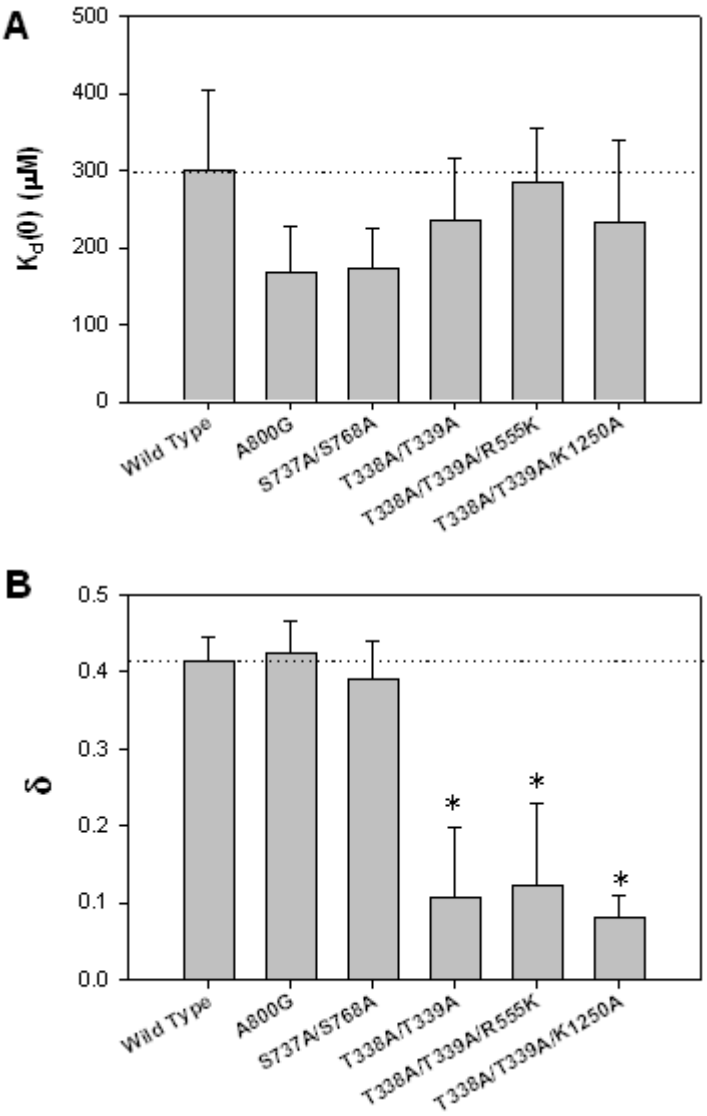

Fig. 4.16 Effect of wt-CFTR and different mutations on the apparent affinity and voltage dependence of block by intracellular $Au(CN)_2^-$

$K_d(0)$ (**A**) and δ (**B**) were estimated using data from individual patches on the blocking effects of 100 μM intracellular $Au(CN)_2^-$. In both cases, *Asterisks* indicate significantly different from wild type CFTR. Mean of data from five to seven patches.

4.5 Mutants Does Not Seriously Disturb Interdomain Interactions

For the R domain mutants H620Q, A800G, S737A, S768A, S737A/S768A and NBD domain mutants T338A/T339A/R555K, T338A/T339A/K12050A, K1250A changed single channel properties implied the flexibility of the CFTR channel pore thereby reflecting the interdomain interactions between TM domains and R domain, TM domains and NBD domains. We also constructed some mutants and find out that single channel property of these mutants did not change too much from those of wild type CFTR. These mutants are K52A, K52A/S737A, K52A/S768A and T338A/T339A/S768A.

Naren et al. mentioned that the NH_2-terminal tail (N-Tail) of CFTR might physically links CFTR to protein components of the membrane traffic machinery, thereby N-Tail has a previously unrecognized role in CFTR channel regulation (Naren et al., 1999) and CFTR activity appears to be governed by the interdomain interactions involving the amino-terminal tail. Therefore, among the highly charged region of the N-Tail that is well conserved across species (residues 46 to 60), we mutated K52 to A52 which was supposed to enhance the Cl^- current of the channel pore (Naren et al., 1999). We also created double mutants K52A/S737A, K52A/S768A to explore the interdomain interactions. Triple mutants T338A/T339A/K464A, T338A/T339A/S737A, and T338A/T339A/S768A were also constructed.

4.5.1 Single Channel Activity

We tested the single channel conductance of these mutants under membrane potential 0 mV and -50 mV. For the mutants K52A, K52A/S737A and K52A/S768A, their single

channel conductances at 0 mV membrane potential are 3.3 pS, 3.3 pS and 3.5 pS, respectively; there is no significant difference from that of wild type CFTR: 3.3 pS. The same situation occured when membrane potential was hold at -50 mV: K52A, K52A/S737A and K52A/S768A had single channel conductances of 6.1 pS, 6.5 pS and 6.1 pS, respectively, which were also very similar as that of wild type CFTR which had a single channel conductance of 6.1 pS. (Fig. 4.17 and Fig. 4.18)

Fig. 4.19 and Fig. 4.20 show the examples of single channel currents of T338A/T339A, T338A/T339A/K464A, T338A/T339A/S737A and T338A/T339A/S768A at membrane potential 0 mV and -50 mV. Here we got some interesting results. At 0 mV (Fig. 4.19), single channel conductances of triple mutants T338A/T339A/K464A and T338A/T339A/S737A were similar as that of double mutant T338A/T339A which had dramatically enhanced single channel current amplitude. While mutant T338A/T339A/S768A showed a single channel conductance as wild type CFTR, just as triple mutants T338A/T339A/R555K and T338A/T339A/K1250A. At -50 mV (Fig. 4.20), triple mutants T338A/T339A/K464A and T338A/T339A/S737A also had similar single channel current amplitude as T338A/T339A. T338A/T339A/S768A had a single channel conductance of 6.8 pS which was close to that of wild type CFTR (6.1 pS) and much lower than that of T338A/T339A, T338A/T339A/K464A and T338A/T339A/S737A (8.9 pS, 9.1 pS, and 9.1 pS, respectively). We can see this more clearly from Fig. 4.21, which compared the single channel current amplitudes of wild type CFTR and mutants at 0 mV and -50 mV membrane potentials.

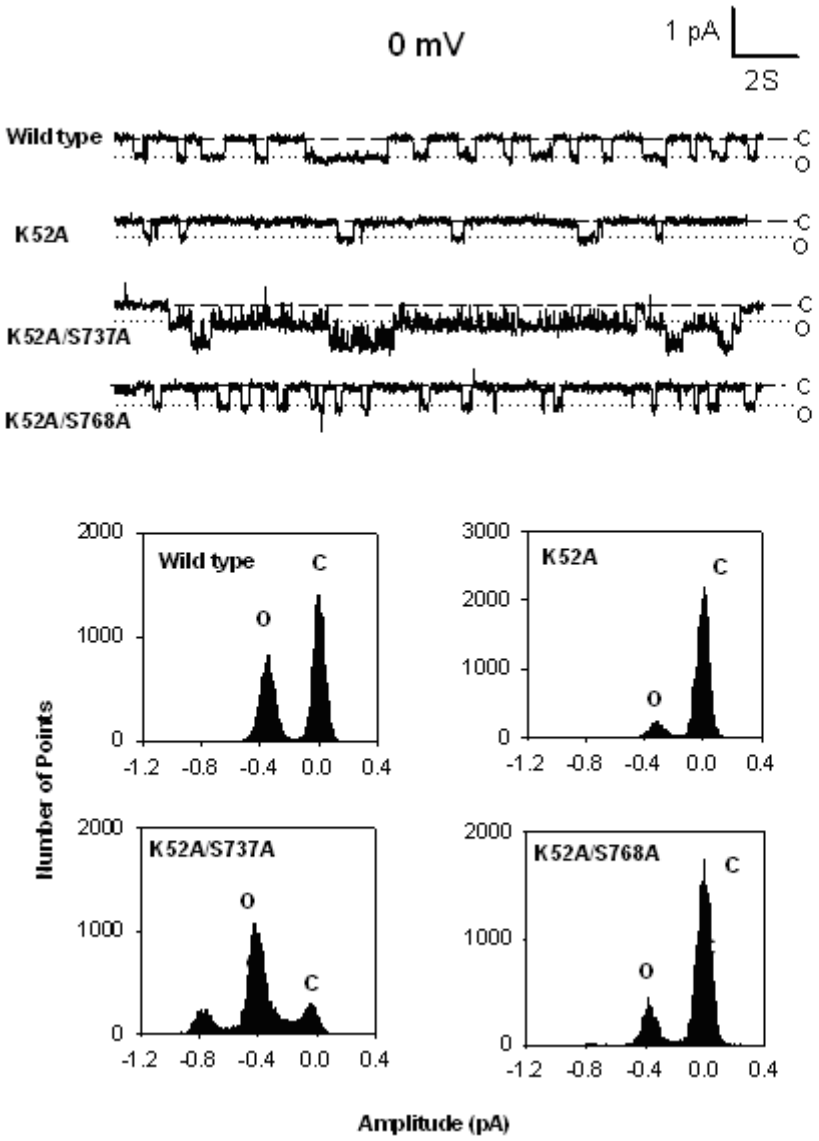

Fig. 4.17 Examples of single channel currents of wt-CFTR, K52A, K52A/S737A, K52A/S768A

Examples of single channel currents of wt-CFTR, K52A, K52A/S737A, K52A/S768A recorded from inside-out patches at membrane potentials of 0 mV. In each case, the open and closed states of the channel are indicated by the short dashed lines and dotted lines, respectively. The unitary current amplitudes are demonstrated from all point histograms prepared from these current traces, and as indicated. Single-channel current amplitudes at 0 mV are 0.35, 0.33, 0.33 and 0.35 pA for wt-CFTR, K52A, K52A/S737A, and K52A/S768A, respectively.

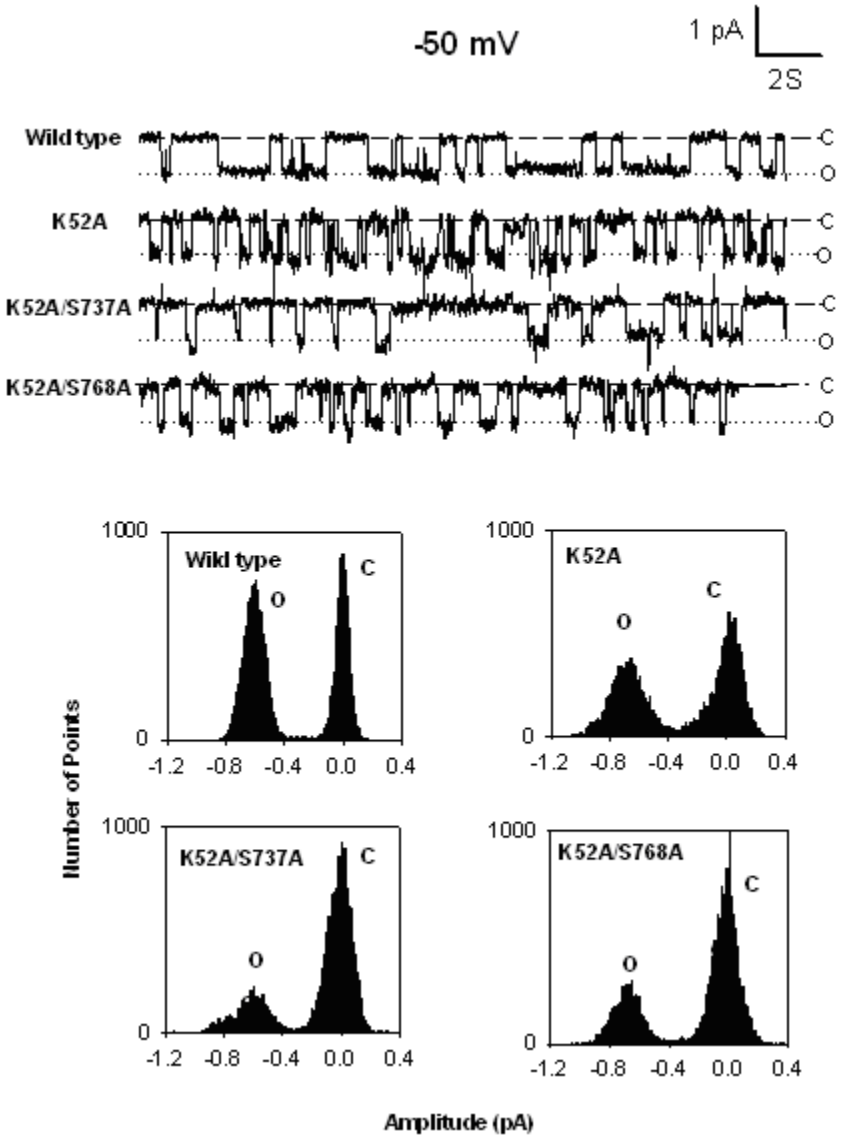

Fig. 4.18 Examples of single channel currents of wt-CFTR, K52A, K52A/S737A, K52A/S768A

Examples of single channel currents of wt-CFTR, K52A, K52A/S737A, K52A/S768A recorded from inside-out patches at membrane potentials of -50 mV. In each case, the open and closed states of the channel are indicated by the short dashed lines and dotted lines, respectively. The unitary current amplitudes are demonstrated from all point histograms prepared from these current traces, and as indicated. Single-channel current amplitudes at -50 mV are 0.61, 0.61, 0.65 and 0.61 pA for wt-CFTR, K52A, K52A/S737A, and K52A/S768A, respectively.

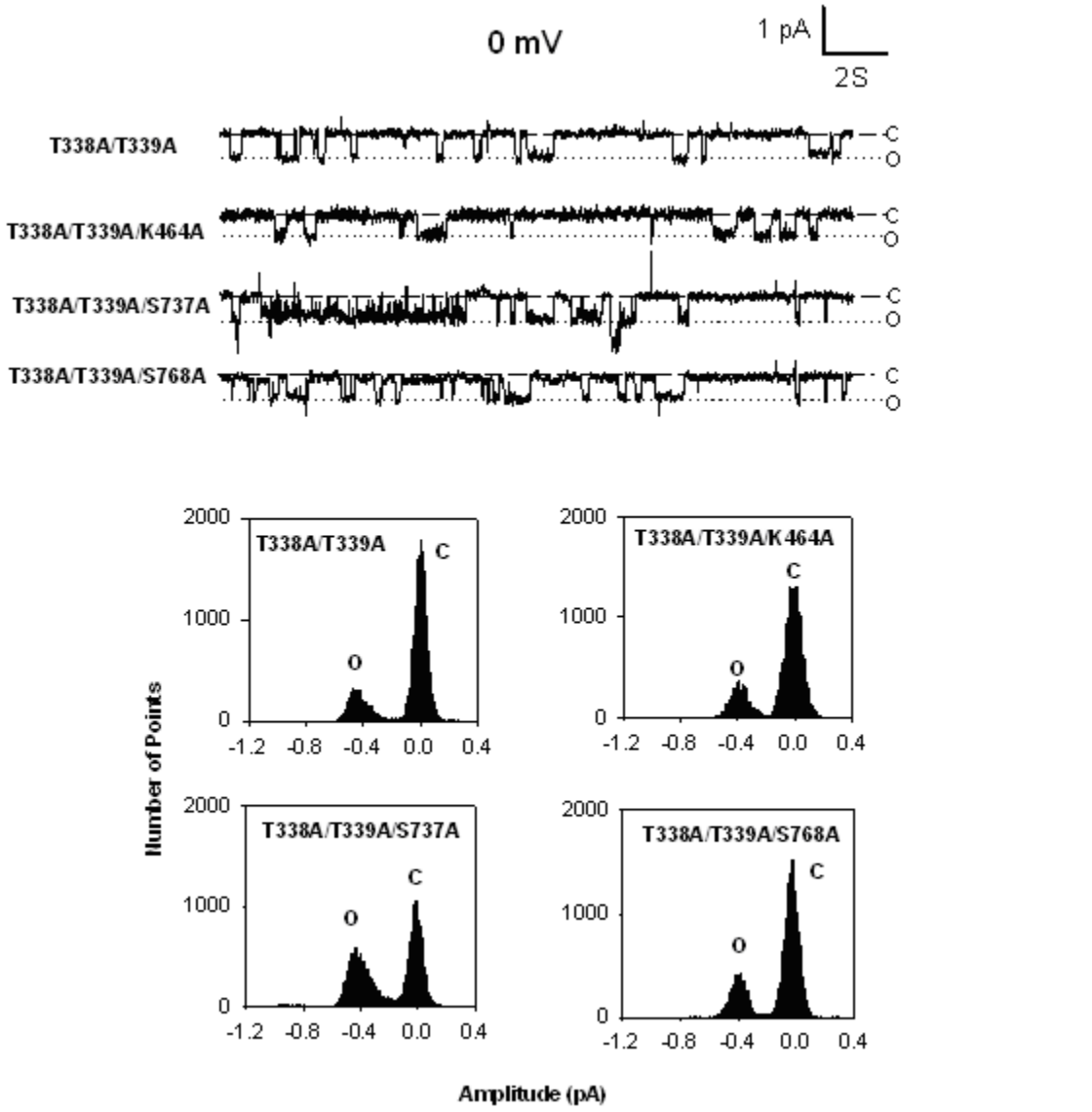

Fig. 4.19 Examples of single channel currents of T338A/T339A, T338A/T339A/K464A, T338A/T339A/S737A, T338A/T339A/S768A

Examples of single channel currents of T338A/T339A, T338A/T339A/K464A, T338A/T339A/S737A, T338A/T339A/S768A recorded from inside-out patches at membrane potentials of 0 mV. In each case, the open and closed states of the channel are indicated by the short dashed lines and dotted lines, respectively. The unitary current amplitudes are demonstrated from all point histograms prepared from these current traces, and as indicated. Single-channel current amplitudes at 0 mV are 0.49, 0.42, 0.47 and 0.35 pA for T338A/T339A, T338A/T339A/K464A, T338A/T339A/S737A, and T338A/T339A/S768A, respectively.

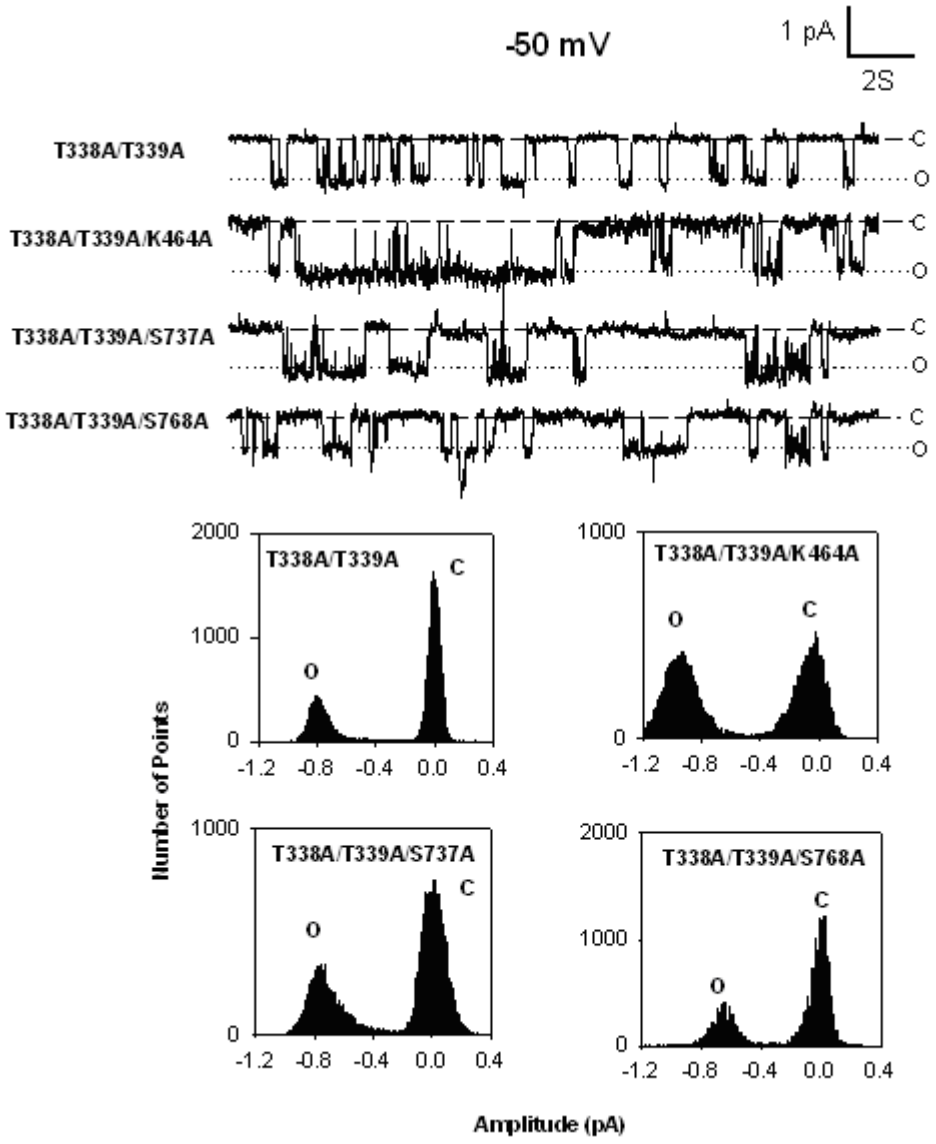

Fig. 4.20 Examples of single channel currents of T338A/T339A, T338A/T339A/K464A, T338A/T339A/S737A, T338A/T339A/S768A

Examples of single channel currents of T338A/T339A, T338A/T339A/K464A, T338A/T339A/S737A, T338A/T339A/S768A recorded from inside-out patches at membrane potentials of -50 mV. In each case, the open and closed states of the channel are indicated by the short dashed lines and dotted lines, respectively. The unitary current amplitudes are demonstrated from all point histograms prepared from these current traces, and as indicated. Single-channel current amplitudes at -50 mV are 0.89, 0.91, 0.91 and 0.68 pA for T338A/T339A, T338A/T339A/K464A, T338A/T339A/S737A, and T338A/T339A/S768A, respectively.

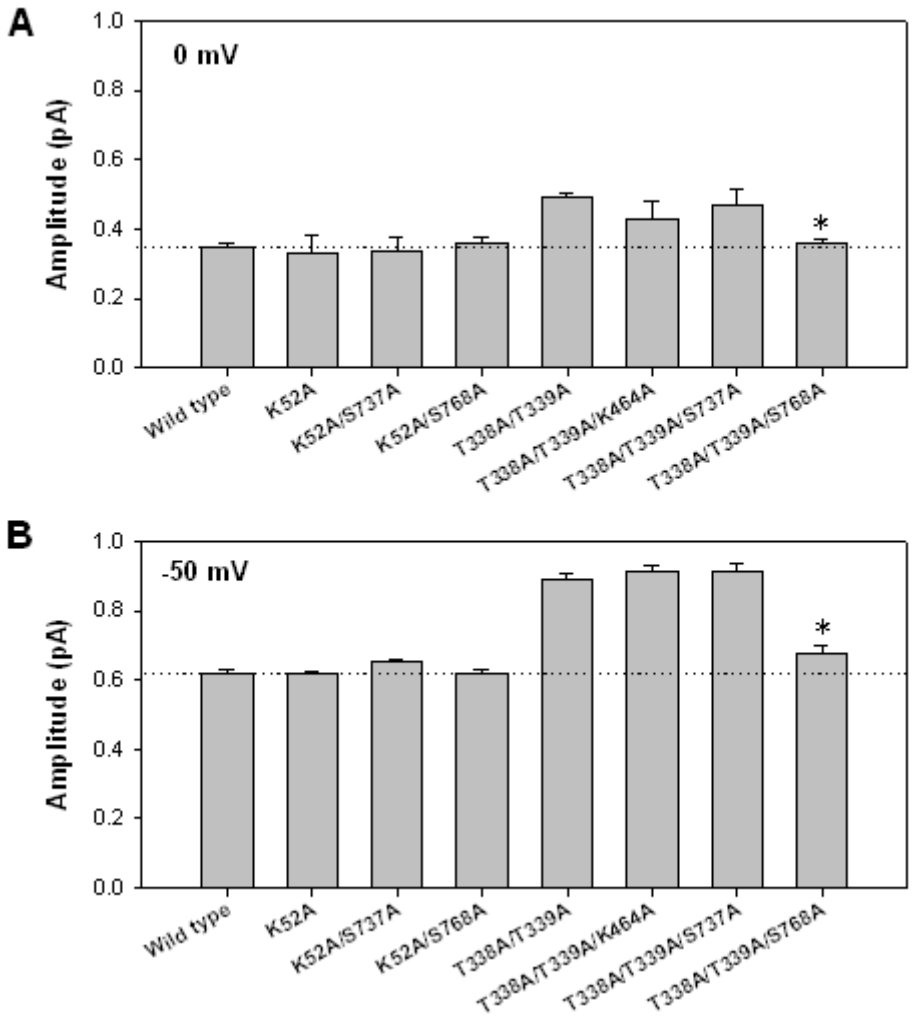

Fig. 4.21 Single channel current amplitudes of wt-CFTR and different CFTR channel variants

Single channel current amplitudes from individual patches of wt-CFTR and different CFTR channel mutants at 0 mV (A) and -50 mV (B) membrane potential were calculated and compared. *Asterisks* indicate a significant difference from T338A/T339A. Mean of data from three to ten patches.

4.5.2 Single Channel Kinetics

4.5.2.1 Closed Dwell Time

Fig. 4.22 shows the closed time histograms of wild type CFTR, K52A, K52A/S737A and K52A/S768A at 0 mV. The mean closed time constant τ_c of wild type CFTR, K52A, K52A/S737A and K52A/S768A is 474.6 ms, 181.6 ms, 99.1 ms and 120.8 ms, respectively. K52A showed a shorter closed state than wild type CFTR, which implied that K52, one residue highly conserved (Naren et al., 1999), might include in the regulation of the gating of CFTR Cl^- channel pore. Double mutants K52A/S737A and K52A/S768A showed a much shorter open state than wild type CFTR and K52A, which was consistent to the previous result of the phosphorylation inhibitory function of R domain residue S737 and S768 (Wilkinson et al., 1997).

Triple mutants T338A/T339A/K464A, T338A/T339A/S737A and T338A/T339A/S768A also showed longer open state and shorter closed state than wild type CFTR, which could be seen from the τ_c value: T339A/K464A (88.8 ms), T338A/T339A/S737A (95.8 ms) and T338A/T339A/S768A (164.1 ms) (Fig. 4.23). But these values had not significant differences from that of double mutant T338A/T339A which carried a τ_c value of 110.7 ms. Fig. 4.24A compared the τ_c of wild type CFTR and all the mutants, we can see that all mutants had significantly lower τ_c value than wild type CFTR.

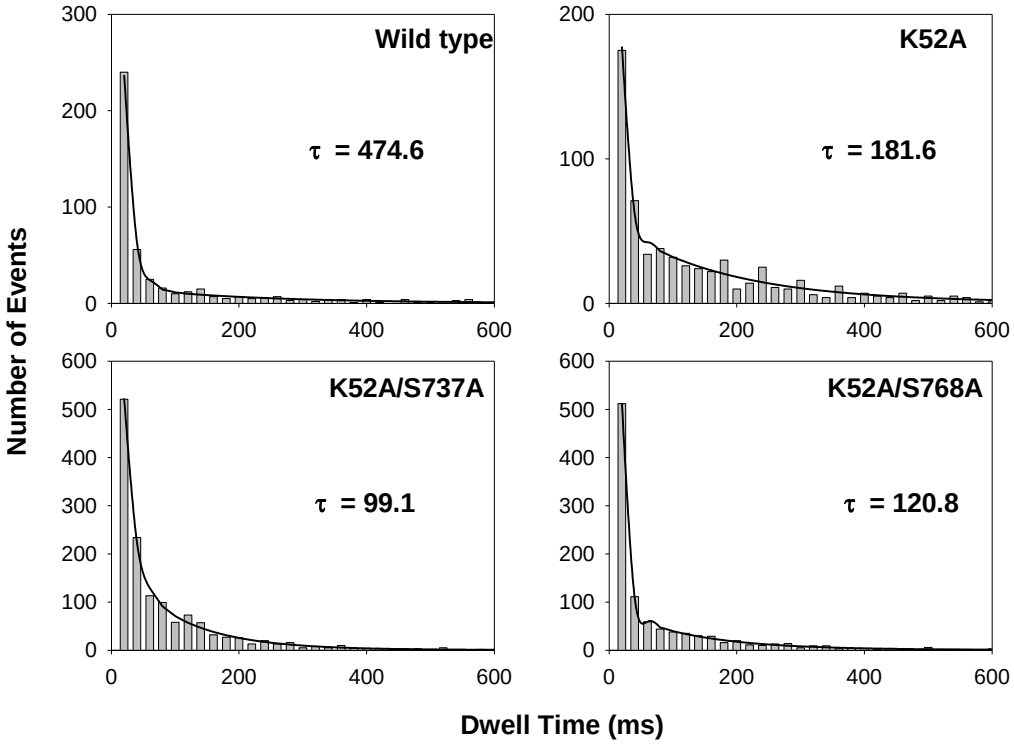

Fig. 4.22 Examples of closed time histograms obtained from single channel recordings of wt-CFTR, K52A, K52A/S737A and K52A/S768A

Examples of closed time histograms obtained from single channel recordings of wt-CFTR, K52A, K52A/S737A and K52A/S768A. Tracings were obtained at 0 mV membrane potential. Data are closed dwell time analysis of 1 channel. The continuous line is the fit of a one-component exponential function and the time constants (τ) are shown for each distribution.

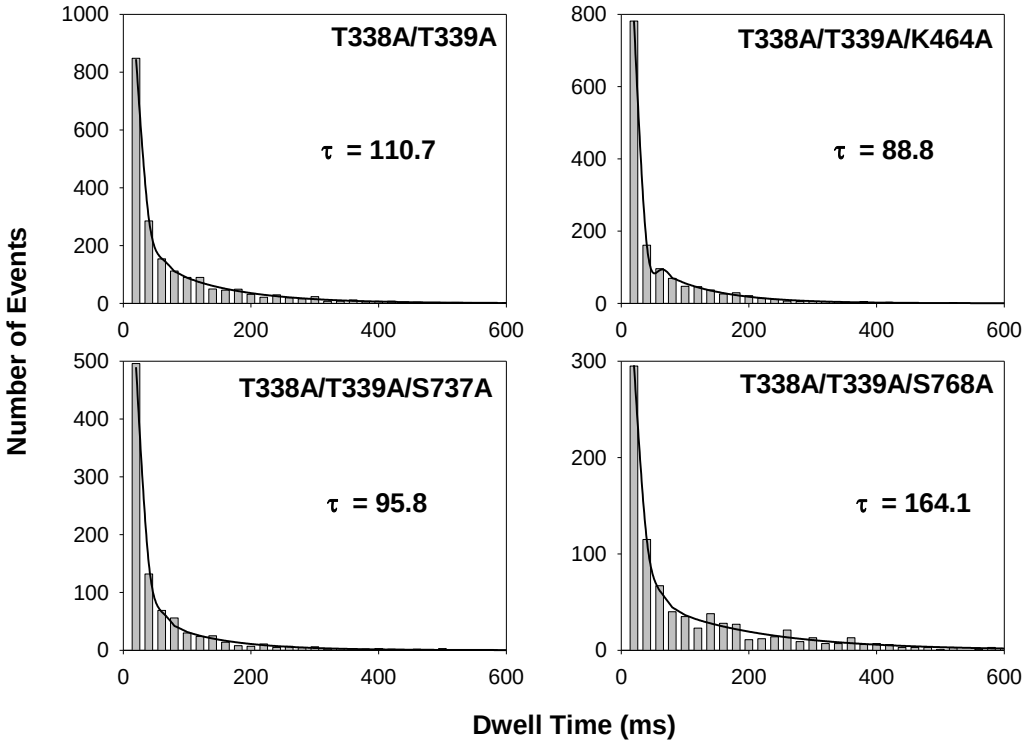

Fig. 4.23 Examples of closed time histograms obtained from single channel recordings of T338A/T339A, T338A/T339A/K464A, T338A/T339A/S737A and T338A/T339A/S768A

Examples of closed time histograms obtained from single channel recordings of T338A/T339A, T338A/T339A/K464A, T338A/T339A/S737A and T338A/T339A/S768A. Tracings were obtained at 0 mV membrane potential. Data are closed dwell time analysis of 1 channel. The continuous line is the fit of a one-component exponential function and the time constants (τ) are shown for each distribution.

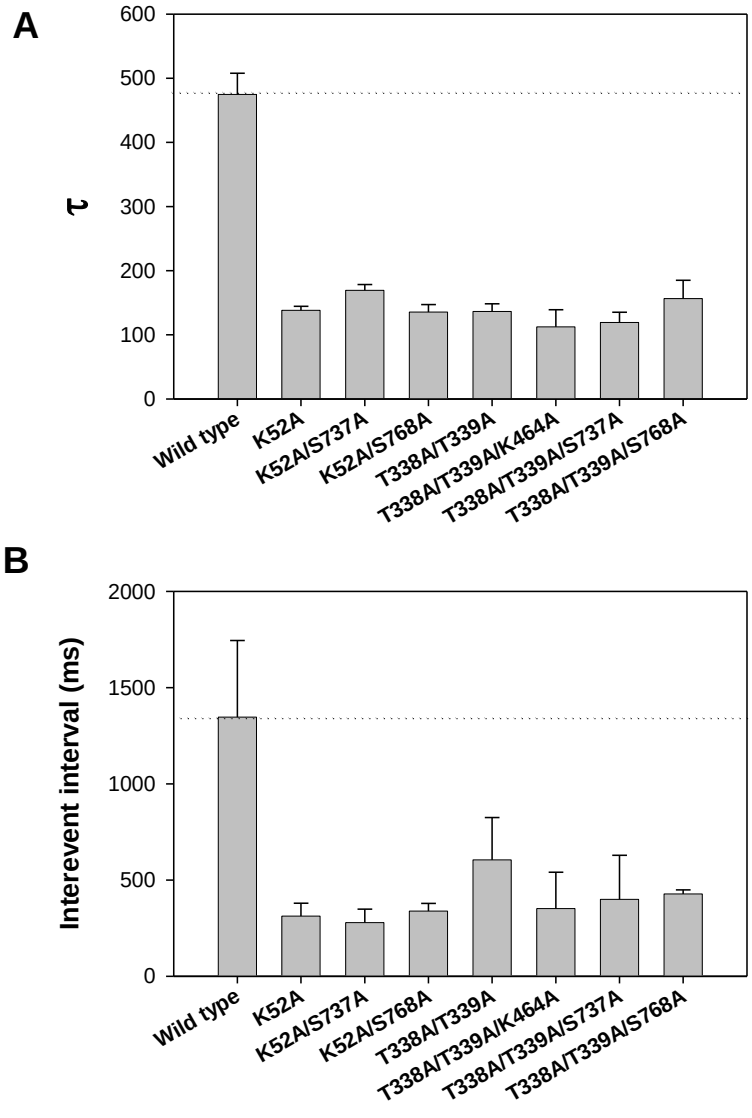

Fig. 4.24 Mean closed time constant τ (ms) and interevent interval (ms) of wt-CFTR and mutants

Panel A shows the mean closed time constant τ of wt-CFTR and other 7 mutants. Each data were from 5 minutes intervals and 5~10 patches. Panel B shows the interevent intervals of wt-CFTR and mutants. Each data also were from 5 minutes intervals and 5~10 patches.

4.5.2.2 Interevent Interval

We also compared the interevent intervals of wild type CFTR and its mutants. As shown in Fig. 4.24B, the interevent interval for wild type CFTR was 1346.6 ± 397.9 ms, while the interevent intervals for other mutants were all smaller than that of wild type CFTR.

4.5.2.3 Open Probability

Besides dwell time and interevent interval, we also analyzed single channel open state probability (P_o). Fig. 4.25 shows that in the presence of ATP and PKA, all the variants had a similar P_o compared with wild type CFTR (0.25 ±0.09, n=5) and no significant difference was shown.

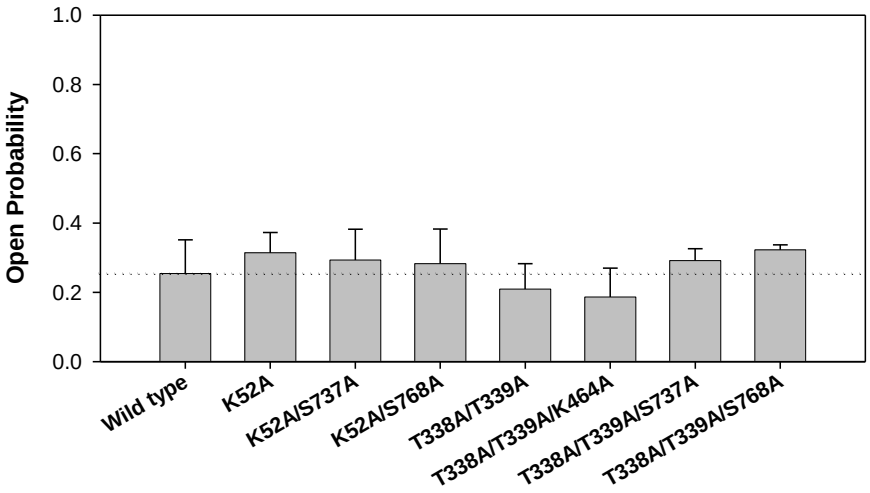

Fig. 4.25 Po for wt-CFTR and other 7 mutants

All measurements were made in the presence of ATP and PKA with membrane potential clamped at -50 mV. Mean of data of 5~10 patches.

5 Molecular Engineering of CFTR Gain of Function Mutants ---- An Implication for Cystic Fibrosis (CF) Gene Therapy

5.1 Introduction

As we mentioned previously, the fundamental principle of these gene therapies is to deliver a normal copy of the CFTR DNA to airway epithelia using a delivery vehicle by instillation or as an aerosol. However, the difficulties in this method, including delivery of the vector to the cell, lack of persistent gene expression, immune responses to viral gene products and directing viral vectors towards on the apical surface of the epithelial cells, limit the achievement of effective gene therapy. Though the difficulties daunt the successful CF airway gene therapy, the potential rewards are great and still worth seeking. By primary focusing on the restoration of CFTR function, cautious evaluating of the methods, utility and safety of different gene therapies directed to compensate the loss of CFTR function; these difficulties will slowly be overcomed. Thus, our purpose is to achieve CFTR gain of function mutants which can compensate the loss of CFTR Cl^- channel function and hence be potentially useful to the gene therapy.

In CFTR, transmembrane helix 6 (Ge et al.) is suggested to be involved in forming pore. Mutations at several positions in TM6 affect biophysical parameters such as single channel conductance, rectification and anion selectivity. Amino acid residues R334, K335, F337, T338, T339 and S341 in TM6, when mutated, significantly affect anion selectivity, suggesting that these residues may line in the pore of CFTR channel (Gong et al., 2002b; Gong and Linsdell, 2003b, 2004; Linsdell et al., 1998). Preliminary findings

also have revealed that mutant T338A can enhance Cl^- channel conductance, which may be regarded as a form of gene gain of function. Based on this mutant, four double mutants were constructed (T338A/R334E, T338A/K335A, T338A/F337A, T338A/T339A, T338A/S341A), with the hope to get the aimed gene forms.

CFTR channel activity is also regulated by nucleotide binding and ATP hydrolysis. The relationship between ATPase activity at the NBDs of CFTR and channel gating has been interpreted in different ways. Here we also constructed double mutant T338A/K1250A and triple mutant T338A/R334E/K1250A to measure their gain of function.

5.2 Type I of CFTR Gain of Function: Augmenting the Amplitude of Channel Conductance

As we mentioned in the introduction part, Class IV mutations include cases where the CFTR gene encodes a protein that is correctly trafficked to the cell membrane, that is activated by cAMP and regulation by ATP appeared to be normal, however, the Cl^- current was much reduced due to a decrease in amplitude of a single channel current. Most of the class IV mutations analyzed to date are located within the membrane-spanning domains, such as TM1, and TM6. These mutations cause a decreased Cl^- current. So sustaining CFTR channel conductance is very crucial for maintaining normal airway surface liquid volume and maximizing CFTR chloride channel conductance, if possible, may provide another way for therapy of CF patients.

Here we investigated the amplitude of single channel conductance of wild type CFTR, single mutant T338A, double mutant T338A/S341A, T338A/R334E, T338A/K335A, T338A/F337A, T338A/T339A, T338A/K1250A, and triple mutant T338A/R334E/K1250A. Fig. 5.1 shows the examples of single channel conductance of wild type CFTR, T338A, T338A/T339A and T338A/K1250A at -50 mV membrane potential. These three mutants have dramatically enhanced the amplitude of single channel conductance. T338A and T338A/T339A showed 0.75 amplitude of pA, 0.89 pA respectively, and T338A/K1250A showed amplitude of 0.72 pA, all are larger than the amplitude of wild type CFTR(0.6 pA).

Fig. 5.2 also lists the examples of single channel conductance of wild type CFTR, T338A, T338A/K335A and T338A/F337A at -50 mV membrane potential. Different from the results of T338A/T339A and T338A/K1250A, both T338A/K335A and T338A/F337A had reduced amplitude of single channel conductance when compared with T338A single mutant. In addition, the amplitudes of these two mutants are similar as that of wild type CFTR.

The single channel conductance of double mutant T338A/S341A, T338A/R334E and triple mutant T338A/R334E/K1250A at -50 mV membrane potential were also compared with that of wild type CFTR in Fig. 5.3. As we can see, single channel conductance amplitudes of these three mutants were significantly reduced. We can see above effects more clearly in Fig. 5.4 which listed the single channel current amplitudes of wild type and different CFTR variants.

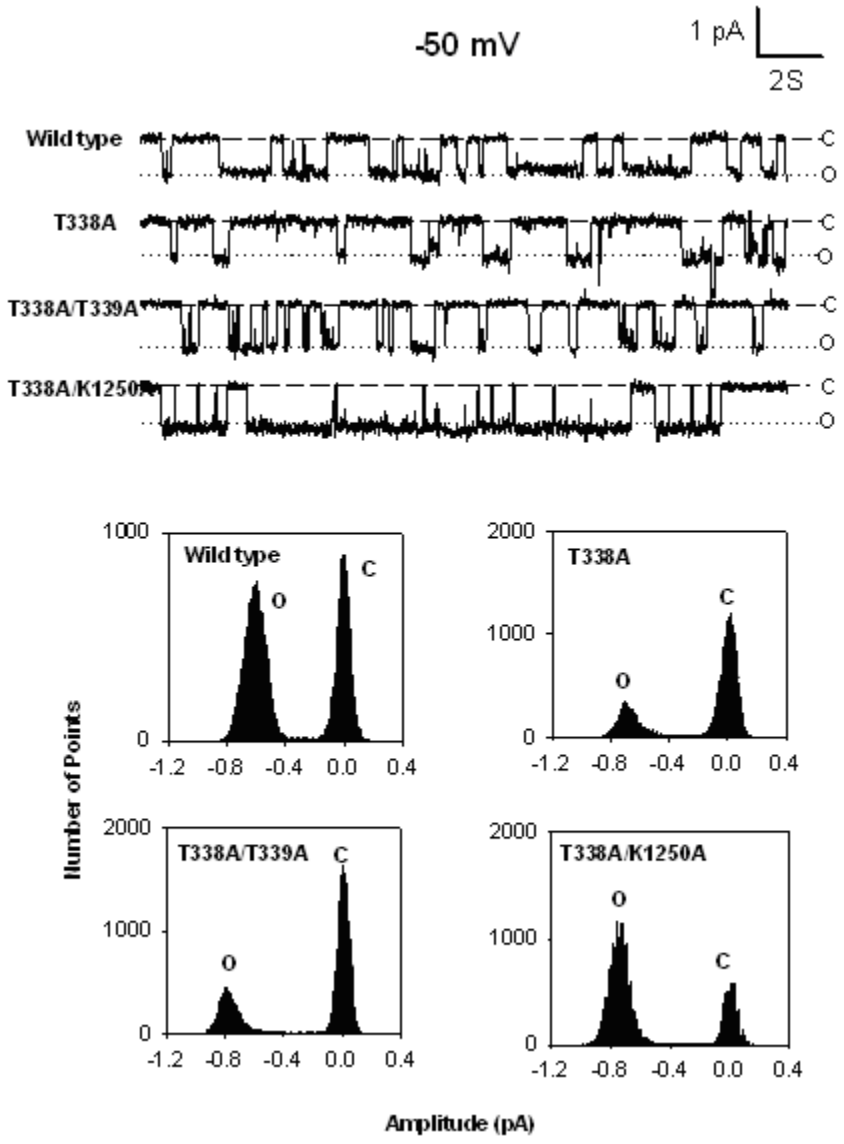

Fig. 5.1 Examples of single channel currents of wt-CFTR, mutants T338A, T338A/T339A and T338A/K1250A

Examples of single channel currents of wt-CFTR, T338A, T338A/T339A and T338A/K1250A recorded from inside-out patches at membrane potentials of -50 mV. In each case, the open and closed states of the channel are indicated by the short dashed lines and dotted lines, respectively. The unitary current amplitudes are demonstrated from all point histograms prepared from these current traces, and as indicated. Single-channel current amplitudes at -50 mV are 0.61, 0.75, 0.89 and 0.72 pA for wt-CFTR, T338A, T338A/T339A and T338A/K1250A, respectively.

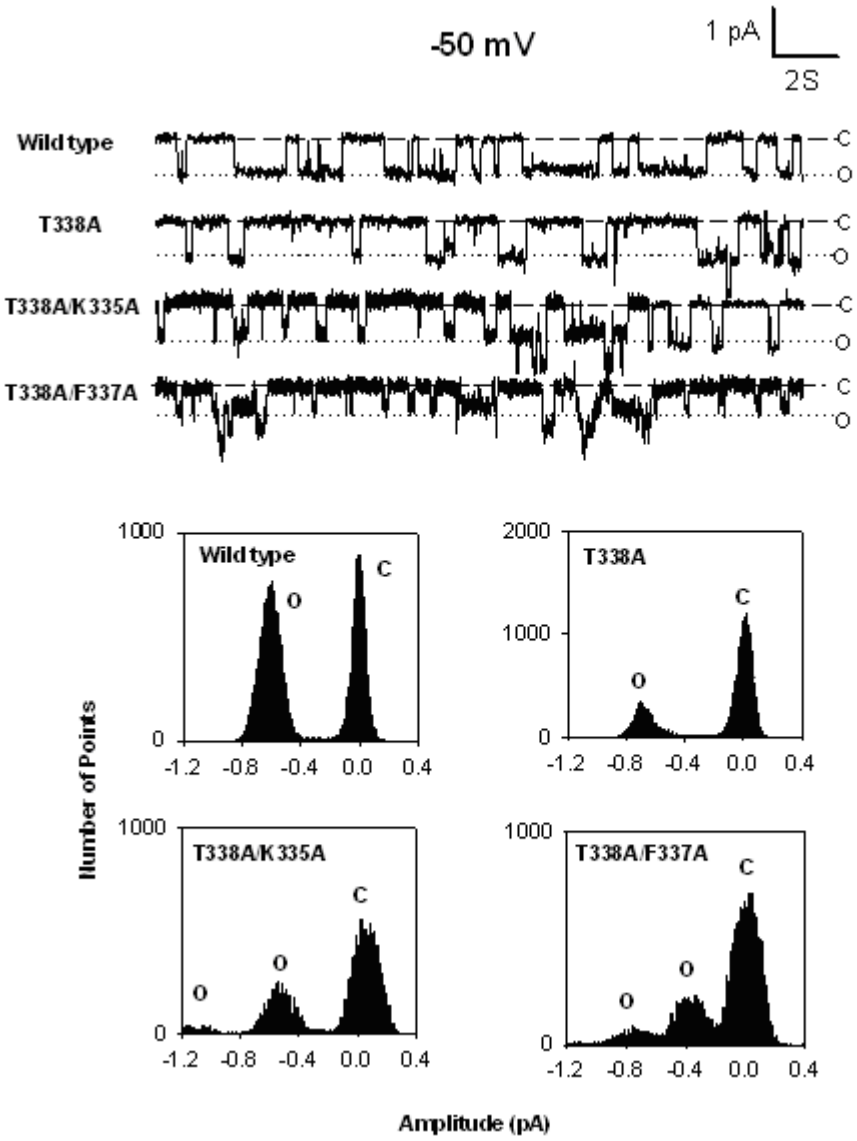

Fig. 5.2 Examples of single channel currents of wt-CFTR, mutants T338A, T338A/K335A and T338A/F337A

Examples of single channel currents of wt-CFTR, T338A, T338A/K335A and T338A/F337A recorded from inside-out patches at membrane potentials of -50 mV. The unitary current amplitudes are demonstrated from all point histograms prepared from these current traces, and as indicated. Single-channel current amplitudes at -50 mV are 0.61, 0.75, 0.58 and 0.39 pA for wt-CFTR, T338A, T338A/K335A and T338A/F337A, respectively.

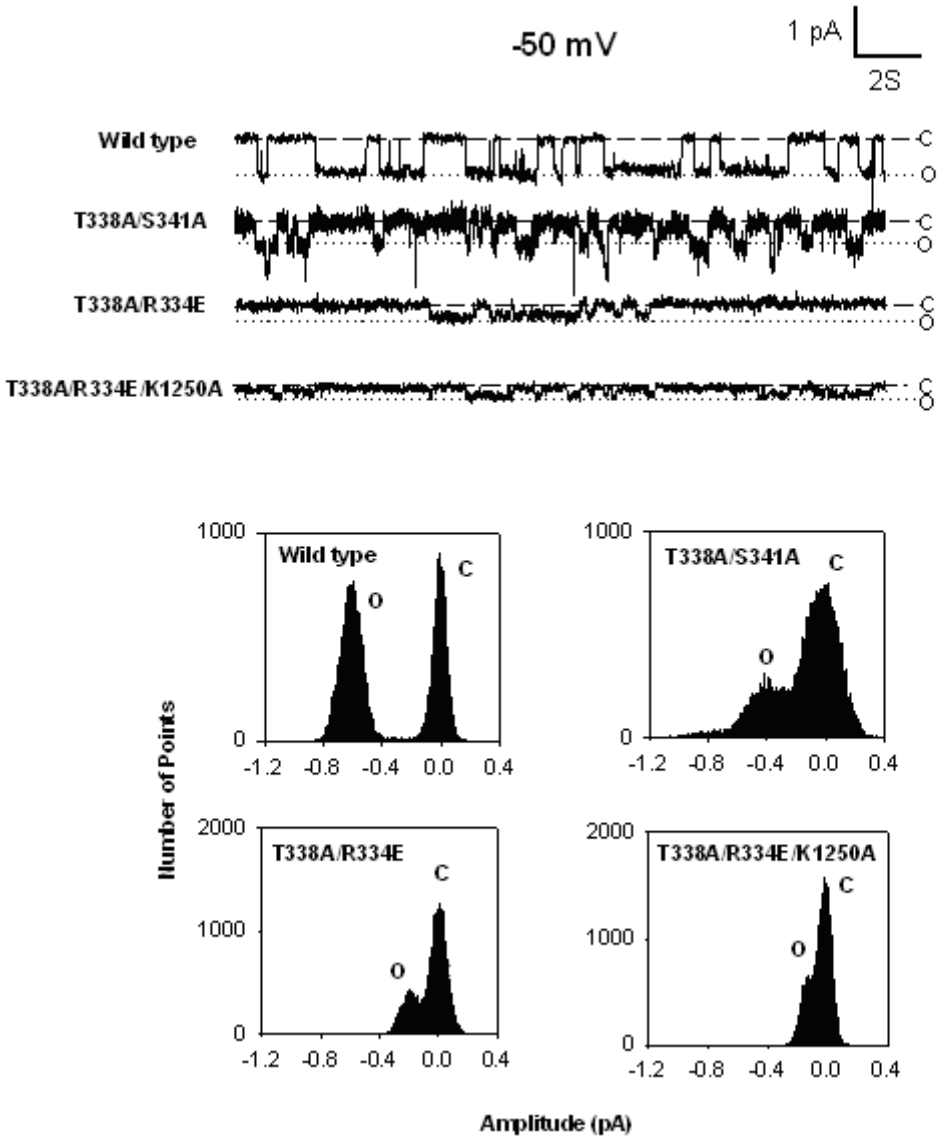

Fig. 5.3 Examples of single channel currents of wt-CFTR, mutants T338A/S341A, T338A/R334E and T338A/R334E/K1250A

Examples of single channel currents of wt-CFTR, T338A/S341A, T338A/R334E and T338A/R334E/K1250A recorded from inside-out patches at membrane potentials of -50 mV. The unitary current amplitudes are demonstrated from all point histograms prepared from these current traces, and as indicated. Single-channel current amplitudes at -50 mV are 0.61, 0.39, 0.20 and 0.18 pA for wt-CFTR, T338A/S341A, T338A/R334E and T338A/R334E/K1250A, respectively.

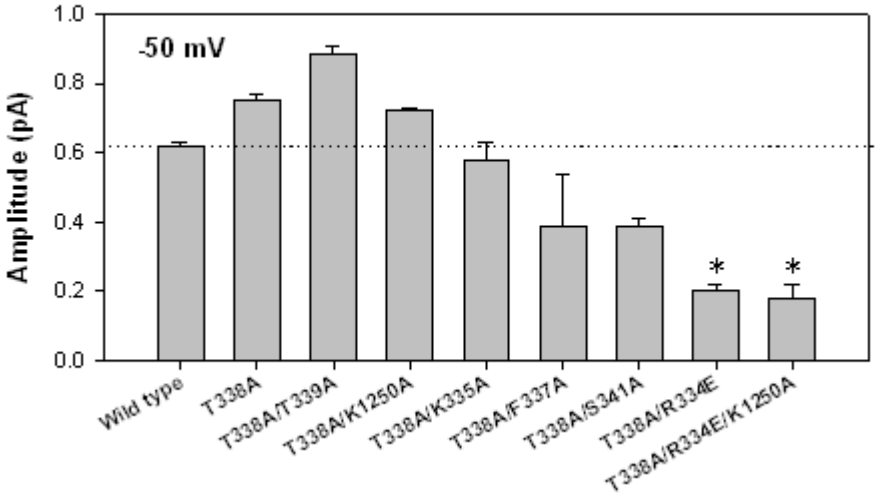

Fig. 5.4 Single channel current amplitudes of wt-CFTR and different CFTR variants

Single channel current amplitudes from individual patches of wt-CFTR and different mutants at -50 mV membrane potential were calculated and compared. *Asterisks* indicate a significant difference from wild type CFTR. Mean of data from three to ten patches.

5.3 Type II of CFTR Gain of Function: Diverting the Direction of Anion Movement through Open CFTR Channel (Rectification)

Rectification is one of the properties in many voltage-gated potassium channels. An inward rectification is a conductance that increases under hyperpolarization and decreases under depolarization. Based on the macroscopic current-voltage *(I-V)* relationships of wild type CFTR and mutations, we quantified the rectification of the *I-V* relationship as the "rectification ratio", the slope conductance at -50 mV as a fraction of that at +50 mV (Gong and Linsdell, 2003b).

Examples of leak-subtracted macroscopic CFTR *I-V* relationships are shown in Fig. 5.5. The macroscopic *I-V* relationship of wild type was linear in the presence of symmetrical Cl^- concentrations. Similarly, T338A single mutant, T338A/K335A, T338A/F337A, T338A/T339A and T338A/K1250A displayed I-V relationship close to linear. Double mutant T338A/S341A showed very slight inward rectification and distinguishingly, strong inward rectification was observed in the double mutant T338A/R334E and T338/R334E/K1250A. As we mentioned above, rectification is one of the properties in many voltaged-gated potassium channels. An inward rectification is a conductance that increases under hyperpolarization and decreases under depolarization. Thus, the inward rectification shown in T338A/S341A, T338A/R334E and T338/R334E/K1250A indicates that there is more Cl^- efflux under hyperpolarization, which is also considered as a type of CFTR gain of function and might be useful for gene therapy. Fig. 5.7 shows the rectification ratio of wild type CFTR and other mutants, we can see the significant

difference between wild type CFTR and T338A/S341A, T338A/R334E, T338/R334E/K1250A more clearly.

Mutant T338A/K335A and T338A/S341A showed severe reduction in macroscopic currents despite the fact that conductance in T338A/K335A was almost the same as wild type. This might be due to the fewer expression of CFTR in T338A/K335A or the lower open probability of CFTR Cl^- channel. Therefore, because of that the effect of 100 μM $Au(CN)_2^-$ might be too faint to be detected, we only added 1 mM $Au(CN)_2^-$ to the intracellular solution.

Fig. 5.6 shows the mean fractions of control current remaining (I/I_0) of wild type CFTR and other mutants after adding of 100 μM and 1 mM $Au(CN)_2^-$ to the intracellular solution. Block of macroscopic CFTR currents by $Au(CN)_2^-$ was examined following current stimulation with PKA and ATP plus PPi. Although in each case $Au(CN)_2^-$ reduced the current amplitude, its blocking effects were more or less altered in most mutants, as shown more clearly in the mean fractional current-voltage relationships. In wild type CFTR, the mean fractional current-voltage relationship showed upward when membrane potential varied from -100 mV to 60 mV, while in T338A, T338A/K335A, T338A/F337A, T338A/T339A, T338A/S341A and T338A/K1250A, it shows "U" shape. Fig. 5.6 also shows that the block by lower concentrations $Au(CN)_2^-$ appeared as less voltage-dependent than block by higher concentrations. The blocking effect of 100 μM $Au(CN)_2^-$ at -100 mV membrane potential was weakened in T338A, T338A/F337A, T338A/T339A and T338A/K1250A. (Due to the very small macroscopic currents of

T338A/K335A and T338A/S341A, 100 μM $Au(CN)_2^-$ was not used in these two double mutants). At positive membrane potential, the blocking effect of 100 μM $Au(CN)_2^-$ was very weak in wild type CFTR, T338A, T338A/F337A, T338A/T339A and T338A/K1250A. Compared with wild type CFTR, the blocking effect of 1 mM $Au(CN)_2^-$ at -100 mV was also weakened in T338A/T339A, T338A/S341A and T338A/K1250A. While in T338A, T338A/K335A and T338A/F337A, the blocking effect of this concentration of $Au(CN)_2^-$ was dramatically weakened. Blocking by 1 mM $Au(CN)_2^-$ in T338A, T338A/K335A, T338A/F337A, T338A/T339A, T338A/S341A and T338A/K1250A at 60 mV was not significantly different from that in wild type CFTR. The most effective blocking effect of both 100 μM and 1 mM $Au(CN)_2^-$ in T338A, T338A/K335A, T338A/F337A, T338A/T339A, T338A/S341A and T338A/K1250A appeared at the membrane potential near 0 mV, presenting a striking contrast to wild type CFTR in which the most effective blocking was at very negative membrane potential. Thereby, at extremely negative membrane potential, in T338A, T338A/K335A, T338A/F337A, T338A/T339A, T338A/S341A and T338A/K1250A, $Au(CN)_2^-$ can permeate through the CFTR channel pore, reconfirming the crucial function of residue T338.

As for double mutant T338A/R334E and triple mutant T338A/R334E/K1250A, the mean fractional current-voltage relationship was flattened when membrane potential varied from -100 mV to 60 mV. This is quite different with the upward slope of wt-CFTR and “U” shape of T338A. That is, at very positive membrane potential, the blocking effects of 100 μM and 1 mM $Au(CN)_2^-$ in T338A/R334E and T338A/R334E/K1250A are very

close to the effects at very negative membrane potential. Also, at very positive membrane potential, say, 60 mV, the blocking effects of 100 μM and 1 mM $Au(CN)_2^-$ in T338A/R334E and T338A/R334E/K1250A are dramatically enhanced. While at very negative membrane potential, the effects are almost the same as that in wild type CFTR.

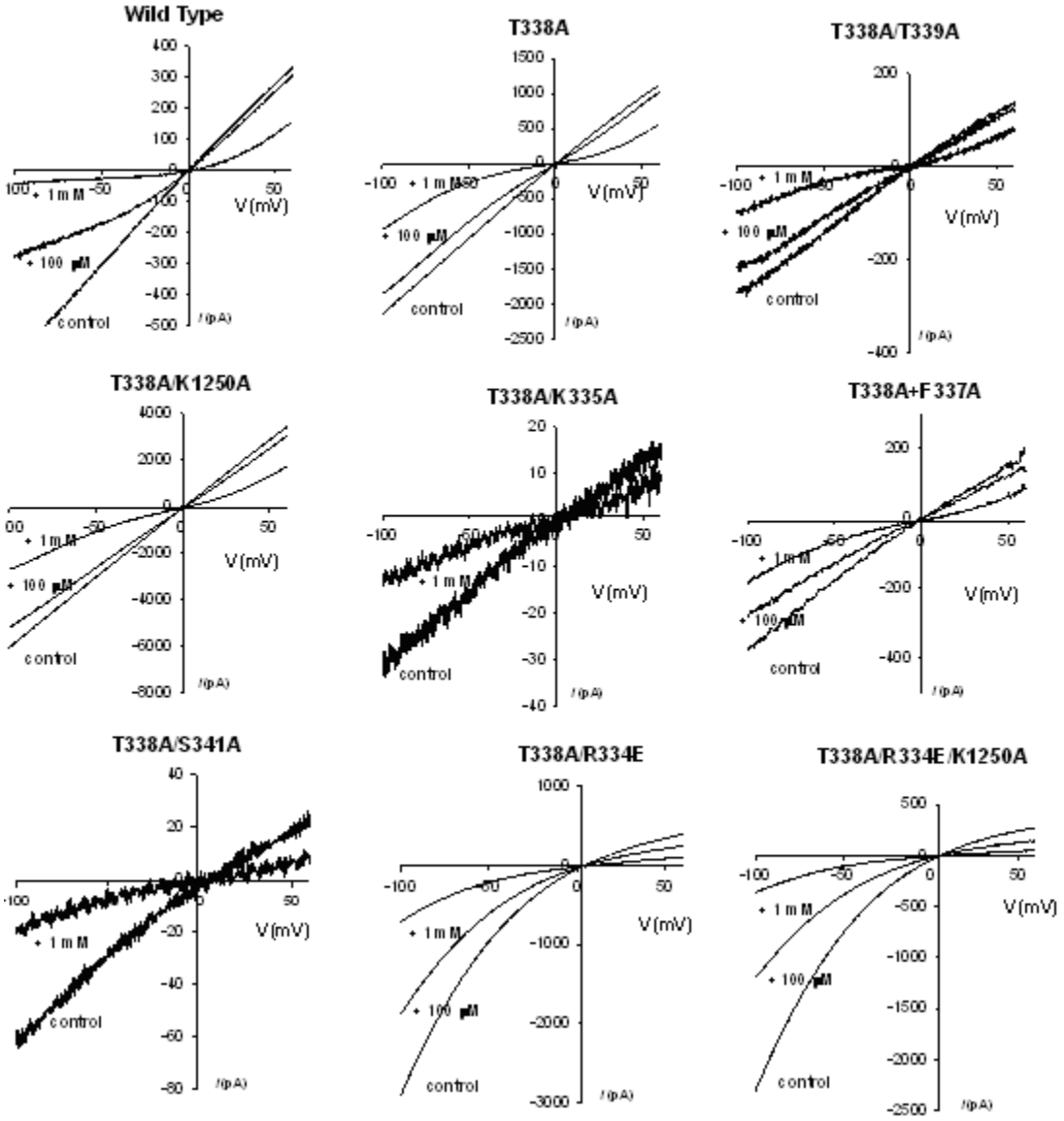

Fig. 5.5 Inhibitory Effects of $Au(CN)_2^-$ in wt-CFTR and other mutants

Examples of leak-subtracted macroscopic currents of wt-CFTR and other mutants recorded in inside-out membrane patches following maximal activation with 50 nM PKA, 1 mM MgATP under symmetrical 154 mM Cl^- concentrations. In each case, currents were recorded before (*Control*) and after additions of 100 µM and 1 mM $Au(CN)_2^-$ to the intracellular solution Mean of data from five to seven patches.

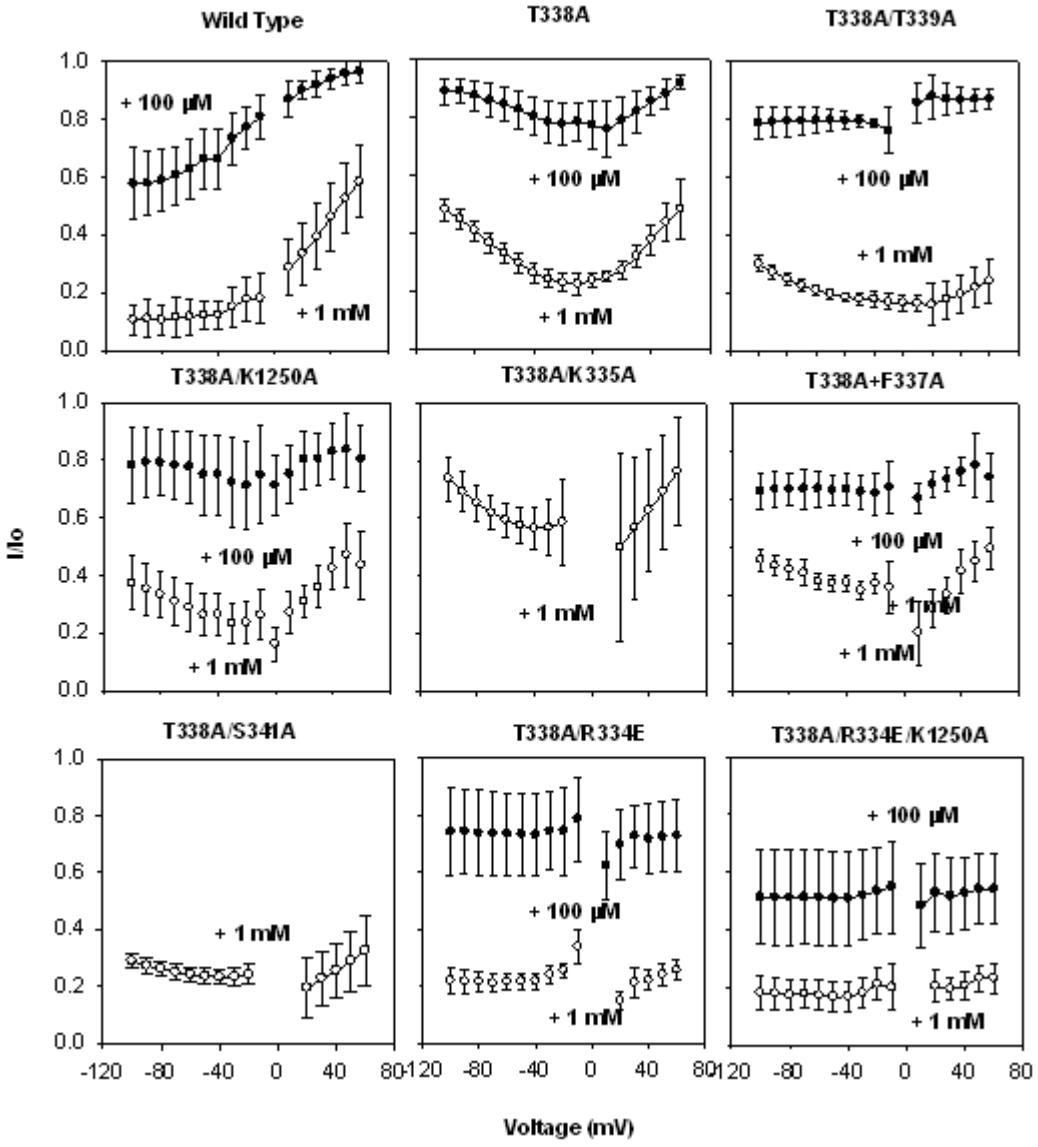

Fig. 5.6 Mean Fractions of Control Current Remaining (I/I_0)

The mean fractions of control current remaining (I/I_0) of wt-CFTR and other mutants are shown, following additions of 100 µM and 1 mM $Au(CN)_2^-$ to the intracellular solution as a function of membrane potential. Mean of data from five to seven patches.

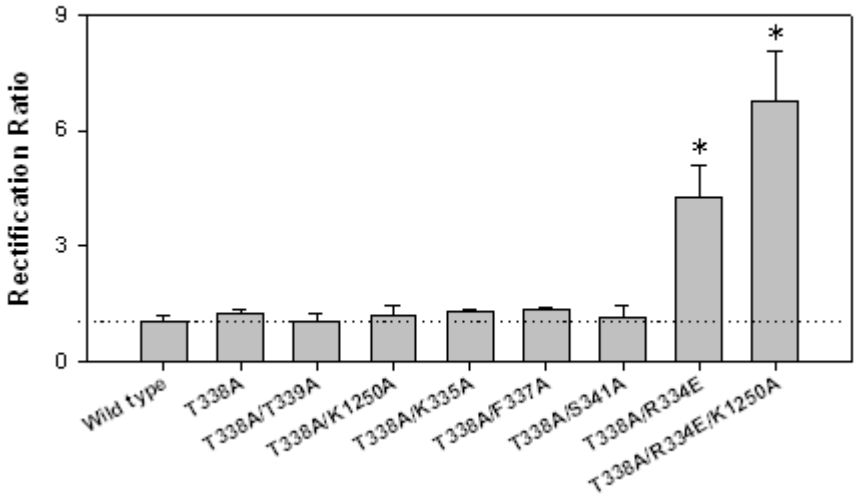

Fig. 5.7 Effect of mutations on rectification of the macroscopic I-V relationship

Rectification was quantified as the rectification ratio as described above, such that a ratio greater than one reflects inward rectification and a ratio less than one outward rectification of the *I-V* curve. *Asterisks* indicate significantly different from wild type CFTR. Mean of data from three to six patches.

5.4 Type III of CFTR Gain of Function: Favouring Physiological Important Ion Permeation (Channel Selectivity)

Ion channels are defined primarily by their ionic selectivity, that is the ability to allow certain ions to pass through at a high rate while effectively excluding others. The most highly selective ion channels are the voltage-gated cation channel superfamily, which may select K^+, Na^+ or Ca^{2+} ions with extremely high fidelity. In these channel types, ionic selectivity is determined at a highly localized region within the pore known as the selectivity filter. However, much less is known about the mechanism of anion permeation and anion selectivity in Cl^- channels. These Cl^- channels are generally much less selective than the cation channels, typically having some permeability to all small monovalent anions (Linsdell, 2001). Like most anion channels, CFTR allows the permeation not only of Cl^-, but also of most small monovalent anions. It has a permeability sequence of $SCN^- > I^- > NO_3^- > Br^- > Cl^- > OOCH^- \geqslant ClO_4^- > F^-$, which is described as similar to a lyotropic sequence, with anions which are more easily dehydrated (lyotropes) having a higher permeability than anions which retain their waters of hydration more strongly (Linsdell et al., 1997b; Tabcharani et al., 1997; Tabcharani et al., 1993).

Previous work, which focused on TM6, has begun to identify the structural determinants of CFTR pore function and to provide clues concerning the mechanism of Cl^- permeation through the pore. Previous investigations of TM6 also have provided evidences that both anion selectivity (in terms of permeability ratios) and anion binding in the CFTR pore are correlated with anion hydration energy, with lyotropic anions showing both high permeability and tight intrapore binding (Gong and Linsdell, 2003a, b, c, 2004). To

uncover the molecular determinations of anion permeability and to create mutants that favour physiological important anion such as HCO_3^- and glutathione permeation, the anion permeabilities of the wild type CFTR and mutants focus on TM6 were examined.

5.4.1 Permeability of Physiological Important Anions

As we mentioned in introduction, HCO_3^- and glutathione play vital physiological roles in nature: HCO_3^- is implicated in pH regulation of pancreatic ducts and glutathione is involved in the regulation of oxidative stressing airways. In fact, permeation of anions other than Cl^- such as HCO_3^- and glutathione through CFTR may be physiologically relevant (Gray et al., 2000; Linsdell and Hanrahan, 1998b; Poulsen et al., 1994; Reddy and Quinton, 2003). To enhance the selectivity of CFTR channels to HCO_3^- and glutathione over to Cl^-, we create some CFTR mutants with the intention to get some mutants that have higher selectivity of HCO_3^- and glutathione. Here we tested the permeability of HCO_3^- and glutathione in wild type CFTR, T338A single mutant, double mutants T338A/R33E, T338A/K1250A and triple mutant T338A/R334E/K1250A.

In biionic permeability of physiological important anions experiments, macroscopic currents were measured using inside-out patches with Cl^- solution in pipette and HCO_3^- /glutathione in the bath. Table. 5.1 summarizes the reversal potentials and permeability ratios for HCO_3^- /glutathione in wild type CFTR and mutants. As shown in Table. 5.1, the permeability for intracellular HCO_3^- in wild type CFTR is near 0.125; while in T338A, T338A/R334E, T338A/K1250A and T338A/R334E/K1250A, the values of P_X/P_{Cl} are bigger than that of wild type CFTR. That is to say, the permeabilities of HCO_3^- in these

mutations are larger than that in wild type CFTR. The permeability in T338A/R334E is close to that in T338A. While in T338A/R334E and T338A/R334E/K1250A, we noticed a significant enhancement in the permeability. However, for the intracellular glutathione, we see a different situation. The permeability in these mutants has no significant difference with that in wild type CFTR. Fig. 5.8 shows the relative permeabilities of HCO_3^- and glutathione in wild type CFTR and mutants; we can see these results more clearly from Fig. 5.8.

Table. 5.1 Summary of E_{Rev} and P_X/P_{Cl}

Mutants	Intracellular HCO_3^-		Intracellular glutathione	
	E_{Rev} (mV)	P_X/P_{Cl}	E_{Rev} (mV)	P_X/P_{Cl}
Wild Type	-53.00 ± 1.83	0.125 ± 0.009	-48.25 ± 4.79	0.153 ± 0.003
T338A	-37.16 ± 1.81	0.233 ± 0.016	-47.70 ± 5.16	0.156 ± 0.032
T338A/R334E	-19.02 ± 3.46	0.477 ± 0.063	-41.96 ± 3.43	0.194 ± 0.027
T338A/K1250A	-33.11 ± 8.17	0.285 ± 0.102	-51.79 ± 5.60	0.133 ± 0.029
T338A/R334E/K1250A	-20.31 ± 2.48	0.452 ± 0.044	-27.91 ± 14.79	0.361 ± 0.190

Table. 5.1. Summary of mean reversal potentials (E_{Rev}) measured with intracellular anions in wt-CFTR and different mutants. Relative permeabilities (P_X/P_{Cl}) were calculated from the reversal potentials using functions in **Data Analysis**.

We also tested the permeability of HCO_3^- and glutathione in single mutant F337A and double mutant T338A/F337A. Table. 5.2 and Fig. 5.9 summarize the reversal potentials and permeability ratios for HCO_3^- /glutathione in wild type CFTR and its mutants. We

can see very clearly that the permeabilities of HCO_3^- in all these mutations were larger than in wild type CFTR. The permeability of HCO_3^- in F337A was greater than in T338A and T338A/F337A; while that in T338A/F337A was greater than that in T338A. As for the permeability of glutathione, there is no big difference between wild type CFTR and its mutants.

Table. 5.2 Summary of E_{Rev} and P_X/P_{Cl}

Mutants	Intracellular HCO_3^-		Intracellular glutathione	
	E_{Rev} (mV)	P_X/P_{Cl}	E_{Rev} (mV)	P_X/P_{Cl}
Wild Type	-53.00 ± 1.83	0.125 ± 0.009	-48.25 ± 4.79	0.153 ± 0.003
T338A	-37.16 ± 1.81	0.233 ± 0.016	-47.70 ± 5.16	0.156 ± 0.032
F337A	-26.77 ± 7.84	0.363 ± 0.108	-47.96 ± 3.43	0.155 ± 0.040
T338A/F337A	-33.11 ± 6.27	0.290 ± 0.100	-49.42 ± 9.55	0.151 ± 0.052

Table. 5.2. Summary of mean reversal potentials (E_{Rev}) measured with intracellular anions in wt-CFTR and different mutants. Relative permeabilities (P_X/P_{Cl}) were calculated from the reversal potentials using functions in **Data Analysis**.

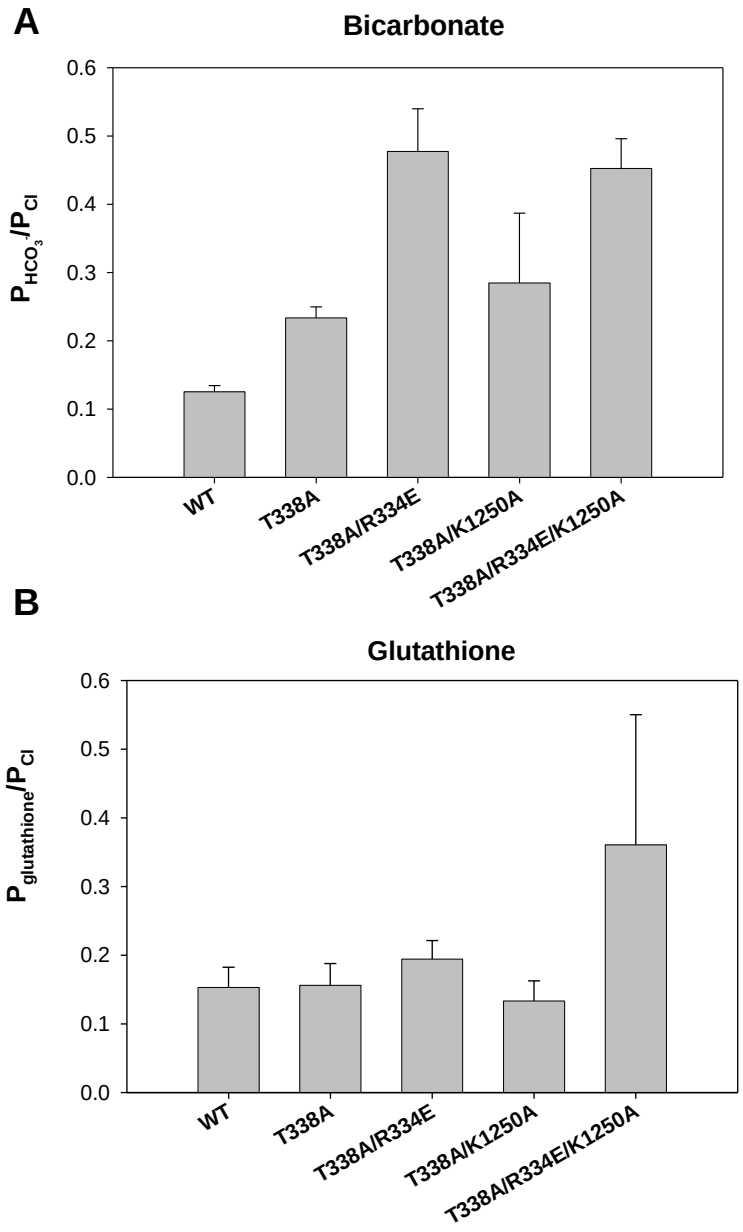

Fig. 5.8 Relative permeabilities (P_X / P_{Cl}) of HCO_3- and glutathione in wt-CFTR and mutants

HCO_3^- and glutathione were contained in bath solution (intracellular). Panel A shows the relative permeabilities of HCO_3^- while panel B shows the relative permeabilities of glutathione. Mean of data from three to six patches.

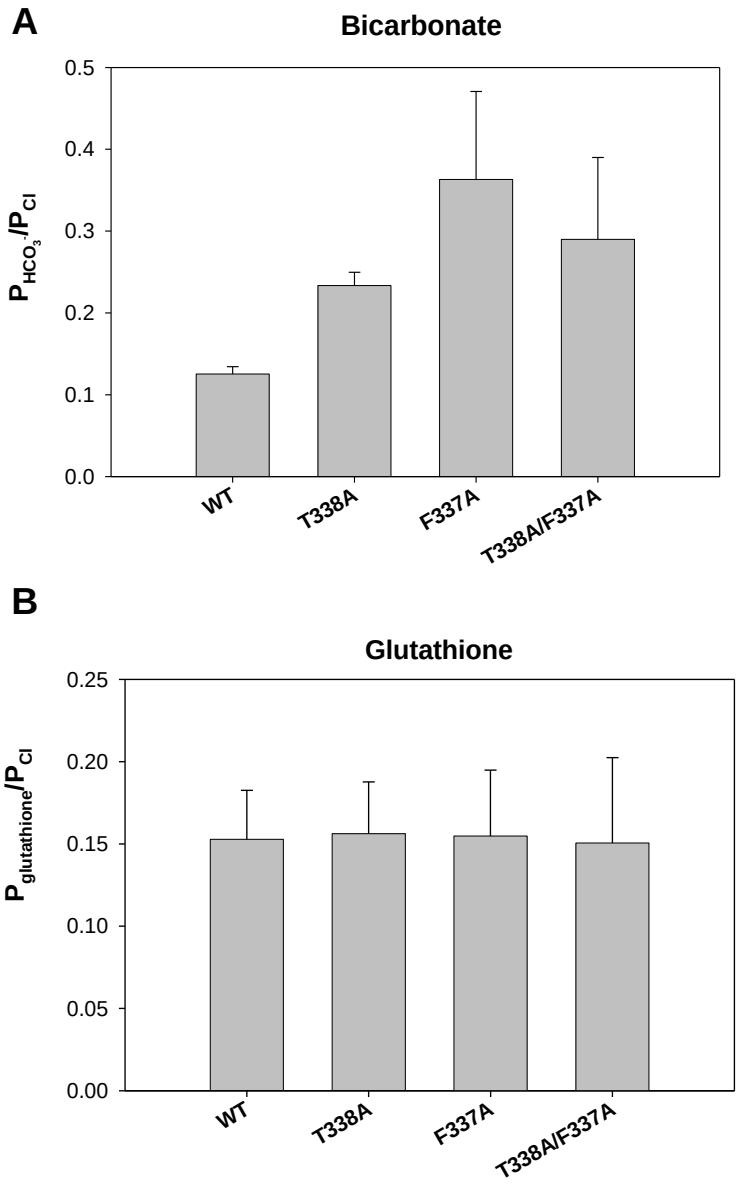

Fig. 5.9 Relative permeabilities (P_X / P_{Cl}) of HCO3- and glutathione in wt-CFTR and mutants

HCO_3^- and glutathione were contained in bath solution (intracellular). Panel A shows the relative permeabilities of HCO_3^- while panel B shows the relative permeabilities of glutathione. Mean of data from three to six patches.

5.4.2 Permeability of Extracellular Anions

In biionic permeability of extracellular anions experiments, macroscopic currents were measured using inside-out patches with Cl^- solution in bath and different anions in the pipette. Here we tested the permeabilities of extracellular anions Br^-, F^-, $HCOO^-$, NO_3^-, ClO_4^-, SCN^-, HCO_3^- and gluconate in wild type CFTR, T338A, T338A/R334E, T338A/K1250A and T338A/R334E/K1250A. We also tested the permeabilities of these ions in F337A and T338A/F337A.

Table. 5.3 Summary of P_X/P_{Cl}

	Wild Type	T338A	T338A/R334E	T338A/K1250A	T338A/R334E/K1250A
Br^-	1.50 ± 0.07	2.03 ± 0.03	1.67 ± 0.04	1.82 ± 0.09	1.74 ± 0.08
F^-	0.11 ± 0.02	0.09 ± 0.02	0.32 ± 0.02	0.07 ± 0.02	0.28 ± 0.03
$HCOO^-$	0.18 ± 0.02	0.29 ± 0.03	0.36 ± 0.03	0.21 ± 0.02	0.40 ± 0.04
NO_3^-	1.37 ± 0.12	1.84 ± 0.04	2.13 ± 0.23	1.55 ± 0.35	1.57 ± 0.30
ClO_4^-	0.11 ± 0.01	1.44 ± 0.12	0.99 ± 0.09	1.17 ± 0.12	0.97 ± 0.16
SCN^-	2.08 ± 0.09	7.34 ± 0.82	9.00 ± 0.55	6.63 ± 0.36	8.60 ± 0.55
HCO_3^-	0.09 ± 0.01	0.11 ± 0.02	0.68 ± 0.06	0.12 ± 0.02	0.59 ± 0.02
gluconate	≈ 0	≈ 0	≈ 0	≈ 0	≈ 0

Table. 5.3. Summary of relative permeabilities (P_X/P_{Cl}) which were calculated from the reversal potentials using functions in **Data Analysis**.

Table. 5.3 and Fig. 5.10 show the permeability ratios of extracellular anions Br^-, F^-, $HCOO^-$, NO_3^-, ClO_4^-, SCN^-, HCO_3^- and gluconate in wild type CFTR, T338A, T338A/R334E, T338A/K1250A and T338A/R334E/K1250A. Wild type CFTR had a

permeability sequence of $SCN^- > Br^- > NO_3^- > Cl^- > HCOO^- > F^- \geq ClO_4^- > HCO_3^- >$ gluconate. The permeabilities of ClO_4^- and SCN^- were significantly enhanced in T338A, T338A/R334E, T338A/K1250A and T338A/R334E/K1250A. The permeabilities of NO_3^- and Br^- were also enhanced in these four mutants. Moreover, we saw great enhancement of the permeabilities of F^- and HCO_3^- in T338A/R334E and T338A/R334E/K1250A.

Table. 5.4 Summary of P_X/P_{Cl}

	Wild Type	T338A	F337A	T338A/F337A
Br^-	1.50 ±0.07	2.03 ±0.03	0.43 ±0.05	1.40 ±0.03
F^-	0.11 ±0.02	0.09 ±0.02	0.34 ±0.05	0.17±0.02
$HCOO^-$	0.18 ±0.02	0.29 ±0.03	0.19 ±0.04	0.43 ±0.05
NO_3^-	1.37 ±0.12	1.84 ±0.04	1.06 ±0.03	2.11 ±0.15
ClO_4^-	0.11 ±0.01	1.44 ±0.12	0.27 ±0.01	0.61 ±0.06
SCN^-	2.08 ±0.09	7.34 ±0.82	0.82 ±0.03	7.40 ±0.80
gluconate	≈ 0	≈ 0	≈ 0	≈ 0

Table. 5.4. Summary of relative permeabilities (P_X/P_{Cl}) which were calculated from the reversal potentials using functions in **Data Analysis**.

Table. 5.4 and Fig. 5.11 show the permeability ratios of extracellular anions Br^-, F^-, $HCOO^-$, NO_3^-, ClO_4^-, SCN^- and gluconate in wild type CFTR, T338A, F337A and T338A/F337A. The permeabilities of all these extracellular anions in F337A were declined except ClO_4^- , which was more permeable in F337A than in wild type CFTR. While in T338A, almost all anions were more permeable than in wild type CFTR. For double mutant T338A/F337A, the permeabilities of most extracellular anions were between T338A and F337A.

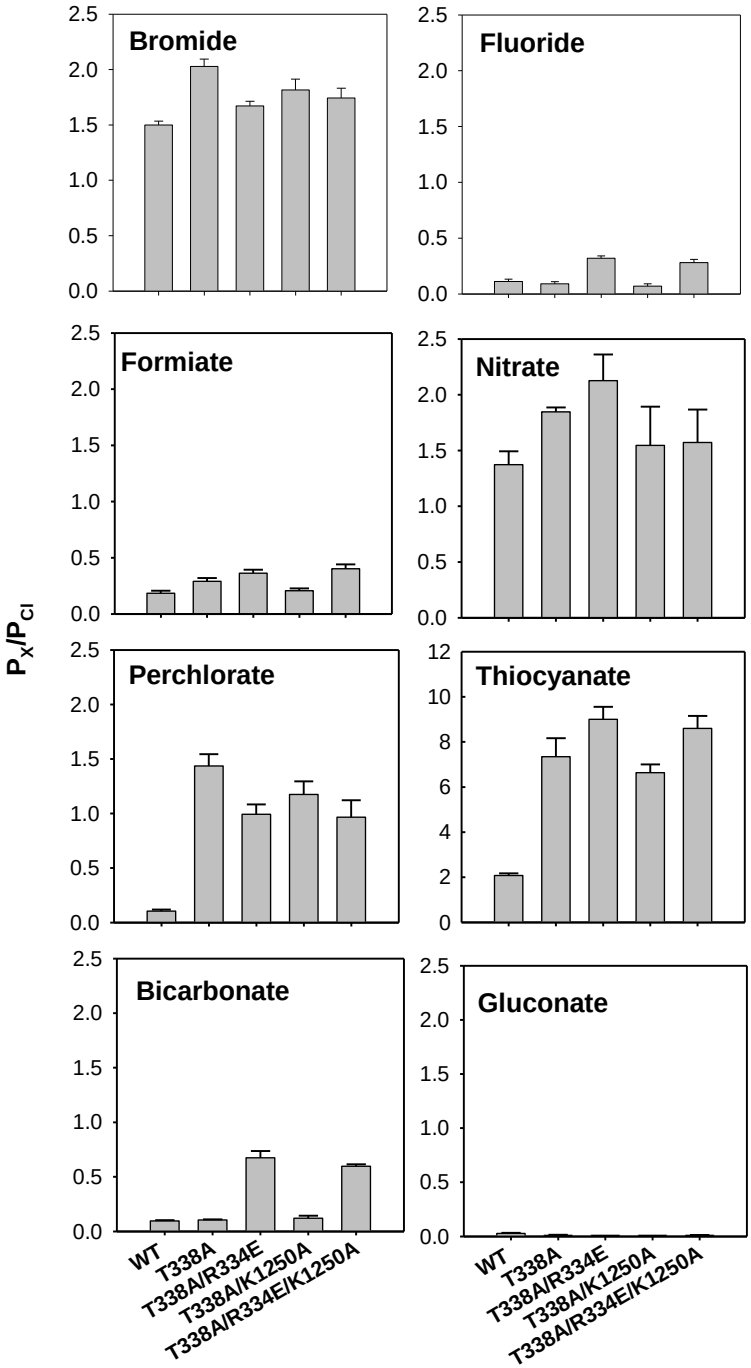

Fig. 5.10 Relative permeabilities (P_X / P_{Cl}) of extracellular anions in wt-CFTR, T338A, T338A/R334E, T338A/K1250A and T338A/R334E/K1250A

Cl^- was contained in bath solution (intracellular) while different anions were contained in pipette solution (extracellular). Mean of data from three to six patches.

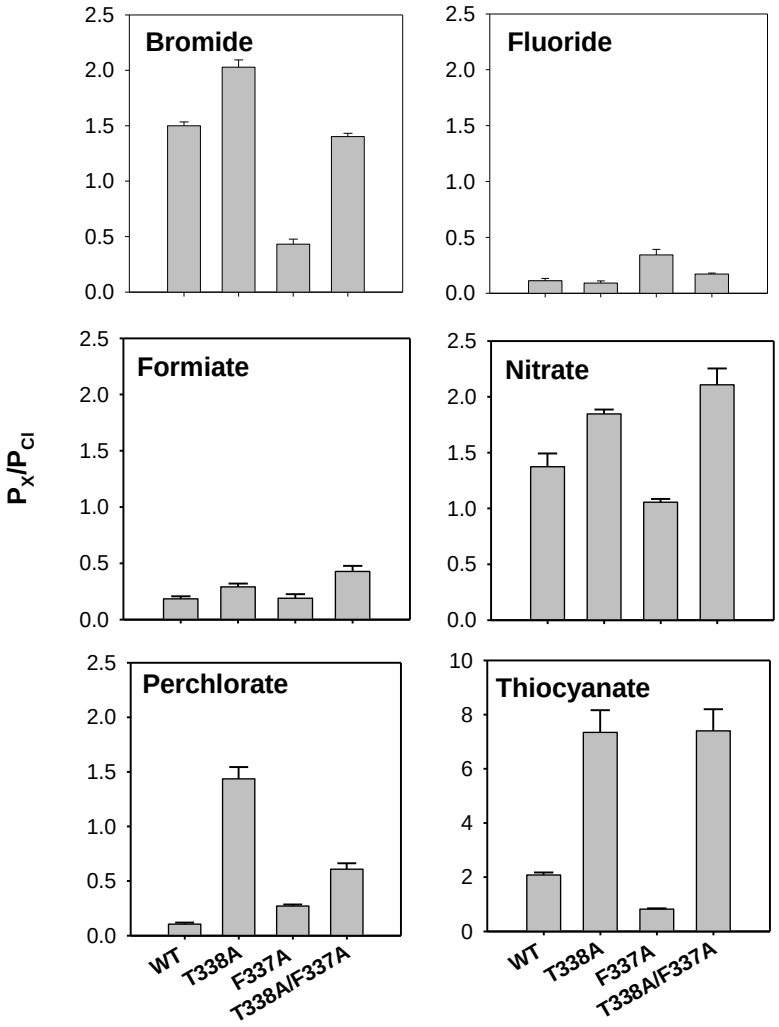

Fig. 5.11 Relative permeabilities (P_X / P_{Cl}) of extracellular anions in wt-CFTR, T338A, F337A and T338A/F337A

Cl^- was contained in bath solution (intracellular) while different anions were contained in pipette solution (extracellular). Mean of data from three to six patches.

6 Discussion

6.1 CFTR Channel Pore Is Made up From A CFTR Monomer

Despite the progress in elucidating domains involved in CFTR channels function, the structural basis for chloride conductance through CFTR remains incompletely understood. Fundamental questions remain as to how many CFTR polypeptides constitute the channel, although there are controversial reports concerning whether CFTR channel is a monomer (Chen et al., 2002; Marshall et al., 1994) or a dimmer (Eskandari et al., 1998; Ramjeesingh et al., 2003; Ramjeesingh et al., 2001; Schillers et al., 2004; Zerhusen et al., 1999). Furthermore, the possible interactions among the CFTR proteins have not been demonstrated at the cell membranes if they can form a dimer or an oligomer. Quaternary structure of CFTR at the cell membranes is fundamental importance to understand the molecular basis for CF pathogenesis. Since nearly all known ion channels are homo- or hetero-oligomers (Hille, 2001), the possibility that CFTR may posses a quaternary structure also has to be considered.

We first tested whether CFTR is monomeric or oligomeric by analyzing the population of channel conductance from cells co-expressing two mutants with different single channel properties. Our results suggest that CFTR channel pore is made up from a monomer. Coexpression of various pairs of CFTR channel pore-forming single mutants within sixth transmembrane region and the mutant (K1250A) which affects CFTR channel gating into the low CFTR protein expressive CHO cells, no hybrid channels were observed in our numerous recordings (Fig. 3.3 and Fig. 3.4). To further confirm these mutated CFTR

channels, we also tested the sensitivity of the channels to probe $Au(CN)_2^-$. From our results we confirmed that the channels observed were indeed from the individual mutants, not from a hybrid channel (Fig. 3.5). Our CFTR double mutant experiments support the notion that mutations at two different sites of CFTR channel pore region would affect their single channel properties (Fig. 3.1 and Fig. 3.2). In addition, we could not detect any hybrid channels when we coexpressed a double mutant and a single mutant which are mutated at the corresponded site of one of the double mutation (Fig. 3.4a and Fig. 3.4b). Lastly, the experiments of single channel recordings in the high CFTR protein expressing BHK cells demonstrate that CFTR channel pore is made up of CFTR monomer (Fig. 3.7). The data from all of our single channel recordings obtained from both CHO and BHK cells provides evidence that CFTR monomer forms a CFTR channel pore.

6.2 CFTR Can Exist As Dimer or even Multimer in the Cell Membranes

Our findings also provide direct functional evidence to support the notion that CFTR can exist as dimer or even multimer in the cell membranes (Ramjeesingh et al., 2003; Ramjeesingh et al., 2001) (Fig. 3.6, Fig. 3.7 and Fig. 3.8). There are also several lines of evidence that support CFTR protein can form a dimer and even multimeric complex using functional assays in this study. Firstly, CFTR single channel recordings in stably transfected BHK cells show two types (with high open probability or low open probability) of single channel kinetics existed in BHK cells (Fig. 3.6b, 3.6c, 3.6e to 3.6g). One of them shows a gating behaviour similar to the Torpedo ClC-0 channel, two barrel-pores in one channel (Fig. 3.6b) (Dutzler, 2004; Dutzler et al., 2003). Secondly, cotransfecting a double mutant (T338A/T339A) and a single mutant (R334K) into CFTR high expressive BHK cells which high express CFTR, we were able to record traces in

which R334K channel(s) opened only when T338A/T339A channel had been activated – a dependent gating mechanism (Fig. 3.7). Lastly, we further demonstrated that two CFTR channels sometimes show a coupled gating mechanism- two physically connected CFTR channels can open and close simultaneously. In summary, the central finding is that CFTR proteins can be assembled into macromolecular complexes in the cell membranes. These CFTR macromolecular complexes functionally up-regulate individual CFTR channel activity via two novel gating mechanisms-dependent gating and coupled gating.

Taken together, our data show that physical and functional association among the CFTR channels in the epithelial cells can be preserved. Our findings (single monomer CFTR channel pore with dependent or coupled gatings in oligomer) seemingly can solve many contradictions regarding whether CFTR is a monomer or dimer (multimer) among previous reports (Chen et al., 2002; Eskandari et al., 1998; Marshall et al., 1994; Ramjeesingh et al., 2003; Ramjeesingh et al., 2001; Schillers et al., 2004; Zerhusen et al., 1999). Our findings that CFTR associates with itself to form an oligomer which can significantly alter the function of individual CFTR channel pores further establish new molecular mechanisms. How do these CFTR proteins exert such an influence on the gatings shown in present study? Obviously, these inter-CFTR protein interactions involve the domains from different CFTR molecules and dynamic restructuring of the CFTR proteins. Several CFTR channel domains have been identified as important for the conformational changes within the single CFTR protein that occur during the activation of the CFTR channels (Mense et al., 2006; Vergani et al., 2005b; Wang et al., 2000). We hypothesize that CFTR proteins most likely form oligomers by the interactions of the nucleotide binding domains from different CFTR molecules. As there are no direct

evidence showing that CFTR can form an oligomer by the interaction of membrane spanning domains and regulatory domains among the CFTR proteins, but there are wealth of evidence showing that two nucleotide binding domains (NBD) can form a dimmer (Mense et al., 2006; Vergani et al., 2005b), we reason that CFTR dimer formation mainly by NBD1 (head) interacts with NBD2 (tail) from another CFTR protein (Fig. 3.6f). Furthermore, CFTR can form an oligomer by a head-tail-head-tail structure which has a dependent gating or a coupled gating or both mechanism to up-regulate CFTR channel function (Fig. 3.6f), although we cannot ruled out that other accessory proteins such as CFTR-associated protein 70 (CAP70), may link the carboxy termini of two CFTR molecules which enhances channel open probability (Wang et al., 2000). However, this possibility is rendered unlikely if we consider the inside-out membrane-patch excision. We believe that the multimer formation of CFTR may be more common than we previously thought in native epithelial cells. The biological significance for self-assembly of CFTR proteins in cell membranes appears to regulate intrinsic function by either a dependent gating or a coupled gating mechanism or by both mechanisms. Through dependent gating mechanism, activation of one CFTR channel might activate all of the CFTR channels interacted. Coupled gating provides a mechanism for the concerted activation of CFTR channels during electrolyte secretion in epithelial cells.

6.3 Evidence for CFTR Interdomain Interaction—MSD- or NBD- R Domain?

It is well known that phosphorylation of CFTR by PKA in R domain is required for the nucleotide-dependent channel activity of CFTR (Chang et al., 1993; Chappe et al., 2005;

Mathews et al., 1998; Seibert et al., 1999; Seibert et al., 1995). The 10 dibasic consensus sites for PKA phosphorylation on R domain act in a coordinated manner and not a single residue seems to be critical for R domain function (Chang et al., 1993). The mechanisms of phosphorylation-dependent regulation still remain unknown. A suggestion is that R domain may present "loose" structure which permits R domain interaction via the multiple phosphoserine residues with multiple regions of the protein. Studies suggest that residues 760-783 may have an inhibitory effect on CFTR gating (Xie et al., 2002) while other studies also show that residues 708-831 can engage in stimulatory interactions after phosphorylation (Winter and Welsh, 1997). These results raise the possibilities that R domain may interact with and modify the NBDs to enhance the nucleotide-dependent gating to the channel open state. Howell et al. also reported that the phosphorylation of R domain controls the interaction between NBD1-NBD2 (Howell et al., 2004). However, the interdomain interaction of R domain with other regions of the CFTR is still unclear.

Here we tested the interdomain interaction of R domain with other domains through the single channel conductance of mutations in R domain. Two mutations, H620Q and A800G were reported to increase intrinsic chloride transport activities. Moreover, they showed a significantly increased P_0 when compared with wild type CFTR (Vankeerberghen et al., 1998). We tested the single channel activity and single channel kinetics of these two mutants. Consistent with previous results, our results showed that both H620Q and A800G had a higher open probability than wild type CFTR (Fig. 4.12). H620Q and A800G also have lower mean closed time constant τ and interevent interval than wild type CFTR does (Fig. 4.11). As for the single channel conductance, we got

very interesting result. H620 shows similar conductance as wild type CFTR, but A800G shows a reduced single channel conductance when compared with wild type CFTR. (Fig. 4.1 and Fig. 4.2) Other than these two mutations, we also tested the single channel activity and kinetics of single mutants S737A, S768A and double mutant S373A/S768A. S737 and S768A are reported as inhibitory residues due to the possibility that individual phosphoserines have differential sensitivity to PKA (Wilkinson et al., 1997). In our experiments, S737A and S768A show similar single channel conductance as wild type CFTR (Fig. 4.3 and Fig. 4.4) and these two mutations prolong the channel open period (Fig. 4.9) and open probability (Fig. 4.12). For double mutant S737A/S768A, we also get very interesting results. This double mutant shows a reduced single channel conductance (Fig. 4.3 and Fig. 4.4) while in the meanwhile shows a prolonged open state (Fig. 4.9). It is widely accepted that R domain itself is not highly structured when phosphorylated or dephosphorylated. But phosphorylation of R domain by PKA was proposed to enhance ATP binding or hydrolysis (Gadsby and Nairn, 1999; Li et al., 1996) or it may be permissive for transmission of the conformational perturbation caused by ATP binding at the NBDs to the channel pore. So there is no direct connection between R domain and TM domains which may be involved the formation of the CFTR channel pore. Then how can mutations in R domain effect the single channel conductance property?

Our results show that mutations in R domain not affect only the gating ability of CFTR channel pore but also the single channel conductance property. All the mutations prolong the channel open duration and this confirms that R domain phosphorylation enhances ATP interaction with the NBDs. The reduced single channel conductances in mutant

A800G and S737A/S768A raise the possibility that R domain interacts with MSD domain, therefore affecting the channel pore structure. R domain is predominantly unstructured in solution (Ostedgaard et al., 2000), and other ABC transporters which do not contain a region homologous to R domain might contain a central region connecting NBD and MSD that includes PKA motifs. So a defined amino acid sequence might not be the determinant factor of channel activity whereas PKA consensus motifs, a certain degree of flexibility and an optimal length might be the key factors. These observations suggest that the functional R domain is predominantly random coil (Ostedgaard et al., 2001). Then how will an R domain regulate CFTR channel pore activity? Ostedgaard et al. suggested four possibilities: (A) Phosphorylation might induce a conformational change in small discrete regions; (B) Introduction of negative charge by phosphorylation may be sufficient to initiate activity; (C) Phosphorylation may not directly change conformation but may be required before the R domain can interact with other sites within CFTR; (D) R domain may adopt a more ordered structure only upon contact with the rest of CFTR (Ostedgaard et al., 2001).

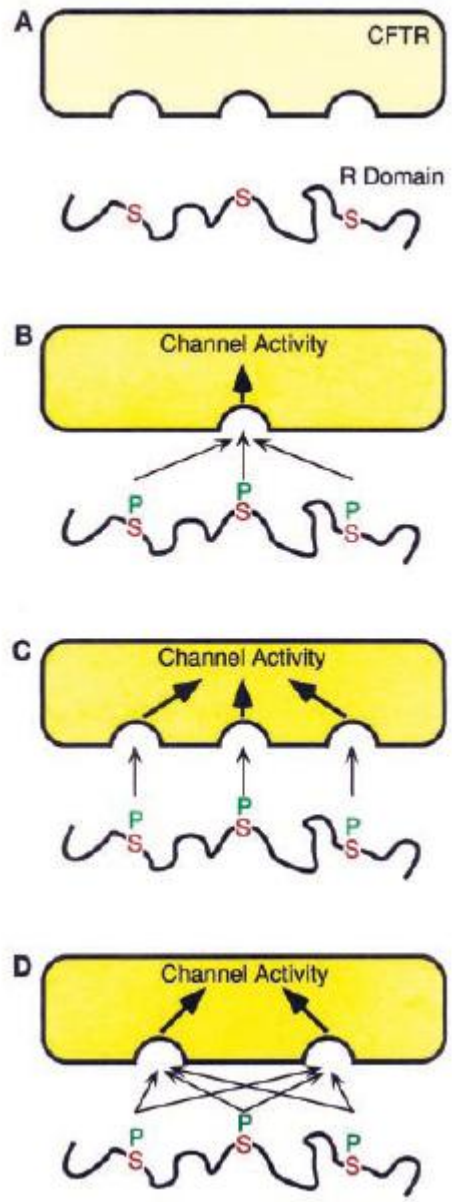

Fig. 6.1 Model of Stimulatory Interaction of R domain with the rest of CFTR

(Ostedgaard et al., 2001)

Fig 6.1 which comes from the published paper of Ostedgaard et al. in 2001 shows these models. Our results prefer the model D: R domain might interact nonspecficly with multiple sites on the rest of CFTR. In such a model, R domain which is predominantly unstructured would allow multiple different phosphoserines to stimulate and effect differently and quantitatively. The unstructured R domain has a large flexibility to interact with NBDs and MSDs.

6.4 Flexibility of the CFTR Channel Pore—Interaction of NBD and TM Domain

CFTR is a member of the ABC superfamily of membrane transport proteins and the dimeric assembly of NBDs is reported to be essential for ATPase function in ABC transporter (Aleksandrov et al., 2001; Kidd et al., 2004). The NBDs of ABC superfamily contain several conserved motifs including Walker A, Walker B, ABC signature motif and Q, P loop, which are involved in ATP binding and hydrolysis (Hopfner et al., 2000). In prokaryotic ABC transporters, NBD dimers show a head-to-tail configuration with Walker A motif of one NBD domain juxtaposed to ABC signature motif of the other NBD domain to form two nucleotide binding sites at the interface (Ward et al., 2007). The NBDs of CFTR are structurally asymmetric whereas prokaryotic NBDs are symmetric. CFTR NBDs are predicted to interact also in a head to tail orientation (Ramjeesingh et al., 1999). Each NBD of CFTR was reported to be able to bind nucleotide and heterodimeriztion of the NBDs is necessary to confer optimal ATPase activity (Kidd et al., 2004). Gadsby et al. recently suggested a model of gating which coupled with ATP hydrolysis (Gadsby et al., 2006; Vergani et al., 2005a). In this model, ATP binding to both NBDs promotes dimeriztion and conformational changes leading to

channel gating to the open state. Hydrolysis of nucleotide at one site precedes channel closing. R domain phosphorylation by PKA can accelerate the association of NBD domains. Nucleotides binding to NBDs cause the proper interaction of the two MSD that in turn permits Cl^- ions to move through the channel (Randak and Welsh, 2003; Randak and Welsh, 2005). Associations between NBDs and MSD domain may provide the conduit of communication from nucleotide-dependent conformational changes in NBD domains to the gating of transmembrane channels in CFTR. Lewis et al. proposed the homology models of CFTR MSD1-NBD1 based on the structure of mNBD1 docked on to the corresponding region of the MsbA and BtuCD structures (Lewis et al., 2004). Locher et al. identified a plausible interface between the MSD domain and the NBD domains, suggesting that helical segments (L1-L2) extending from the MSD intercalate with and provide a docking site for the NBD domains (Locher et al., 2002). However, at present, there is no accurate evidence how NBD domains interact with MSD domain.

Our results showed the gating control of CFTR by NBD domains. Triple mutants T338A/T339A/R555K and T338A/T339A/K1250A present a longer open time than wild type CFTR (Fig. 4.10 and Fig. 4.11). T338A/T339A/K1250 also shows a dramatically enhanced open probability than wild type CFTR (Fig. 4.12). R555 was reported to play a critical role in the formation of the NBD1-NBD2 dimer and mutation of R555 can act as a F508del-CFTR revertant by rescuing its cell surface expression and enhancing channel gating (Teem et al., 1996). Different gating patterns of channel gating have been reported for R555K. Our results showed that R555K can alter the closed time interval between bursts. Our results of T338A/T339A/K1250A also showed this characteristic. An

interesting finding of our results is that mutants T338A/T339A/R555K and T338A/T339A/K1250A show a lower single channel conductance than double mutant T338A/T339A. (Fig. 4.5 and Fig. 4.6) T338A/T339A, a double amino acid substitution in TM6 of CFTR, was reported to significantly increase channel conductance and also increase permeability to several large anions (Linsdell et al., 1997a). Our results are consistent with these results (Fig. 4.5 and Fig. 4.6). The explanation for T338A/T339A gain of function is that an apparent increase in the functional diameter of the CFTR channel pore increases the permeability to extracellular formate, acetate, propanoate and pyruvate ions (Linsdell et al., 1997a). This diameter effect did not show in T338, so it is possible that both T338 and T339 are located near physical constriction in the CFTR channel pore, and that simultaneous mutagenesis of both residues is necessary to influence functional pore diameter. Therefore, T338 and T339 might provide structural stability to the TM6 helix of CFTR via intra-helix hydrogen bonding. Triple mutation of T338A/T339A/R555K and T338A/T339A/K1250A might disrupt the orientation of the helix, leading to alteration of the single channel conductance. However, how can mutations in NBD1 and NBD2 change the pore properties which are mainly determined by TM domains? We believe that CFTR channel pore has a flexible structure which can interact with NBD domains. Interdomain interaction between NBD and MSD domains can change the conformation, thereby affecting the channel pore properties. The rectification ratios of triple mutants T338A/T339A/R555K and T338A/T339A/K1250A are larger than that of wild type CFTR and double mutant T338A/T339A. (Fig. 4.15) The values of δ in T338A/T339A/R555K and T338A/T339A/K1250A also have significant differences from that of wild type CFTR. (Fig. 4.16B)

Another interesting result we got is that triple mutant T338A/T339A/S768A showed a lower single channel conductance than double mutant T338A/T339A. (Fig. 4.19 and Fig. 4.20) This confirms the flexible structure of CFTR channel pore which not only can interact with NBD domains but also has direct interaction with R domain. These interdomain interactions can have some influences on the channel pore properties.

We also tested the interdomain interaction between N tail and R domain. As we mentioned early, NH_2-terminal tail (N-Tail) of CFTR might physically links CFTR to protein components of the membrane traffic machinery, thereby has a previously unrecognized role in CFTR channel regulation (Naren et al., 1999). And CFTR activity appears to be governed by the interdomain interactions involving the amino-terminal tail. Among the highly charged region of the N-Tail that is well conserved across species (residues 46 to 60), we mutated K52 to A52 which is supposed to enhance the Cl^- current of the channel pore (Naren et al., 1999). Our results show that mutant K52A, double mutants K52A/S73A and K52A/S768A did not change the CFTR channel pore properties too much and carrying almost the same single channel conductance as wild type CFTR. (Fig. 4.17 and Fig. 4.18) However, all these three mutants altered the interevent interval (Fig. 4. 24), revealing that N tail may be involved in the regulation of CFTR channel pore gating.

6.5 Gene Therapy for CF

The science of gene therapy has a turbulent history. Initially perceived as a revolutionary new technology with the promise to cure almost any disease, provided that we understand its genetic or molecular basis-enthusiasm rapidly, waned as clinical trial failed to show efficacy. CF is a disorder that results in a complex spectrum of disease phenotypes. We focus on CFTR's function as an ion channel to explain CF pathology. Several reasons has explained why the CFTR ion channel function is important. First, in exocrine tissues and intestine, the pathophysiology of CF appears to be explained well by CFTR's channel function. Second, the pathophysiology of CF generally varies with the capacity of different epithelia to express alternate ion channel pathway. Finally, most mutations that can interfere the procession of CFTR only affect the magnitude of the CFTR Cl^- conductance in a milder form (Pilewski and Frizzell, 1999). The amount of CFTR required by each organ to remain phenotypically normal varies and, similarly, the extent to which each organ contributes to the CF phenotype varies substantially. The type of mutation in the CFTR gene is clearly directly linked to CF phenotype in the case of pancreatic function, whereas CFTR mutations have a more variable impact on pulmonary phenotype where modifier genes and environmental effects also contribute to disease severity. Here, we hypothesize that CFTR gene can be genetically modified to maximize its lost function. These specific new forms of gene, because of their maximized functions, can efficiently compensate the functional losses in various CF patients even at under lower efficiency of gene transfer.

6.5.1 T338A/T339A with Increased Conductance Suggests the Possibility for Gene Therapy

Previous investigations showed that amino acid substitutions carried out for T338 strongly affected unitary Cl^- conductance, with both increases and decreases in conductance depending on the amino acid substituted. Strongly altered anion selectivity was observed in T338 mutants. This suggests the role of T338 in CFTR anion permeability. In contrast to mutations at T338, most mutations at T339 resulted in a reduced expression of CFTR protein and failure to express any detectable PKA- and ATP-dependent current (Linsdell et al., 1998).

When two polar threonine residues near the middle TM6 were simultaneously replaced by smaller, nonpolar alanines, double mutant T338A/T339A showed a larger saturating conductance than wild type CFTR, suggesting that conductance of the wild type may be limited by the rate of Cl^- flux through this narrow region. Conductance can be elevated due to a reduction in nonspecific frictional interactions between the permeating ion and the pore walls. Thus, the increased conductance in this double mutant indicates an increase in the dimensions of the narrowest part of the pore. As we said previously, one possible interpretation of this is that threonine residues 338 and/or 339 might contribute to the narrowest part of the pore, either directly or via an allosteric effect on a constricted region that is physically located elsewhere. Anion binding properties were not strongly altered in this double mutant. However, the P_X/P_{Cl} values of T338A/T339A for extracellular anions were higher than those of wild type, suggesting the increased anion

permeability. This might be also due to the increase in the dimensions of the selective pore of this mutant.

T338A/T339A with increased conductance may be useful in elevating Cl^- current in gene therapy for CF. Furthermore, the anions permeability are also enhanced in this double mutant, strengthening the possibility in replacement therapy for CF. It also suggests the possibility of other mutations which can be developed in TM6 for the gene therapy.

6.5.2 F337 is a Potential Residue for Developing New Gene Forms for Gene Therapy

F337 is a putative pore-lining phenylalanine residue whose mutants can dramatically alter the relative permeability of different anions. Single mutants F337A and F337S can enhance HCO_3^-, glutathione and some large organic anions (some native antibiotics) permeation. Thus, F337 is regarded as a potential residue for CFTR gene gain of function. When simultaneously mutated to alanines, double mutant T338A/F337A showed a larger conductance than F337A single mutant, increasing the possibility for its application in gene therapy. F337A and T338A/F337A both have increased intracellular HCO_3^- permeability. For the intracellular glutathione permeability, F337A and T338A/F337A have no significant differences from wild type CFTR. The permeabilities of extracellular anions (Br^-, F^-, $HCOO^-$, NO_3^-, ClO_4^-, SCN^- and gluconate) in F337A were all declined except ClO_4^- which was more permeable in F337A than in wild type CFTR. In T338A, almost all anions were more permeable than in wild type CFTR. For the double mutant T338A/F337A, the permeabilities of most the extracellular anions were between T338A and F337A. One possible explanation for the weaken anion permeability in F337A is that

anions are able to pass through the pores of F337A with more of their associated waters of hydration intact than that happen in wild type CFTR channel pore, so reducing the degree of anion dehydration required for permeation. The reduction of anion dehydration in determining permeability in F337A may result from the decrease in the degree of anion dehydration and the increase in the strength of the interaction between permeating anions and the channel pore. In addition, enhanced permeability in T338A/F337A might result from the alteration in the functional dimensions of the pore associated with T338A.

6.5.3 R334E with Strong Inward Rectification Strengthens the Efflux of Cl^-

R334 is a key anion binding site near the external end of TM6 which plays a crucial role in coordinating the concurrent binding of multiple anions (Gong and Linsdell, 2003b, 2004). Previous results suggested that R334 makes a strong contribution to anion binding in the CFTR pore. All mutations at this position induced inward rectification of the I-V relationship. Removal of the positive charge at position 334 reduces anion entry from the extracellular solution and causes inward rectification (Linsdell, 2005a). The importance of this anion attraction in the normal permeation mechanism is underscored by the finding that the unitary Cl^- conductance of CFTR is reduced by removal of the fixed charge at position 334 (Ge et al., 2004; Gong and Linsdell, 2004). The locations of R334, in pore inner and outer vestibules respectively, implies that a short, narrow section of the pore between these residues contributes a major barrier to anion flux; this section may also contain the anion selectivity filter that includes transmembrane helix 6 residue F337 (Gong and Linsdell, 2003a).

Our results showed that T338A/R334E and T338A/R334E/K1250A show strong inward rectification which indicates that there is more Cl^- efflux under hyperpolarization, and this enhanced Cl^- efflux is also regarded as a type of CFTR gain of function that might be useful for gene therapy. However, T338A/R334E and T338A/R334E/K1250A also have a drastic reduction in unitary Cl^- conductance. As for the permeability of physiological important anions HCO_3^- and glutathione, there is a significant enhancement in T338A/R334E and in T338A/R334E/K1250A. These imply that R334 is a potential target residue for gene therapy.

6.5.4 T338A/S341A with Inward Rectification also Strengthens the Efflux of Cl^-

Residue S341 is also suggested to lie in the selectivity region. Mutations in it affect conductance, selectivity, and sensitivity to blockade by DPC, NPPB and glibenclamide (McCarty and Zhang, 2001). Among these mutants, S341A shows a strong inward rectification. As mentioned previously, rectification is one of the properties in many voltaged-gated potassium channels. An inward rectification is a conductance that increases under hyperpolarization and decreases under depolarization. Thus, S341A can increase the efflux of Cl^- under hyperpolarization, which is regarded as a type of CFTR gain of function. Strong inward rectification was also observed in T338A/S341A. However, the small conductance, low macroscopic currents in this double mutant weaken its possibility in CF gene therapy application.

6.6 The Asymmetrical Structure of CFTR Pore

CFTR pore seems to show an asymmetrical structure between cytoplasm and extracellular loops. Here, the permeability properties of intracellular and extracellular anions in different CFTR mutants might also lead to such a conclusion.

The permeabilities for intracellular anions in wild type CFTR, T338A, F337A and T338A/F337A are higher than those for extracellular anions. For example, our results show that when gluconate was presented extracellular, no reversal potentials were observed, whereas when placed intracellular, it showed negative reversal potential near -60 mV. The voltage-dependent blocking by 100 μM and 1000 μM $Au(CN)_2^-$ also indicates the asymmetry of CFTR pore. In wild type CFTR, T338A, F337A and T338A/F337A, the blocking effect of higher concentration $Au(CN)_2^-$ for extracellular anions was observably stronger than that of lower concentration $Au(CN)_2^-$. However, for intracellular anions, the blocking effect of higher concentration $Au(CN)_2^-$ was not so distinguishing from that of lower concentration blocker. These observations not only can be interpreted by the asymmetry of CFTR pore, but also support the hypothesis that CFTR pore is presumed to narrow towards its extracellular end, forming a restricted region where discrimination between different permeant anions takes place (Gong et al., 2002b).

One thing should be mentioned is that although the mutants T338A, F337A, T338A/F337A show an asymmetrical pore structure, it is not sure whether the asymmetry

is the authentic reflection of the CFTR structure, or it is due to the conformation changes by the alanine substituting.

As the most common inherited disease in the Caucasian population, CF has been one of the most extensively studied genetic diseases in gene therapy. Despite the numerous obstacles encountered including vector inflammation, inefficient delivery, and vector production, enthusiasm for cystic fibrosis gene therapy remains high. There is still a tremendous amount of work to be done in order to develop an artificial new CFTR gene with a gain of function for CFTR gene therapy. We believe that we are now at the crucial point of being able to define the physiological importance of anion binding and understand more on the precise mechanism of anion permeation through the CFTR channel pore. We have some clues to develop such a gene so far and may encounter many obstacles in future, but these obstacles are not insurmountable. By continuing to identify the potential CFTR mutants and by maintaining a strong focus on improving CFTR gene function, gene therapy will surely improve the outcome of therapy of CF.

7 Reference

Alberti, S., Bohse, K., Arndt, V., Schmitz, A., and Hohfeld, J. (2004). The cochaperone HspBP1 inhibits the CHIP ubiquitin ligase and stimulates the maturation of the cystic fibrosis transmembrane conductance regulator. Mol Biol Cell *15*, 4003-4010.

Aleksandrov, L., Mengos, A., Chang, X., Aleksandrov, A., and Riordan, J.R. (2001). Differential interactions of nucleotides at the two nucleotide binding domains of the cystic fibrosis transmembrane conductance regulator. J Biol Chem *276*, 12918-12923.

Alexis, N.E., Muhlebach, M.S., Peden, D.B., and Noah, T.L. (2006). Attenuation of host defense function of lung phagocytes in young cystic fibrosis patients. J Cyst Fibros *5*, 17-25.

Anderson, M.P., Berger, H.A., Rich, D.P., Gregory, R.J., Smith, A.E., and Welsh, M.J. (1991). Nucleoside triphosphates are required to open the CFTR chloride channel. Cell *67*, 775-784.

Barinaga, M. (1992). Novel function discovered for the cystic fibrosis gene. Science *256*, 444-445.

Basso, C., Vergani, P., Nairn, A.C., and Gadsby, D.C. (2003). Prolonged nonhydrolytic interaction of nucleotide with CFTR's NH2-terminal nucleotide binding domain and its role in channel gating. J Gen Physiol *122*, 333-348.

Baukrowitz, T., Hwang, T.C., Nairn, A.C., and Gadsby, D.C. (1994). Coupling of CFTR Cl- channel gating to an ATP hydrolysis cycle. Neuron *12*, 473-482.

Bilan, F., Thoreau, V., Nacfer, M., Derand, R., Norez, C., Cantereau, A., Garcia, M., Becq, F., and Kitzis, A. (2004). Syntaxin 8 impairs trafficking of cystic fibrosis transmembrane conductance regulator (CFTR) and inhibits its channel activity. J Cell Sci *117*, 1923-1935.

Bobadilla, J.L., Macek, M., Jr., Fine, J.P., and Farrell, P.M. (2002). Cystic fibrosis: a worldwide analysis of CFTR mutations--correlation with incidence data and application to screening. Hum Mutat *19*, 575-606.

Brown, C. (2008). Current progress in cystic fibrosis: is this a disease elusive to therapy? Pulm Pharmacol Ther *21*, 585-587.

Cantiello, H.F. (2001). Electrodiffusional ATP movement through CFTR and other ABC transporters. Pflugers Arch *443 Suppl 1*, S22-27.

Cantiello, H.F., Jackson, G.R., Jr., Prat, A.G., Gazley, J.L., Forrest, J.N., Jr., and Ausiello, D.A. (1997). cAMP activates an ATP-conductive pathway in cultured shark rectal gland cells. Am J Physiol *272*, C466-475.

Carson, M.R., Travis, S.M., and Welsh, M.J. (1995). The two nucleotide-binding domains of cystic fibrosis transmembrane conductance regulator (CFTR) have distinct functions in controlling channel activity. J Biol Chem *270*, 1711-1717.

Chang, X.B., Tabcharani, J.A., Hou, Y.X., Jensen, T.J., Kartner, N., Alon, N., Hanrahan, J.W., and Riordan, J.R. (1993). Protein kinase A (PKA) still activates CFTR chloride channel after mutagenesis of all 10 PKA consensus phosphorylation sites. J Biol Chem *268*, 11304-11311.

Chappe, V., Hinkson, D.A., Howell, L.D., Evagelidis, A., Liao, J., Chang, X.B., Riordan, J.R., and Hanrahan, J.W. (2004). Stimulatory and inhibitory protein kinase C consensus sequences regulate the cystic fibrosis transmembrane conductance regulator. Proc Natl Acad Sci U S A *101*, 390-395.

Chappe, V., Irvine, T., Liao, J., Evagelidis, A., and Hanrahan, J.W. (2005). Phosphorylation of CFTR by PKA promotes binding of the regulatory domain. EMBO J *24*, 2730-2740.

Chen, J.H., Chang, X.B., Aleksandrov, A.A., and Riordan, J.R. (2002). CFTR is a monomer: biochemical and functional evidence. J Membr Biol *188*, 55-71.

Cheng, J., Wang, H., and Guggino, W.B. (2004). Modulation of mature cystic fibrosis transmembrane regulator protein by the PDZ domain protein CAL. J Biol Chem *279*, 1892-1898.

Cheng, S.H., Rich, D.P., Marshall, J., Gregory, R.J., Welsh, M.J., and Smith, A.E. (1991). Phosphorylation of the R domain by cAMP-dependent protein kinase regulates the CFTR chloride channel. Cell *66*, 1027-1036.

Cheung, M., and Akabas, M.H. (1997). Locating the anion-selectivity filter of the cystic fibrosis transmembrane conductance regulator (CFTR) chloride channel. J Gen Physiol *109*, 289-299.

Csanady, L., Seto-Young, D., Chan, K.W., Cenciarelli, C., Angel, B.B., Qin, J., McLachlin, D.T., Krutchinsky, A.N., Chait, B.T., Nairn, A.C., *et al.* (2005). Preferential Phosphorylation of R-domain Serine 768 Dampens Activation of CFTR Channels by PKA. J Gen Physiol *125*, 171-186.

Dahan, D., Evagelidis, A., Hanrahan, J.W., Hinkson, D.A., Jia, Y., Luo, J., and Zhu, T. (2001). Regulation of the CFTR channel by phosphorylation. Pflugers Arch *443 Suppl 1*, S92-96.

Dalemans, W., Barbry, P., Champigny, G., Jallat, S., Dott, K., Dreyer, D., Crystal, R.G., Pavirani, A., Lecocq, J.P., and Lazdunski, M. (1991). Altered chloride ion channel kinetics associated with the delta F508 cystic fibrosis mutation. Nature *354*, 526-528.

Dawson, D.C., Smith, S.S., and Mansoura, M.K. (1999). CFTR: mechanism of anion conduction. Physiol Rev *79*, S47-75.

Dork, T., Dworniczak, B., Aulehla-Scholz, C., Wieczorek, D., Bohm, I., Mayerova, A., Seydewitz, H.H., Nieschlag, E., Meschede, D., Horst, J., *et al.* (1997). Distinct spectrum of CFTR gene mutations in congenital absence of vas deferens. Hum Genet *100*, 365-377.

Dutzler, R. (2004). The structural basis of ClC chloride channel function. Trends Neurosci *27*, 315-320.

Dutzler, R., Campbell, E.B., and MacKinnon, R. (2003). Gating the selectivity filter in ClC chloride channels. Science *300*, 108-112.

Eskandari, S., Wright, E.M., Kreman, M., Starace, D.M., and Zampighi, G.A. (1998). Structural analysis of cloned plasma membrane proteins by freeze-fracture electron microscopy. Proc Natl Acad Sci U S A *95*, 11235-11240.

Fischer, H., Illek, B., and Machen, T.E. (1998). Regulation of CFTR by protein phosphatase 2B and protein kinase C. Pflugers Arch *436*, 175-181.

Gadsby, D.C., Dousmanis, A.G., and Nairn, A.C. (1998). ATP hydrolysis cycles and the gating of CFTR Cl- channels. Acta Physiol Scand Suppl *643*, 247-256.

Gadsby, D.C., and Nairn, A.C. (1999). Control of CFTR channel gating by phosphorylation and nucleotide hydrolysis. Physiol Rev *79*, S77-S107.

Gadsby, D.C., Vergani, P., and Csanady, L. (2006). The ABC protein turned chloride channel whose failure causes cystic fibrosis. Nature *440*, 477-483.

Ge, N., Muise, C.N., Gong, X., and Linsdell, P. (2004). Direct comparison of the functional roles played by different transmembrane regions in the cystic fibrosis transmembrane conductance regulator chloride channel pore. J Biol Chem *279*, 55283-55289.

Gong, X., Burbridge, S.M., Cowley, E.A., and Linsdell, P. (2002a). Molecular determinants of Au(CN)(2)(-) binding and permeability within the cystic fibrosis transmembrane conductance regulator Cl(-) channel pore. J Physiol *540*, 39-47.

Gong, X., Burbridge, S.M., Lewis, A.C., Wong, P.Y., and Linsdell, P. (2002b). Mechanism of lonidamine inhibition of the CFTR chloride channel. Br J Pharmacol *137*, 928-936.

Gong, X., and Linsdell, P. (2003a). Coupled movement of permeant and blocking ions in the CFTR chloride channel pore. J Physiol *549*, 375-385.

Gong, X., and Linsdell, P. (2003b). Molecular determinants and role of an anion binding site in the external mouth of the CFTR chloride channel pore. J Physiol *549*, 387-397.

Gong, X., and Linsdell, P. (2003c). Mutation-induced blocker permeability and multiion block of the CFTR chloride channel pore. J Gen Physiol *122*, 673-687.

Gong, X., and Linsdell, P. (2004). Maximization of the rate of chloride conduction in the CFTR channel pore by ion-ion interactions. Arch Biochem Biophys *426*, 78-82.

Gong, X.D., Linsdell, P., Cheung, K.H., Leung, G.P., and Wong, P.Y. (2002c). Indazole inhibition of cystic fibrosis transmembrane conductance regulator Cl(-) channels in rat epididymal epithelial cells. Biol Reprod *67*, 1888-1896.

Gong, X.D., and Wong, P.Y. (2000). Characterization of Lonidamine and AF2785 blockade of the cyclic AMP-activated chloride current in rat epididymal cells. J Membr Biol *178*, 225-233.

Gong, X.D., Wong, Y.L., Leung, G.P., Cheng, C.Y., Silvestrini, B., and Wong, P.Y. (2000). Lonidamine and analogue AF2785 block the cyclic adenosine 3', 5'-monophosphate-activated chloride current and chloride secretion in the rat epididymis. Biol Reprod *63*, 833-838.

Gray, M., O'Reilly, C., Winpenny, J., and Argent, B. (2000). Anion interactions with CFTR and consequences for HCO3- transport in secretory epithelia. J Korean Med Sci *15 Suppl*, S12-15
.
Gray, M.A., O'Reilly, C., Winpenny, J., and Argent, B. (2001). Functional interactions of HCO3- with cystic fibrosis transmembrane conductance regulator. Jop *2*, 207-211.

Grimard, V., Li, C., Ramjeesingh, M., Bear, C.E., Goormaghtigh, E., and Ruysschaert, J.M. (2004). Phosphorylation-induced conformational changes of cystic fibrosis transmembrane conductance regulator monitored by attenuated total reflection-Fourier transform IR spectroscopy and fluorescence spectroscopy. J Biol Chem *279*, 5528-5536.

Grubb, B.R., Pickles, R.J., Ye, H., Yankaskas, J.R., Vick, R.N., Engelhardt, J.F., Wilson, J.M., Johnson, L.G., and Boucher, R.C. (1994). Inefficient gene transfer by adenovirus vector to cystic fibrosis airway epithelia of mice and humans. Nature *371*, 802-806.

Guinamard, R., and Akabas, M.H. (1999). Arg352 is a major determinant of charge selectivity in the cystic fibrosis transmembrane conductance regulator chloride channel. Biochemistry *38*, 5528-5537.

Gunderson, K.L., and Kopito, R.R. (1995). Conformational states of CFTR associated with channel gating: the role ATP binding and hydrolysis. Cell *82*, 231-239.

Haardt, M., Benharouga, M., Lechardeur, D., Kartner, N., and Lukacs, G.L. (1999). C-terminal truncations destabilize the cystic fibrosis transmembrane conductance regulator without impairing its biogenesis. A novel class of mutation. J Biol Chem *274*, 21873-21877.

Hanrahan, J.W., and Wioland, M.A. (2004). Revisiting cystic fibrosis transmembrane conductance regulator structure and function. Proc Am Thorac Soc *1*, 17-21.

Hasegawa, H., Skach, W., Baker, O., Calayag, M.C., Lingappa, V., and Verkman, A.S. (1992). A multifunctional aqueous channel formed by CFTR. Science *258*, 1477-1479.

Hille, B. (2001). Ion channels of excitable membranes, Third edn (Sunderland, Massachusetts, USA, Sinauer Associates, Inc.).

Himmel, B., and Nagel, G. (2004). Protein kinase-independent activation of CFTR by phosphatidylinositol phosphates. EMBO Rep *5*, 85-90.

Hopfner, K.P., Karcher, A., Shin, D.S., Craig, L., Arthur, L.M., Carney, J.P., and Tainer, J.A. (2000). Structural biology of Rad50 ATPase: ATP-driven conformational control in DNA double-strand break repair and the ABC-ATPase superfamily. Cell *101*, 789-800.

Howell, L.D., Borchardt, R., Kole, J., Kaz, A.M., Randak, C., and Cohn, J.A. (2004). Protein kinase A regulates ATP hydrolysis and dimerization by a CFTR (cystic fibrosis transmembrane conductance regulator) domain. Biochem J *378*, 151-159.

Johnson, L.G., Olsen, J.C., Sarkadi, B., Moore, K.L., Swanstrom, R., and Boucher, R.C. (1992). Efficiency of gene transfer for restoration of normal airway epithelial function in cystic fibrosis. Nat Genet *2*, 21-25.

Kidd, J.F., Ramjeesingh, M., Stratford, F., Huan, L.J., and Bear, C.E. (2004). A heteromeric complex of the two nucleotide binding domains of cystic fibrosis transmembrane conductance regulator (CFTR) mediates ATPase activity. J Biol Chem *279*, 41664-41669.

Kim, J.Y., Han, W., Namkung, W., Lee, J.H., Kim, K.H., Shin, H., Kim, E., and Lee, M.G. (2004). Inhibitory regulation of cystic fibrosis transmembrane conductance regulator anion-transporting activities by Shank2. J Biol Chem *279*, 10389-10396.

Ko, S.B., Zeng, W., Dorwart, M.R., Luo, X., Kim, K.H., Millen, L., Goto, H., Naruse, S., Soyombo, A., Thomas, P.J., *et al.* (2004). Gating of CFTR by the STAS domain of SLC26 transporters. Nat Cell Biol *6*, 343-350.

Kogan, I., Ramjeesingh, M., Li, C., Kidd, J.F., Wang, Y., Leslie, E.M., Cole, S.P., and Bear, C.E. (2003). CFTR directly mediates nucleotide-regulated glutathione flux. Embo J *22*, 1981-1989.

Kunzelmann, K. (1999). The cystic fibrosis transmembrane conductance regulator and its function in epithelial transport. Rev Physiol Biochem Pharmacol *137*, 1-70.

Kunzelmann, K. (2001). CFTR: interacting with everything? News Physiol Sci *16*, 167-170.

Lader, A.S., Wang, Y., Jackson, G.R., Jr., Borkan, S.C., and Cantiello, H.F. (2000a). cAMP-activated anion conductance is associated with expression of CFTR in neonatal mouse cardiac myocytes. Am J Physiol Cell Physiol *278*, C436-450.

Lader, A.S., Xiao, Y.F., O'Riordan, C.R., Prat, A.G., Jackson, G.R., Jr., and Cantiello, H.F. (2000b). cAMP activates an ATP-permeable pathway in neonatal rat cardiac myocytes. Am J Physiol Cell Physiol *279*, C173-187.

Lee, M.G., Choi, J.Y., Luo, X., Strickland, E., Thomas, P.J., and Muallem, S. (1999). Cystic fibrosis transmembrane conductance regulator regulates luminal Cl-/HCO3- exchange in mouse submandibular and pancreatic ducts. J Biol Chem *274*, 14670-14677.

Lewis, H.A., Buchanan, S.G., Burley, S.K., Conners, K., Dickey, M., Dorwart, M., Fowler, R., Gao, X., Guggino, W.B., Hendrickson, W.A., *et al.* (2004). Structure of nucleotide-binding domain 1 of the cystic fibrosis transmembrane conductance regulator. EMBO J *23*, 282-293.

Li, C., Ramjeesingh, M., Wang, W., Garami, E., Hewryk, M., Lee, D., Rommens, J.M., Galley, K., and Bear, C.E. (1996). ATPase activity of the cystic fibrosis transmembrane conductance regulator. J Biol Chem *271*, 28463-28468.

Linsdell, P. (2001). Relationship between anion binding and anion permeability revealed by mutagenesis within the cystic fibrosis transmembrane conductance regulator chloride channel pore. J Physiol *531*, 51-66.

Linsdell, P. (2005a). Location of a common inhibitor binding site in the cytoplasmic vestibule of the CFTR chloride channel pore. J Biol Chem.

Linsdell, P. (2005b). Location of a common inhibitor binding site in the cytoplasmic vestibule of the cystic fibrosis transmembrane conductance regulator chloride channel pore. J Biol Chem *280*, 8945-8950.

Linsdell, P. (2006). Mechanism of chloride permeation in the cystic fibrosis transmembrane conductance regulator chloride channel. Exp Physiol *91*, 123-129.

Linsdell, P., Evagelidis, A., and Hanrahan, J.W. (2000). Molecular determinants of anion selectivity in the cystic fibrosis transmembrane conductance regulator chloride channel pore. Biophys J *78*, 2973-2982.

Linsdell, P., and Gong, X. (2002). Multiple inhibitory effects of Au(CN)(2-) ions on cystic fibrosis transmembrane conductance regulator Cl(-) channel currents. J Physiol *540*, 29-38.

Linsdell, P., and Hanrahan, J.W. (1998a). Adenosine triphosphate-dependent asymmetry of anion permeation in the cystic fibrosis transmembrane conductance regulator chloride channel. J Gen Physiol *111*, 601-614.

Linsdell, P., and Hanrahan, J.W. (1998b). Glutathione permeability of CFTR. Am J Physiol *275*, C323-326.

Linsdell, P., Tabcharani, J.A., and Hanrahan, J.W. (1997a). Multi-Ion mechanism for ion permeation and block in the cystic fibrosis transmembrane conductance regulator chloride channel. J Gen Physiol *110*, 365-377.

Linsdell, P., Tabcharani, J.A., Rommens, J.M., Hou, Y.X., Chang, X.B., Tsui, L.C., Riordan, J.R., and Hanrahan, J.W. (1997b). Permeability of wild-type and mutant cystic fibrosis transmembrane conductance regulator chloride channels to polyatomic anions. J Gen Physiol *110*, 355-364.

Linsdell, P., Zheng, S.X., and Hanrahan, J.W. (1998). Non-pore lining amino acid side chains influence anion selectivity of the human CFTR Cl- channel expressed in mammalian cell lines. J Physiol *512 (Pt 1)*, 1-16.

Liu, D.T., Tibbs, G.R., and Siegelbaum, S.A. (1996). Subunit stoichiometry of cyclic nucleotide-gated channels and effects of subunit order on channel function. Neuron *16*, 983-990.

Locher, K.P., Lee, A.T., and Rees, D.C. (2002). The E. coli BtuCD structure: a framework for ABC transporter architecture and mechanism. Science *296*, 1091-1098.

Macek, M., Jr., Vavrova, V., Bohm, I., Stuhrmann, M., Reis, A., Duspivova, R., Macek, M., Sperling, K., Krawczak, M., and Schmidtke, J. (1990). Frequency of the delta F508 mutation and flanking marker haplotypes at the CF locus from 167 Czech families. Hum Genet *85*, 417-418.

Marshall, J., Fang, S., Ostedgaard, L.S., O'Riordan, C.R., Ferrara, D., Amara, J.F., Hoppe, H.t., Scheule, R.K., Welsh, M.J., Smith, A.E., *et al.* (1994). Stoichiometry of recombinant cystic fibrosis transmembrane conductance regulator in epithelial cells and its functional reconstitution into cells in vitro. J Biol Chem *269*, 2987-2995.

Mastrocola, T., Porcelli, A.M., and Rugolo, M. (1998). Role of CFTR and anion exchanger in bicarbonate fluxes in C127 cell lines. FEBS Lett *440*, 268-272.

Mathews, C.J., Tabcharani, J.A., and Hanrahan, J.W. (1998). The CFTR chloride channel: nucleotide interactions and temperature-dependent gating. J Membr Biol *163*, 55-66.

McCarty, N.A. (2000). Permeation through the CFTR chloride channel. J Exp Biol *203*, 1947-1962.

McCarty, N.A., and Zhang, Z.R. (2001). Identification of a region of strong discrimination in the pore of CFTR. Am J Physiol Lung Cell Mol Physiol *281*, L852-867.

McDonough, S., Davidson, N., Lester, H.A., and McCarty, N.A. (1994). Novel pore-lining residues in CFTR that govern permeation and open-channel block. Neuron *13*, 623-634.

McIntosh, I., and Cutting, G.R. (1992). Cystic fibrosis transmembrane conductance regulator and the etiology and pathogenesis of cystic fibrosis. Faseb J *6*, 2775-2782.

Mense, M., Vergani, P., White, D.M., Altberg, G., Nairn, A.C., and Gadsby, D.C. (2006). In vivo phosphorylation of CFTR promotes formation of a nucleotide-binding domain heterodimer. Embo J *25*, 4728-4739.

Meyer, K.C., Sharma, A., Brown, R., Weatherly, M., Moya, F.R., Lewandoski, J., and Zimmerman, J.J. (2000). Function and composition of pulmonary surfactant and surfactant-derived fatty acid profiles are altered in young adults with cystic fibrosis. Chest *118*, 164-174.

Naren, A.P., Cormet-Boyaka, E., Fu, J., Villain, M., Blalock, J.E., Quick, M.W., and Kirk, K.L. (1999). CFTR chloride channel regulation by an interdomain interaction. Science *286*, 544-548.

Ostedgaard, L.S., Baldursson, O., Vermeer, D.W., Welsh, M.J., and Robertson, A.D. (2000). A functional R domain from cystic fibrosis transmembrane conductance regulator is predominantly unstructured in solution. Proc Natl Acad Sci U S A *97*, 5657-5662.

Ostedgaard, L.S., Baldursson, O., and Welsh, M.J. (2001). Regulation of the cystic fibrosis transmembrane conductance regulator Cl- channel by its R domain. J Biol Chem *276*, 7689-7692.

Pietrement, C., Da Silva, N., Silberstein, C., James, M., Marsolais, M., Van Hoek, A., Brown, D., Pastor-Soler, N., Ameen, N., Laprade, R., *et al.* (2008). Role of NHERF1, cystic fibrosis transmembrane conductance regulator, and cAMP in the regulation of aquaporin 9. J Biol Chem *283*, 2986-2996.

Pilewski, J.M., and Frizzell, R.A. (1999). Role of CFTR in airway disease. Physiol Rev *79*, S215-255.

Poulsen, J.H., Fischer, H., Illek, B., and Machen, T.E. (1994). Bicarbonate conductance and pH regulatory capability of cystic fibrosis transmembrane conductance regulator. Proc Natl Acad Sci U S A *91*, 5340-5344.

Prat, A.G., Reisin, I.L., Ausiello, D.A., and Cantiello, H.F. (1996). Cellular ATP release by the cystic fibrosis transmembrane conductance regulator. Am J Physiol *270*, C538-545.

Proesmans, M., Vermeulen, F., and De Boeck, K. (2008). What's new in cystic fibrosis? From treating symptoms to correction of the basic defect. Eur J Pediatr.

Pusch, M. (2004). Structural insights into chloride and proton-mediated gating of CLC chloride channels. Biochemistry *43*, 1135-1144.

Quinton, P.M. (1999). Physiological basis of cystic fibrosis: a historical perspective. Physiol Rev *79*, S3-S22.

Quinton, P.M., and Reddy, M.M. (1992). Control of CFTR chloride conductance by ATP levels through non-hydrolytic binding. Nature *360*, 79-81.

Raghuram, V., Mak, D.D., and Foskett, J.K. (2001). Regulation of cystic fibrosis transmembrane conductance regulator single-channel gating by bivalent PDZ-domain-mediated interaction. Proc Natl Acad Sci U S A *98*, 1300-1305.

Ramjeesingh, M., Kidd, J.F., Huan, L.J., Wang, Y., and Bear, C.E. (2003). Dimeric cystic fibrosis transmembrane conductance regulator exists in the plasma membrane. Biochem J *374*, 793-797.

Ramjeesingh, M., Li, C., Garami, E., Huan, L.J., Galley, K., Wang, Y., and Bear, C.E. (1999). Walker mutations reveal loose relationship between catalytic and channel-gating activities of purified CFTR (cystic fibrosis transmembrane conductance regulator). Biochemistry *38*, 1463-1468.

Ramjeesingh, M., Li, C., Kogan, I., Wang, Y., Huan, L.J., and Bear, C.E. (2001). A monomer is the minimum functional unit required for channel and ATPase activity of the cystic fibrosis transmembrane conductance regulator. Biochemistry *40*, 10700-10706.

Randak, C., and Welsh, M.J. (2003). An intrinsic adenylate kinase activity regulates gating of the ABC transporter CFTR. Cell *115*, 837-850.

Randak, C.O., and Welsh, M.J. (2005). ADP inhibits function of the ABC transporter cystic fibrosis transmembrane conductance regulator via its adenylate kinase activity. Proc Natl Acad Sci U S A *102*, 2216-2220.

Reddy, M.M., and Quinton, P.M. (2003). Control of dynamic CFTR selectivity by glutamate and ATP in epithelial cells. Nature *423*, 756-760.

Reigada, D., and Mitchell, C.H. (2005). Release of ATP from retinal pigment epithelial cells involves both CFTR and vesicular transport. Am J Physiol Cell Physiol *288*, C132-140.

Reisin, I.L., Prat, A.G., Abraham, E.H., Amara, J.F., Gregory, R.J., Ausiello, D.A., and Cantiello, H.F. (1994). The cystic fibrosis transmembrane conductance regulator is a dual ATP and chloride channel. J Biol Chem *269*, 20584-20591.

Riordan, J.R., Rommens, J.M., Kerem, B., Alon, N., Rozmahel, R., Grzelczak, Z., Zielenski, J., Lok, S., Plavsic, N., Chou, J.L., *et al.* (1989). Identification of the cystic fibrosis gene: cloning and characterization of complementary DNA. Science *245*, 1066-1073.

Rosenfeld, M.A., Yoshimura, K., Trapnell, B.C., Yoneyama, K., Rosenthal, E.R., Dalemans, W., Fukayama, M., Bargon, J., Stier, L.E., Stratford-Perricaudet, L., *et al.* (1992). In vivo transfer of the human cystic fibrosis transmembrane conductance regulator gene to the airway epithelium. Cell *68*, 143-155.

Rotoli, B.M., Bussolati, O., Dall' Asta, V., Hoffmann, E.K., Cabrini, G., and Gazzola, G.C. (1996). CFTR expression in C127 cells is associated with enhanced cell shrinkage and ATP extrusion in Cl(-)-free medium. Biochem Biophys Res Commun *227*, 755-761.

Rowntree, R.K., and Harris, A. (2003). The phenotypic consequences of CFTR mutations. Ann Hum Genet *67*, 471-485.

Saeed, Z., Wojewodka, G., Marion, D., Guilbault, C., and Radzioch, D. (2007). Novel pharmaceutical approaches for treating patients with cystic fibrosis. Curr Pharm Des *13*, 3252-3263.

Schillers, H., Shahin, V., Albermann, L., Schafer, C., and Oberleithner, H. (2004). Imaging CFTR: a tail to tail dimer with a central pore. Cell Physiol Biochem *14*, 1-10.

Schreiber, R., Pavenstadt, H., Greger, R., and Kunzelmann, K. (2000). Aquaporin 3 cloned from Xenopus laevis is regulated by the cystic fibrosis transmembrane conductance regulator. FEBS Lett *475*, 291-295.

Schultz, B.D., Singh, A.K., Devor, D.C., and Bridges, R.J. (1999). Pharmacology of CFTR chloride channel activity. Physiol Rev *79*, S109-144.

Schwiebert, E.M. (1999). ABC transporter-facilitated ATP conductive transport. Am J Physiol *276*, C1-8.

Schwiebert, E.M., Benos, D.J., Egan, M.E., Stutts, M.J., and Guggino, W.B. (1999). CFTR is a conductance regulator as well as a chloride channel. Physiol Rev *79*, S145-166.

Schwiebert, E.M., Egan, M.E., Hwang, T.H., Fulmer, S.B., Allen, S.S., Cutting, G.R., and Guggino, W.B. (1995). CFTR regulates outwardly rectifying chloride channels through an autocrine mechanism involving ATP. Cell *81*, 1063-1073.

Seibert, F.S., Chang, X.B., Aleksandrov, A.A., Clarke, D.M., Hanrahan, J.W., and Riordan, J.R. (1999). Influence of phosphorylation by protein kinase A on CFTR at the cell surface and endoplasmic reticulum. Biochim Biophys Acta *1461*, 275-283.

Seibert, F.S., Tabcharani, J.A., Chang, X.B., Dulhanty, A.M., Mathews, C., Hanrahan, J.W., and Riordan, J.R. (1995). cAMP-dependent protein kinase-mediated phosphorylation of cystic fibrosis transmembrane conductance regulator residue Ser-753 and its role in channel activation. J Biol Chem *270*, 2158-2162.

Sheppard, D.N., Gray, M.A., Gong, X., Sohma, Y., Kogan, I., Benos, D.J., Scott-Ward, T.S., Chen, J.H., Li, H., Cai, Z., *et al.* (2004). The patch-clamp and planar lipid bilayer techniques: powerful and versatile tools to investigate the CFTR Cl- channel. J Cyst Fibros *3 Suppl 2*, 101-108.

Sheppard, D.N., Rich, D.P., Ostedgaard, L.S., Gregory, R.J., Smith, A.E., and Welsh, M.J. (1993). Mutations in CFTR associated with mild-disease-form Cl- channels with altered pore properties. Nature *362*, 160-164.

Sheppard, D.N., and Welsh, M.J. (1999). Structure and function of the CFTR chloride channel. Physiol Rev *79*, S23-45.

Smith, J.J., Karp, P.H., and Welsh, M.J. (1994). Defective fluid transport by cystic fibrosis airway epithelia. J Clin Invest *93*, 1307-1311.

Smith, P.C., Karpowich, N., Millen, L., Moody, J.E., Rosen, J., Thomas, P.J., and Hunt, J.F. (2002). ATP binding to the motor domain from an ABC transporter drives formation of a nucleotide sandwich dimer. Mol Cell *10*, 139-149.

Smith, S.S., Liu, X., Zhang, Z.R., Sun, F., Kriewall, T.E., McCarty, N.A., and Dawson, D.C. (2001). CFTR: covalent and noncovalent modification suggests a role for fixed charges in anion conduction. J Gen Physiol *118*, 407-431.

Sprague, R.S., Ellsworth, M.L., Stephenson, A.H., Kleinhenz, M.E., and Lonigro, A.J. (1998). Deformation-induced ATP release from red blood cells requires CFTR activity. Am J Physiol *275*, H1726-1732.

Stead, R.J., Hodson, M.E., Batten, J.C., Adams, J., and Jacobs, H.S. (1987). Amenorrhoea in cystic fibrosis. Clin Endocrinol (Oxf) *26*, 187-195.

Strausbaugh, S.D., and Davis, P.B. (2007). Cystic fibrosis: a review of epidemiology and pathobiology. Clin Chest Med *28*, 279-288.

Super, M. (2000). CFTR and disease: implications for drug development. Lancet *355*, 1840-1842.

Tabcharani, J.A., Linsdell, P., and Hanrahan, J.W. (1997). Halide permeation in wild-type and mutant cystic fibrosis transmembrane conductance regulator chloride channels. J Gen Physiol *110*, 341-354.

Tabcharani, J.A., Rommens, J.M., Hou, Y.X., Chang, X.B., Tsui, L.C., Riordan, J.R., and Hanrahan, J.W. (1993). Multi-ion pore behaviour in the CFTR chloride channel. Nature *366*, 79-82.

Teem, J.L., Carson, M.R., and Welsh, M.J. (1996). Mutation of R555 in CFTR-delta F508 enhances function and partially corrects defective processing. Receptors Channels *4*, 63-72.

Vais, H., Zhang, R., and Reenstra, W.W. (2004). Dibasic phosphorylation sites in the R domain of CFTR have stimulatory and inhibitory effects on channel activation. Am J Physiol Cell Physiol *287*, C737-745.

Vankeerberghen, A., Wei, L., Jaspers, M., Cassiman, J.J., Nilius, B., and Cuppens, H. (1998). Characterization of 19 disease-associated missense mutations in the regulatory domain of the cystic fibrosis transmembrane conductance regulator. Hum Mol Genet *7*, 1761-1769.

Vergani, P., Basso, C., Mense, M., Nairn, A.C., and Gadsby, D.C. (2005a). Control of the CFTR channel's gates. Biochem Soc Trans *33*, 1003-1007.

Vergani, P., Lockless, S.W., Nairn, A.C., and Gadsby, D.C. (2005b). CFTR channel opening by ATP-driven tight dimerization of its nucleotide-binding domains. Nature *433*, 876-880.

Wang, S., Raab, R.W., Schatz, P.J., Guggino, W.B., and Li, M. (1998). Peptide binding consensus of the NHE-RF-PDZ1 domain matches the C-terminal sequence of cystic fibrosis transmembrane conductance regulator (CFTR). FEBS Lett *427*, 103-108.

Wang, S., Yue, H., Derin, R.B., Guggino, W.B., and Li, M. (2000). Accessory protein facilitated CFTR-CFTR interaction, a molecular mechanism to potentiate the chloride channel activity. Cell *103*, 169-179.

Ward, A., Reyes, C.L., Yu, J., Roth, C.B., and Chang, G. (2007). Flexibility in the ABC transporter MsbA: Alternating access with a twist. Proc Natl Acad Sci U S A *104*, 19005-19010.

Wilkinson, D.J., Strong, T.V., Mansoura, M.K., Wood, D.L., Smith, S.S., Collins, F.S., and Dawson, D.C. (1997). CFTR activation: additive effects of stimulatory and inhibitory phosphorylation sites in the R domain. Am J Physiol *273*, L127-133.

Wine, J.J. (2003). Rules of conduct for the cystic fibrosis anion channel. Nat Med *9*, 827-828.

Winter, M.C., and Welsh, M.J. (1997). Stimulation of CFTR activity by its phosphorylated R domain. Nature *389*, 294-296.

Xie, J., Adams, L.M., Zhao, J., Gerken, T.A., Davis, P.B., and Ma, J. (2002). A short segment of the R domain of cystic fibrosis transmembrane conductance regulator contains channel stimulatory and inhibitory activities that are separable by sequence modification. J Biol Chem *277*, 23019-23027.

Zerhusen, B., Zhao, J., Xie, J., Davis, P.B., and Ma, J. (1999). A single conductance pore for chloride ions formed by two cystic fibrosis transmembrane conductance regulator molecules. J Biol Chem *274*, 7627-7630.

Zhang, Z.R., McDonough, S.I., and McCarty, N.A. (2000a). Interaction between permeation and gating in a putative pore domain mutant in the cystic fibrosis transmembrane conductance regulator. Biophys J *79*, 298-313.

Zhang, Z.R., Zeltwanger, S., and McCarty, N.A. (2000b). Direct comparison of NPPB and DPC as probes of CFTR expressed in Xenopus oocytes. J Membr Biol *175*, 35-52.

Zhou, Z., Hu, S., and Hwang, T.C. (2002). Probing an open CFTR pore with organic anion blockers. J Gen Physiol *120*, 647-662.

Zielenski, J. (2000). Genotype and phenotype in cystic fibrosis. Respiration *67*, 117-133.